NOTE TO USERS

Delineation of the Fractured-Rock and Unconsolidated Overburden Ground-Water Flow Systems, on the Southern Part of Manhattan, New York, Through Use of Advanced Borehole-Geophysical Techniques

By

Frederick Stumm

A dissertation submitted to the Graduate Committee in Earth and Environmental Sciences
In partial fulfillment of the requirements for the degree in Doctor of Philosophy,
The City University of New York

2005

INFORMATION TO USERS

The quality of this reproduction is dependent upon the quality of the copy submitted. Broken or indistinct print, colored or poor quality illustrations and photographs, print bleed-through, substandard margins, and improper alignment can adversely affect reproduction.

In the unlikely event that the author did not send a complete manuscript and there are missing pages, these will be noted. Also, if unauthorized copyright material had to be removed, a note will indicate the deletion.

ProQuest Information and Learning Company
300 North Zeeb Road
P.O. Box 1346
Ann Arbor, MI 48106-1346

This manuscript has been read and accepted for the Graduate Faculty in Earth and Environmental Sciences in satisfaction of the dissertation requirement for the degree of Doctor of Philosophy.

4/29/05
Date

Chair of Examining Committee

5/2/05
Date

Executive Officer

Accepted_____
(date)

Dr. Allan Ludman

Dr. Shafiul Chowdhury

Dr. Patricia Kenyon

Dr. Yehuda Klein
Supervisory Committee

The City University of New York

Abstract

DELINEATION OF THE FRACTURED-ROCK AND UNCONSOLIDATED OVERBURDEN GROUND-WATER FLOW SYSTEMS, ON THE SOUTHERN PART OF MANHATTAN, NEW YORK, THROUGH USE OF ADVANCED BOREHOLE-GEOPHYSICAL TECHNIQUES

By

Frederick Stumm

Advisor: Professor Allan Ludman

Advanced borehole-geophysical techniques were used to assess the geohydrology of crystalline bedrock in 31 of 64 boreholes on the southern part of Manhattan Island, N.Y. Ten wells were screened in the unconsolidated overburden (glacial aquifer) to determine water-table elevation, transmissivity, and chloride concentration. The borehole-logging techniques included natural gamma, single-point resistance, short-normal resistivity, mechanical and acoustic caliper, magnetic susceptibility, borehole-fluid temperature and resistivity, borehole-fluid specific conductance, dissolved oxygen, pH, redox, heat-pulse flowmeter (at selected boreholes), borehole deviation, acoustic and optical televiewer, and borehole radar (at selected boreholes). The boreholes penetrated gneiss, schist, and other crystalline bedrock that has an overall southwest to northwest-dipping foliation. Most of the fractures penetrated are nearly horizontal or have moderate- to high-angle northwest or eastward dip azimuths. Heat-pulse flowmeter logs obtained under pumping and nonpumping (ambient) conditions, together with other geophysical logs, indicate transmissive fracture zones in each borehole. The 60-

megahertz directional borehole-radar logs delineated the location and orientation of several radar reflectors that did not intersect the projection of the borehole.

Fifty-three faults had mean orientation populations of N12°W, 66°W or N11°W, 70°E. Seventy-seven transmissive fractures delineated using the heat-pulse flowmeter had mean orientations of N11°E, 14°SE (majority) and N23°E, 57°NW (minority). The first potentiometric-surface and water-table maps were completed for southern Manhattan of the bedrock and glacial aquifer, respectively. Bedrock transmissivity ranged from 0.7 to 871 feet squared per day. Glacial aquifer transmissivity ranged from 2 to 93,000 feet squared per day. Chloride concentrations ranged from 25 to 17,800 milligrams per liter in the bedrock, and 28 to 15,250 milligrams per liter in the glacial aquifer. Three areas of saltwater intrusion in the bedrock and three wedges of saltwater intrusion in the glacial aquifer were delineated. The fractured-rock ground-water flow system within the study area is a highly interconnected continuum that responds as far as 3,200 feet away to hydraulic stresses.

ACKNOWLEDGEMENTS

I wish to thank Professor Shafiul Chowdhury, for his advice and assistance in completing this study. His guidance and moral support throughout this endeavor was invaluable. I would also like to thank Professor Alan Ludman for his immeasurable help in organizing this manuscript and for always being supportive throughout these past few years. I will always be indebted to his advice and guidance. My thanks are also extended to Professor Kenyon for expanding my horizons in surface geophysics, and to Professor Klein for his advice and review of the manuscript. To Professor Jeffrey Osleeb, for his advice and support along the many twists and turns that exist in this program.

I would like to extend my sincere appreciation to my colleagues at the United States Geological Survey who were supportive of my research and assisted in the many long hours of fieldwork. A special thank you is extended to Anthony Chu for all his support, advice, and most importantly friendship, and to Jack Monti Jr. for all of his help as well. I wish to also thank my colleagues at the New York City Department of Environmental Protection for their support and assistance during this study.

Most important of all, my heartfelt appreciation to my wife Dina, without her support, love, and understanding I would have never been able to finish this endeavor. To my sons Jacob and Joshua who had to sometimes put up with a Dad who always had homework of his own, your hugs and kisses kept me going. To my mother and father who taught me to never give up and to always do my best, thank you for all your love and support. And to Dina's parents thank you for your understanding and help.

TABLE OF CONTENTS

LIST OF TABLES

LIST OF FIGURES

LIST OF APPENDICES

1. Introduction

This study began in 1998 as a cooperative research project between the U.S. Geological Survey (USGS) and the New York City Department of Environmental Protection (NYCDEP) to apply advanced borehole geophysical methods to provide a comprehensive geologic and hydrologic assessment of the crystalline bedrock in southeastern New York. This provides a unique opportunity to characterize the fractured-rock and unconsolidated overburden ground-water flow systems in an intensely urbanized environment.

Water is supplied to New York City through two Water Tunnels (numbers one and two) constructed in 1917 and 1938, respectively. In 1970, the NYCDEP began construction of a third tunnel to supply water to New York City in the event that one of the two existing water tunnels should require repair. The third water tunnel in southern Manhattan is planned in three sections; the North Water-Tunnel, the Midtown Water-Tunnel, and the South Water-Tunnel.

Sixty-four boreholes were drilled by the NYCDEP during 1998-2004 to identify the type of rock and its degree of fracturing in the boreholes at the proposed tunnel depths within the study area. However, the cores from these boreholes are not oriented; the hydraulic characteristics of the fractures cannot be determined from the cores; and the fracture and foliation orientations, and the vertical deviation of the boreholes cannot be determined from the cores. Ten overburden wells were also installed to delineate the hydraulic head, transmissivity, and chloride concentration of the unconsolidated overburden ground-water flow system.

Statement of Problem and Hypotheses

This thesis will attempt to delineate the ground-water flow system of the fractured bedrock aquifers in southern Manhattan to a depth of about 600 feet below land surface. It will attempt to quantify the ground-water flow system by determining the total borehole (rock mass) and individual fracture transmissivity and hydraulic head within the test boreholes. No systematic study of the fractured-rock ground-water flow system and head distribution in Manhattan has been done. Subsurface engineering projects require the detailed spatial information on the orientation of faults, fractures and transmissive fractures that this study will provide. Some major questions this study will attempt to answer are: 1) the spatial and depth distribution of foliation/fracture strike and dip within the study area, 2) determine which fractures encountered in the boreholes are transmissive and quantify their transmissivity, 3) determine whether there is a preferred orientation to the transmissive fractures in southern Manhattan, and 4) determine if patterns exist in the distribution of transmissivity and hydraulic head that may indicate interconnectivity of the fracture networks. There are several hypotheses proposed for this study:

1. There are structural patterns to the major population orientations of both foliation and fractures.
2. There are patterns to the distribution of hydraulic head in both boreholes and fractures indicating a continuum or inter-connectivity of transmissive fractures, with recharge zones in the center of the island and discharge zones along the coastline.
3. Transmissive fractures have similar structural trends or orientations in southern Manhattan.
4. The unconsolidated overburden aquifer is a separate ground-water flow system from the bedrock.

The advanced borehole geophysical techniques were applied at 31 of the 64 boreholes in southern Manhattan to identify (1) the location and orientation (true strike and dip) of fractures, and foliation of the rock intersected by the boreholes, (2) the hydraulic characteristics of transmissive fracture zones, and (3) major fractures or faults that lie as much as 90 ft beyond the borehole (at selected boreholes). In addition, 10 wells screened in the unconsolidated overburden were also studied to determine the hydraulic characteristics of that system.

Purpose and Scope

The purpose of this study was to determine the hydrologic and structural characteristics of the fractured-rock and unconsolidated overburden ground-water flow systems in southern Manhattan through use of advanced borehole geophysical techniques. The geophysical and hydraulic data collected at 15 selected boreholes of the 31 geophysically logged are presented here. The geophysical logs and stereonets at 26 of the 31 boreholes have been recently published (Stumm and Chowdhury, 2003, Stumm and others 2001; 2004). Included in this study are the geophysical and hydrologic analyses and interpretations of these data and the hydraulic and chloride concentration data collected at additional wells.

This study (1) briefly describes the geophysical methods used; (2) presents geophysical logs, stereonet plots of fractures and foliations in each selected borehole; and summarizes the geophysical interpretations of fractures, faults, and foliation in each borehole; (3) presents ground-water levels, fluid-temperature, specific conductance, dissolved oxygen, pH, and redox logs, and specific-capacity data; and (4) summarizes the

transmissivity of the bedrock and overburden sediments, locations of transmissive fractures in selected boreholes, regional directions of ground-water flow, and the locations of saltwater intrusion in both the bedrock and unconsolidated overburden ground-water flow systems.

Hydrogeology

Manhattan Island is about 12.5 mi long and 2 mi wide (Fig. 1) and consists of unconsolidated deposits ranging from less than 1 ft thick to more than 250 ft thick overlying metamorphic bedrock. Manhattan Island is bounded on the west by the Hudson River, on the east by the East River, and on the south by New York Harbor each containing saltwater (Fig. 1).

The southern Manhattan study area is underlain by unconsolidated Holocene and glacial deposits of Pleistocene age throughout most of the study area, except in a few areas in the northern part where bedrock outcrops occur. These sediments consist of gravel, sand, silt, and clay underlain by crystalline bedrock of Proterozoic and Paleozoic age (Baskerville, 1982; Merguerian and Baskerville, 1987; Taterka (1987). The bedrock is fractured and appears to be a separate ground-water flow system from the unconsolidated sediment above.

Schopf (1787) was the first to describe the rocks in Manhattan as being mica schist. Merrill (1890) attempted to determine correlations and a stratigraphic sequence to the rocks in Manhattan, naming the major rock types on the island as the Inwood Marble, Manhattan Schist, and Fordham Gneiss. Hobbs (1905) collated over one thousand borehole and well logs and produced the first bedrock contour maps of Manhattan.

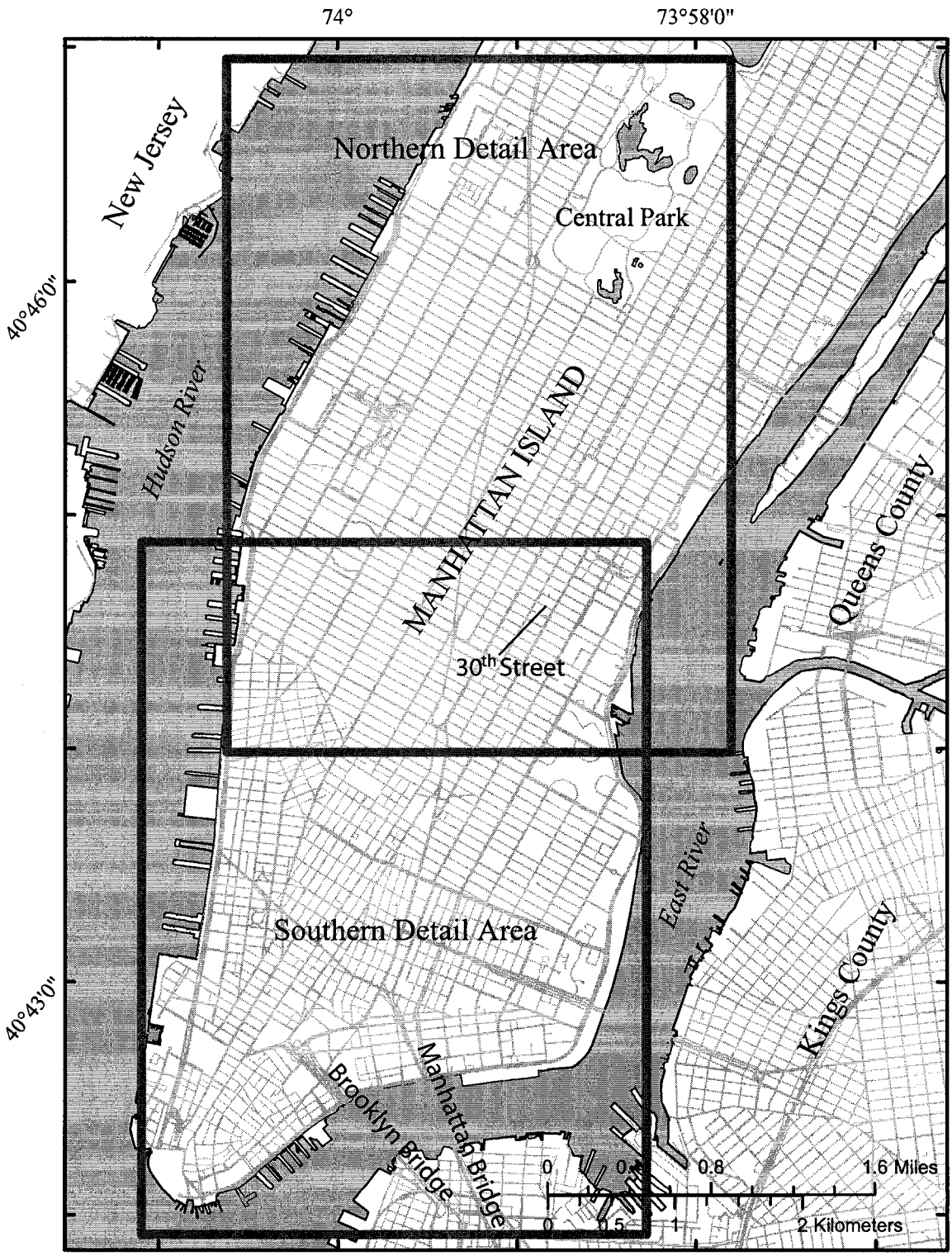

Figure 1. Southern Manhattan Study Area with Northern and Southern Detail Study Areas, Manhattan Island, New York County, N.Y..

Berkey (1910) used tunnel excavations and test boreholes to describe the geology and structural features of the bedrock in southern Manhattan. Murphy and Fluhr (1944) updated the previous work by Hobbs (1905) and produced geologic, soil, and bedrock contour maps. Perlmutter and Arnow (1953) completed the only previous ground-water (reconnaissance) study of the New York City area. Until now, this was the only comprehensive ground-water investigation in Manhattan. Recent workers have mapped the bedrock of Manhattan utilizing outcrops, subsurface drill-core, and Water Tunnel excavations (Fig. 2) (Baskerville, 1982; Merguerian and Baskerville, 1987; Taterka 1987). Baskerville (1994) mapped the geologic and engineering properties of Manhattan, and collated over 80 years worth of subsurface excavation information into a bedrock surface elevation map. Significant differences still persist among recent workers in the interpretation of the stratigraphy and placement of the bedrock formations in Manhattan. It was beyond the scope of this study to attempt to redefine the metamorphic stratigraphy of southern Manhattan. The interpretation by Baskerville (1994) will be used in this study.

Stumm and others (2000, 2001, and 2004); Stumm and Chowdhury (2003) described the fractured-rock ground-water flow system in the southern part of Manhattan for the first time. This study expands upon those preliminary interpretations on the fractured-rock ground-water flow system in southern Manhattan.

Fractured-Rock (Bedrock)

The bedrock underlying the study area has been mapped by various workers as an assemblage of gneiss, schist, amphibolite, marble, granite, and serpentinite. These rocks

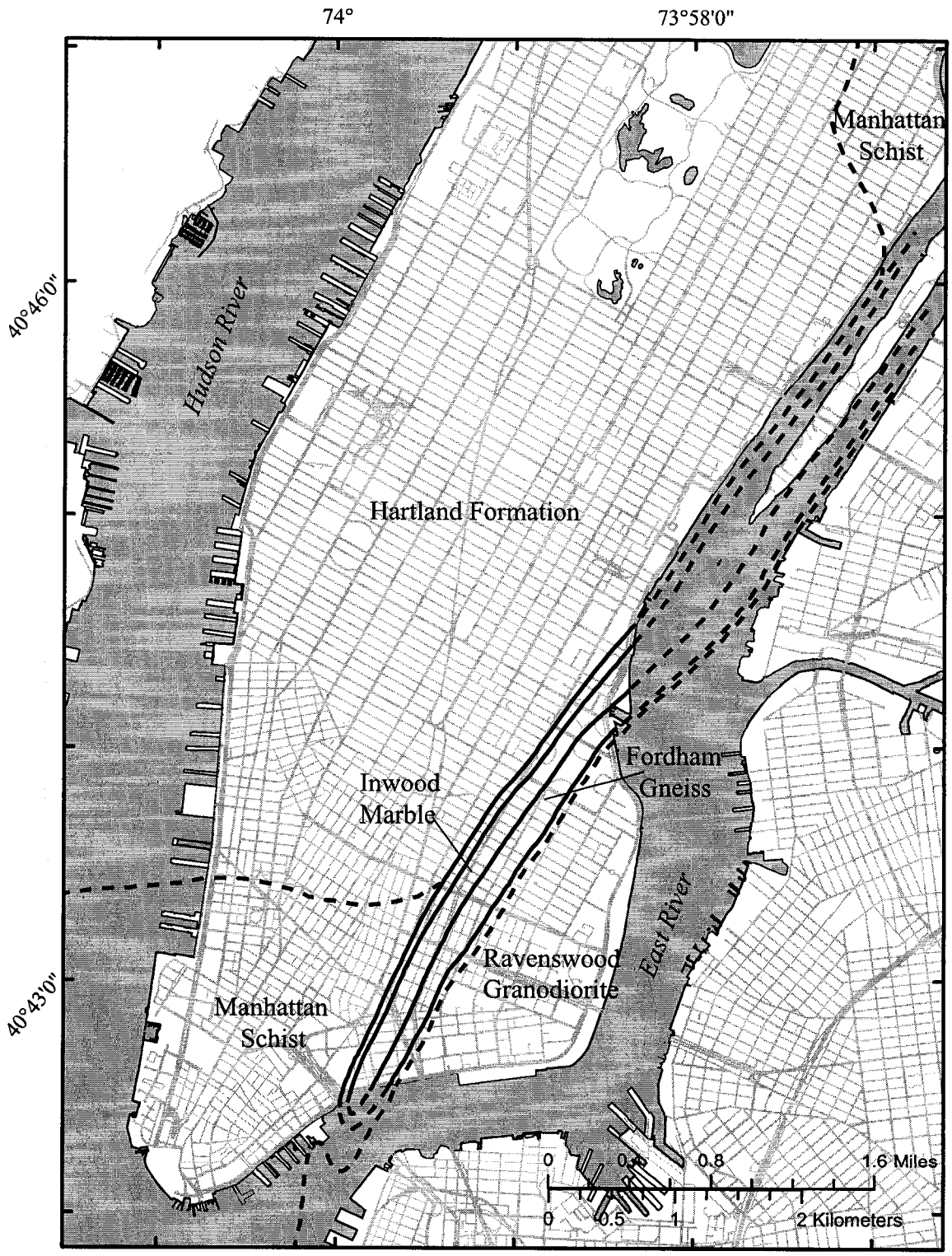

Figure 2. Bedrock geology map of the study area, Manhattan Island, N.Y (Modified from Baskerville, 1994).

include the Manhattan Schist, Hartland Formation, Inwood Marble, Fordham Gneiss, and the Ravenswood Granodiorite (Merguerian, 1983; and Baskerville and Merguerian, 1987; Taterka, 1987, Baskerville and Mose, 1989; Baskerville, 1994; Brock and Brock, 2001; and Merguerian and Sanders, 1993). Relationships proposed by Baskerville (1994) are shown in Figure 2.

Baskerville (1994) describes the Hartland Formation which underlies most of the study area as a gray quartzofelspathic muscovite-biotite-garnet schist with dark-greenish-black quartz-biotite-hornblende amphibolite. He notes that most of the Hartland Formation contains magnetite. The Manhattan Schist consists of a gray sillmanite-muscovite-biotite-kyanite schist and gneiss interlayered with tourmaline-garnet-plagioclase-biotite-quartz schist and gneiss with black amphibolite layers (Baskerville, 1994). Within the study area the Manhattan Schist is in thrust contact with the structurally overlying Hartland Formation. The Inwood Marble is a white coarse-grained calcitic and dolomitic marble in unconformable contact with the Fordham Gneiss (Merguerian and Sanders, 1993; Baskerville, 1994; Brock and Brock, 2001). The Fordham Gneiss is a black and white layered gneiss with quartz, plagioclase, biotite, and garnet. The Ravenswood Granodiorite is a sillmanite-garnet-microcline-plagioclase-biotite-quartz layered gneiss. Baskerville (1994); and Brock and Brock (2001) map the Inwood Marble and Fordham Gneiss as an antiform in the southeastern part of the study area. The Ravenswood Granodiorite is mapped by Baskerville (1994) to be east of the Inwood Marble/Fordham Gneiss antiform. The Inwood Marble, Fordham Gneiss, and Ravenswood Granodiorite do not cropout within the study area. Together these rocks comprise the fractured-rock hydrogeologic system within the study area.

Hobbs (1905) produced the first bedrock surface maps of Manhattan. In 1999 the USGS completed a seismic-reflection survey in the East River and delineated a linear escarpment beneath the Manhattan Bridge (Stumm, unpublished data). Drill-core data from 59 boreholes indicate the fractured-rock surface underlying the study area gently slopes southward from 50 feet above sea level at the surface in the Central Park area to over 250 feet below sea level in the vicinity of the Brooklyn and Manhattan Bridges. These data were interpreted and combined with Baskerville's (1994) bedrock surface map and the 64 newly drilled boreholes to produce a new bedrock surface elevation map (Fig. 3). These data indicate that an anomalously deep buried valley with very steep slopes occupies the southeasternmost part of the study area. The buried valley is more than a mile wide and over 250 feet deep. This buried valley extends offshore based upon unpublished USGS marine seismic-reflection data. It is unclear if the source of this deep buried valley is structural (a fault zone), lithologic (Inwood Marble), glacial erosion, or possibly a combination of all three.

While a large part of the bedrock surface has been eroded by glacial scouring, drill-core data from several bedrock boreholes in the southern part of the study area have reported saprolitic zones up to 50 feet thick. Ground-water flows through the bedrock via an interconnected network of fractures and faults. The rocks are not porous due to their high grade of metamorphism. Borehole geophysical logs were used to delineate the location of fractures, faults, and foliation and determine their 3D orientation as true strike and dip. The application of fluid parameter logs and heat-pulse flowmeter logs facilitated the delineation of transmissive fractures and their transmissivity at selected boreholes.

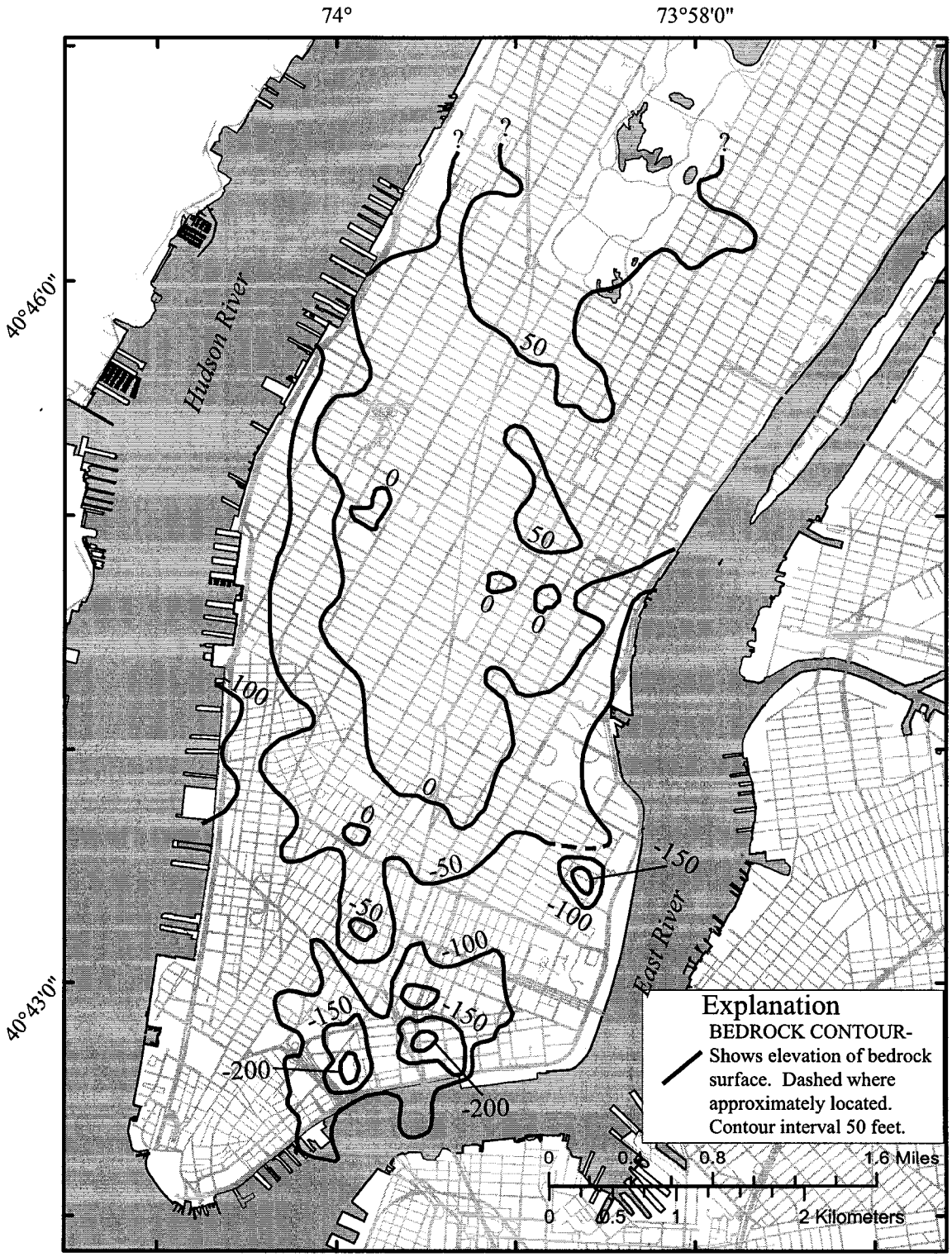

Figure 3. Surface elevation of the bedrock underlying the study area, Manhattan Island, N.Y.

Glacial Aquifer

The name glacial aquifer is introduced here to represent a sequence of unconsolidated Pleistocene-age sediments that overlie the bedrock in the southern Manhattan study area. Unconsolidated gravels, sands, silts, and clay overlie the fractured-rock throughout the study area, except in the northernmost part of the study area where it pinches out and bedrock is exposed. Perlmutter and Arnow (1953) completed the first reconnaissance of the unconsolidated overburden in Manhattan. They included hydrogeologic driller's logs, chloride concentrations, and some data on drawdown and industrial pumpage of the aquifer. There has been no large scale investigation of the unconsolidated aquifer since 1953.

Modern and historical drilling and engineering logs indicate the glacial aquifer currently only extends as far north as about 30th Street, with localized exceptions within the study area. North of the area near 30th Street, drilling data indicate dry sand and silty deposits above bedrock. In addition, bedrock water levels north of this area were consistently below the bedrock surface, whereas the bedrock water levels south of 30th Street were consistently above the bedrock surface.

These data indicate that the glacial aquifer consists of reddish-brown and sometimes gray gravel, sand, silt, and clay. Perlmutter and Arnow (1953) describe the glacial aquifer as consisting of till and ground moraine in the northern part of the study area and stratified drift in the southern part of the study area. Recent drill core data could not confirm this. Split-spoon core analysis of Monroe-4 near the East River within the southern buried valley indicates glacial stratified drift deposits of sandstone and diabase

gravels transported by glacial action from New Jersey. The well extended over 185 ft BLS and cores were taken at 20 ft intervals until bedrock was encountered.

Interpretation of the pre-development water-table is possible using a topographic and hydrographic map by Viele (1865). This map includes the natural stream drainage system, low-lying wetland areas, and topographic features, all overlain with the present street grid in use today. This extraordinary map included the pre-development coastline. Based upon this map showing flowing streams and wetland areas in the northern part of the study area, it appears the pre-development water-table was much higher in 1865 than it is today. The glacial aquifer appears to have been saturated throughout most of the study area during that time. The cause for this dramatic decrease in aquifer extent, saturated thickness, and water-table elevation is potentially due to a reduction in recharge area due to impervious surfaces as a result of urbanization since 1865. Infilling of these ancient stream channels has hidden their location. This is probably the reason why construction in the northern part of the study area (north of 30th Street) may or may not be affected by shallow ground-water inflows. It is a common misconception that underground rivers flow beneath parts of Manhattan Island. In fact, it is simply the existence of small deeply eroded channels infilled with saturated sediment that if encountered during excavation can produce significant quantities of ground-water. Whereas, an excavation north of 30th Street that is not above an eroded channel typically may not encounter ground-water above the bedrock surface at all. Baskerville (1994) included these ancient stream channels in his engineering maps of the study area for the same reason.

Methods

This study employed an array of advanced borehole geophysical probes to acquire information about the physical and hydrogeologic properties of both the fractured-rock and unconsolidated glacial overburden. Data collected during this study included (1) borehole geophysical logs, (2) geologic structure (foliation, fractures, and faults), (3) ground-water levels, transmissivity, and chloride concentrations. Additional data were obtained from the NYCDEP and previous studies.

Sixty-four NX-sized (3-in diameter) boreholes were drilled by the diamond-core method to obtain continuous rock-core samples (Figs. 4 and 5) (Table 1). Ten 2-in diameter overburden wells were installed in unconsolidated sediments in the southern part of Manhattan study area (Figs. 4 and 6) (Table 1). All bedrock boreholes are cased with either steel or Polyvinylchloride (PVC) from land surface through the unconsolidated overburden to the top of bedrock, and are uncased or open from the bedrock surface to the bottom of the drilled depth (except the ten overburden wells). All overburden wells are cased in PVC and screened in the unconsolidated sediments overlying the bedrock. All wells and boreholes were surveyed to determine their location in State Plane northing and easting, and elevation above mean sea level of their top of casing. Sea level in this study refers to the National Geodetic Vertical Datum of 1929 (NGVD of 1929).

Borehole-Geophysical Logging

Borehole-geophysical logs collected in this study included natural gamma, single-point-resistance, short-normal resistivity, mechanical and acoustic caliper, magnetic

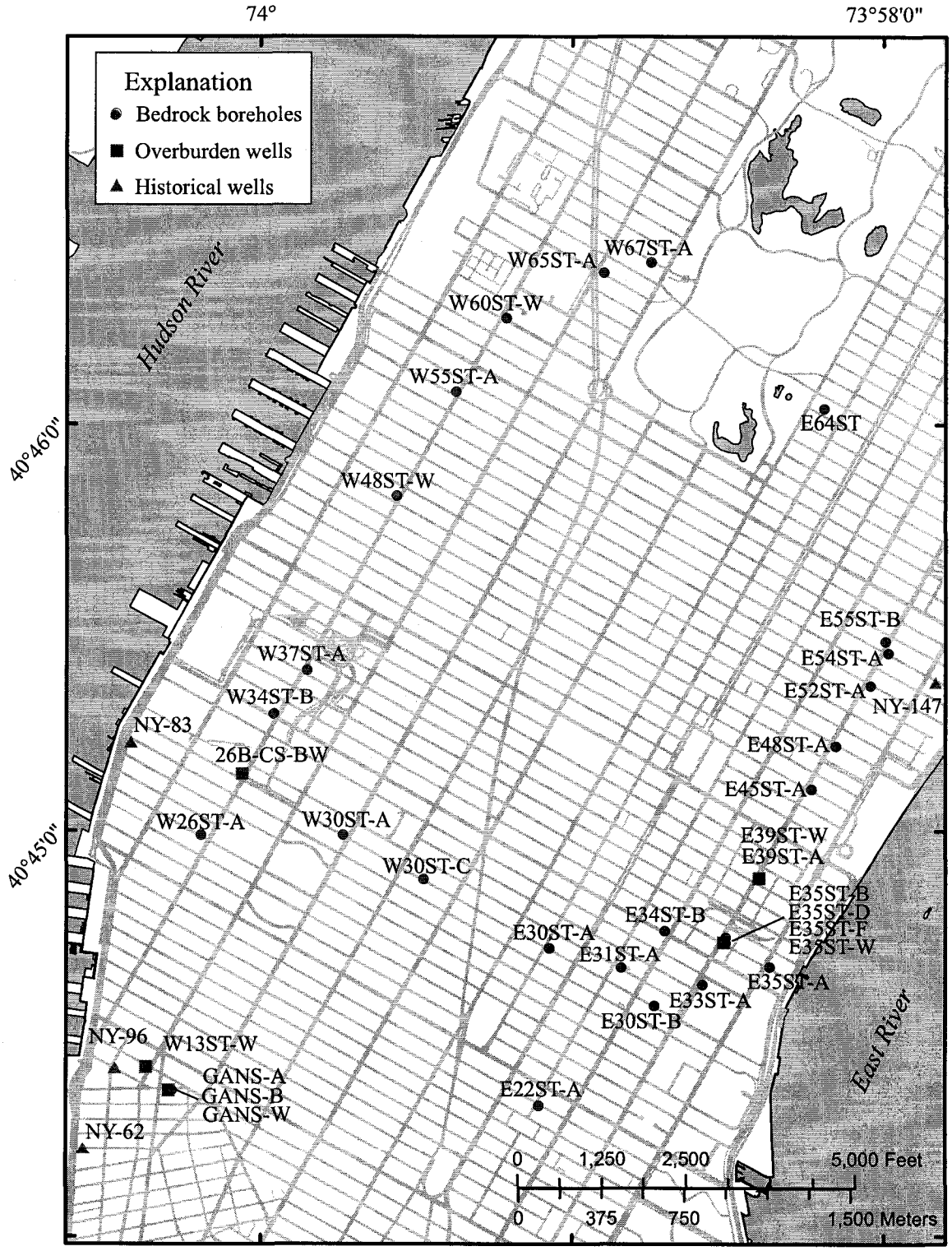

Figure 4. Locations of bedrock boreholes, overburden wells, and historical overburden wells within the northern detail area, Manhattan Island, N.Y. (Location shown in fig.1)

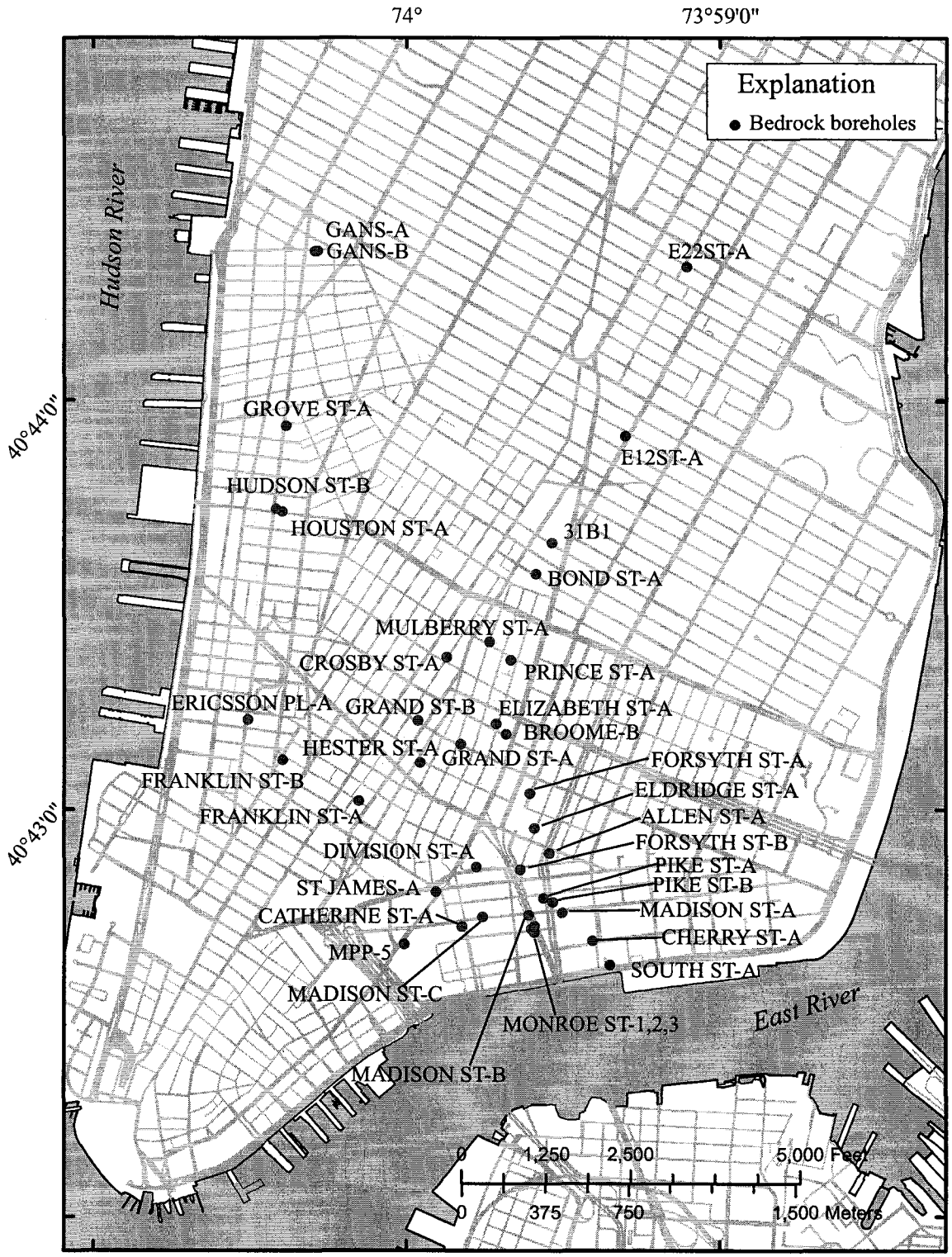

Figure 5. Locations of bedrock borholes within the southern detail area, Manhattan Island, N.Y. (Location shown in fig. 1)

Hydrogeologic unit	Borehole Name	New York State ID Number	Land Surface Elevation in feet	Bottom Depth of Borehole in feet	Casing length in feet
Fractured-Rock (Bedrock)	31B1	NY 185	44.19	653.68	60
	ALLEN ST-A	NY 201	42.26	600.00	226
	BOND ST-A	NY 202	47.37	604.00	92
	BROOME-B	NY 169	38.57	664.82	199
	CATHERINE ST-A	NY 186	19.25	624.00	160
	CHERRY ST-A	NY 190	12.99	600.00	136
	CROSBY ST-A	NY 232	33.47	578.00	125
	DIVISION ST-A	NY 203	42.32	604.30	136
	E12ST-A	NY 205	38.65	538.00	27
	E22ST-A	NY 241	26.68	600.10	42
	E30ST-A	NY 224	38.54	606.00	43
	E30ST-B	NY 226	37.93	595.00	45
	E31ST-A	NY 233	30.29	553.60	61
	E33ST-A	NY 223	22.66	550.20	34
	E34ST-B	NY 198	31.15	635.00	36
	E35ST-A	NY 180	10.50	447.70	14
	E35ST-B	NY 206	18.66	507.00	22
	E35ST-D	NY 207	19.51	599.00	25
	E35ST-F	NY 234	18.60	531.00	29
	E39ST-A	NY 208	35.98	490.50	35
	E45ST-A	NY 209	57.47	489.80	10
	E48ST-A	NY 210	26.89	490.00	105
	E52ST-A	NY 211	38.17	490.00	25
	E54ST-A	NY 212	38.71	490.00	25
	E55ST-B	NY 183	42.60	545.00	18
	E64ST	NY 204	0.00	1500.00	15
	ELDRIDGE ST-A	NY 189	43.54	600.41	232
	ELIZABETH ST-A	NY 178	37.88	600.00	103
	ERICSSON PL-A	NY 213	18.49	525.00	96
	FORSYTH ST-A	NY 175	40.31	600.00	165
	FORSYTH ST-B	NY 182	38.50	600.00	176

NA indicates that no data was available

Table 1. Data from 74 boreholes and wells drilled within the study area, Manhattan Island, N.Y (Part 1 of 2)

Hydrogeologic unit	Borehole Name	New York State ID Number	Land Surface Elevation in feet	Bottom Depth of Borehole in feet	Casing length in feet
Fractured-Rock (Bedrock)	GRAND ST-B	NY 216	25.61	547.40	112
	GROVE ST-A	NY 199	20.87	644.77	71
	HESTER ST-A	NY 229	19.08	NA	100
	HOUSTON ST-A	NY 184	16.57	663.84	NA
	HUDSON ST-B	NY 172	17.32	650.70	108
	MADISON ST-A	NY 196	28.91	NA	NA
	MADISON ST-B	NY 217	33.20	NA	NA
	MADISON ST-C	NY 218	24.99	NA	NA
	MONROE ST-1	NY 173	27.39	677.00	NA
	MONROE ST-2	NY 181	26.44	671.00	NA
	MONROE ST-3	NY 188	28.34	679.00	NA
	MPP-5	NY 179	19.36	644.85	NA
	MULBERRY ST-A	NY 231	42.07	570.00	115
	PIKE ST-A	NY 187	35.10	NA	NA
	PIKE ST-B	NY 174	33.00	NA	NA
	PRINCE ST-A	NY 192	46.87	665.00	120
	SOUTH ST-A	NY 177	6.25	598.00	228
	ST JAMES-A	NY 193	29.21	651.90	NA
	W26ST-A	NY 176	13.25	596.30	30
	W30ST-A	NY 227	31.45	600.00	40
	W30ST-C	NY 240	38.87	600.00	NA
	W34ST-B	NY 219	40.27	625.70	8
	W37ST-A	NY 220	41.32	651.41	15
	W48ST-W	NY246	41.32	31.50	NA
	W55ST-A	NY 221	39.41	650.68	150
	W60ST-W	NY 243	82.01	30.60	NA
	W65ST-A	NY 225	79.33	585.00	19
	W67ST-A	NY 222	82.95	570.75	76
glacial aquifer	26B-W	NY 239	18.86	NA	NA
	28B-2W	NY 248	17.82	100.00	NA
	29B-3W	NY 237	16.85	96.00	NA
	E35ST-C/W	NY 235	18.76	NA	NA
	E39ST-W	NY 242	35.98	NA	NA
	GANS-W	NY 236	19.48	82.50	NA
	GRAND ST-W	NY 244	25.63	66.63	NA
	MONROE ST-4	NY 194	28.57	214.22	NA
	PIKE-W	NY 238	35.10	NA	NA
	W13ST-W	NY 249	16.21	30.30	NA

NA indicates that no data was available

Table 1. Data from 74 boreholes and wells drilled within the study area, Manhattan Island, N.Y (Part 2 of 2)

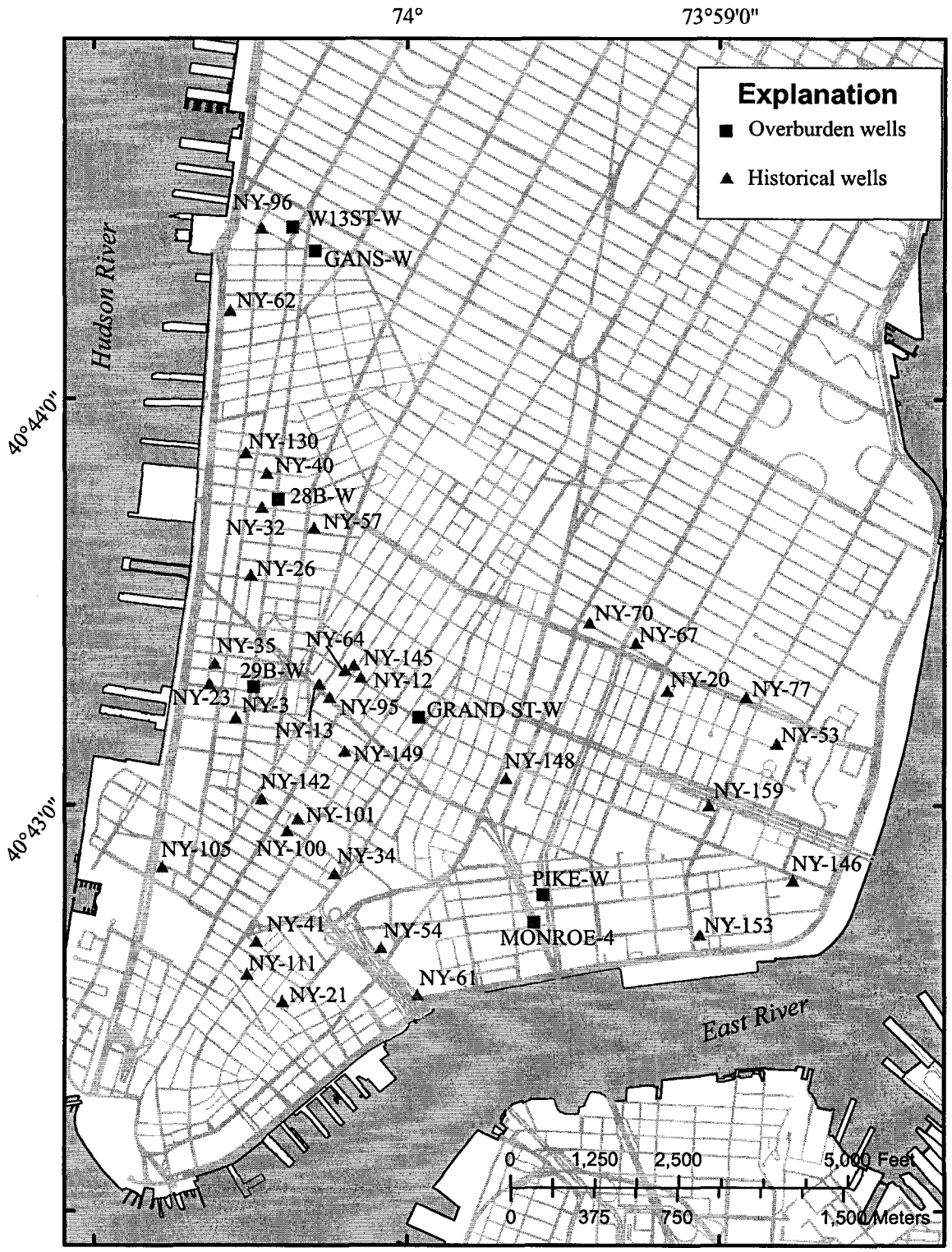

Figure 6. Locations of overburden wells, and historical overburden wells within the southern detail area, Manhattan Island, N.Y. (Location shown in fig.1)

susceptibility borehole-fluid temperature and resistivity, borehole specific conductance, dissolved oxygen (DO), pH, redox, heat-pulse flowmeter (at eight selected boreholes), borehole deviation, acoustic and optical televiewer, and directional borehole radar (at selected boreholes). The logging methods are briefly described below.

Natural-gamma (gamma) logs provide a record of the total gamma radiation detected in a borehole (Keys and McCary, 1971; Keys, 1990) and are most commonly used for litho logic and stratigraphic correlation. Radioisotopes in bedrock minerals such as feldspar and mica are instrumental in lithologic correlation (for example, pegmatite). Clay minerals within fractures may be detected as elevated gamma responses in comparison with those of surrounding rock. A Mount Sopris stratigraphic gamma probe was used in this study.

Single-point resistance (SPR) logs provide a measure of the electrical resistance of the rock or formation, in ohms, and are used to obtain qualitative lithologic information with a depth resolution approximately equal to borehole diameter (Keys and McCary, 1971; Keys, 1990). In some boreholes a Mount Sopris gamma/electric stratigraphic probe was used. Recently, a new combination resistivity/gamma/fluid probe was used from Mount Sopris.

Short-Normal resistivity (R) logs provide a measure of the apparent resistivity in ohm-meters and are used to determine lithology and water-quality (Keys, 1990). The volume of the surrounding material to which normal resistivity probes are sensitive is about twice the electrode spacing (Serra, 1984; Keys, 1990). In this study only 16-inch short-normal resistivity logs from the new Mount Sopris resistivity/gamma/fluid probe were used.

Caliper logs provide information on lithology and the location of major fractures or faults. Mechanical calipers use spring-loaded arms to profile the surface of the borehole wall. Acoustic calipers calculate the distance from the probe to the borehole wall from the traveltime of the acoustic signal emitted from an acoustic televiewer (ATV) to provide high-resolution, compass-oriented logs (Keys, 1990). The Mount Sopris 3-arm caliper was used for the mechanical caliper logs. The acoustic televiewer from either Century Geophysical or ALT Limited was used for the acoustic caliper logs.

Magnetic-susceptibility (MAG) logs provide a record of the variations in magnetic minerals within the surrounding rock. Magnetite is the most common magnetic mineral, and local variations in its abundance may indicate lithologic contacts (McNeill and others, 1996). A Geonics Limited EM-39S probe was used in this study.

Specific Conductance (SpC) logs measure the specific conductance of the fluid column as a function of depth and can provide information on the movement of ground water through the borehole and the location of zones that produce or accept water (Stumm and others, 2004). The SpC log was one parameter measured by an Ocean Seven Idronaut probe.

Dissolved Oxygen (DO) logs provide a qualitative measurement of the dissolved oxygen concentration of the fluid column as a function of depth and can indicate zones within the borehole that produce or accept water (Stumm and others, 2004). The DO log was one parameter measured by an Ocean Seven Idronaut probe.

pH logs provide a qualitative measurement of the relative changes in the pH of the fluid column as a function of depth and can identify zones that produce or accept water

(Stumm and others, 2004). The pH log was one parameter measured by an Ocean Seven Idronaut probe.

Redox logs provide a qualitative measurement of the reduction-oxidation potential of the fluid in the borehole as a function of depth and can indicate zones within the borehole that produce or accept water (Stumm and others, 2004). The Redox log was one parameter measured by an Ocean Seven Idronaut probe.

Temperature logs measure the temperature of the fluid column as a function of depth and can provide information on the movement of ground water through the borehole and the location of zones that produce or accept water (Keys and McCary, 1971; Keys, 1990). Borehole fluid resistivity logs provide a record of the capacity of the fluid to conduct electricity and provide an indication of salinity (Keys, 1990). Temperature logs were collected using Century Geophysical, Mount Sopris, and Idronaut probes.

Heat-pulse flowmeter logs measure vertical flow in boreholes and can indicate which fractures are producing or accepting water in a borehole under pumping and ambient conditions (Keys, 1990). Cross-borehole flowmeter tests can be used to identify connections between fractures (Paillet, 1998). The Mount Sopris heat-pulse flowmeter was used at most boreholes. The Century EM flowmeter was used at only two boreholes.

Acoustic televiewer (ATV) uses a rotating transducer that transmits and receives high-frequency acoustic pulses to produce an image of the intensity of acoustic energy reflection. The ATV provides high-resolution information on the location and strike and dip of fractures or faults within a borehole (Keys, 1990; Williams and Johnson, 2000; 2004). The Century Geophysical ATV probe was only used at three boreholes. ATV logs at a majority of boreholes were collected using the ALT Limited FAC-40 probe.

Borehole-deviation logs provide information on the borehole's angle and direction of deviation from vertical. All deep boreholes deviate from vertical; therefore, deviation logs must be obtained before three-dimensional information on fractures and faults is interpreted (Keys, 1990). After processing, the resulting log indicates the true depth of the borehole, its distance from vertical, and the direction or azimuth of deviation. The ATV probes provided the majority of deviation data.

Optical televiewer (OTV) digitally records a high-resolution optical scan of the borehole wall that can be used to produce a virtual core. The virtual core is oriented to allow for visualization of major faults and fractures as they are imaged within the borehole. Faults and fractures, both opened and sealed, can be viewed in three-dimensional orientations. This system also allows measurement of true strike-and-dip orientation and fracture spacing (Stumm and others, 2000; Williams and Johnson, 2000; 2004). The Raax Borehole Imaging system was used at all boreholes to collect OTV data.

Borehole radar uses a single-hole, 60-MHz directional radar unit (transmitter/receiver) that can detect fracture zones and other structural features at distances as much as 90 ft from the borehole in electrically resistive rocks. The data logs can be used to calculate the orientation of fractures (Singha and others, 2000). The Ramac 60-MHz directional radar system from the USGS Branch of Geophysics was used.

Geologic-Structure Analysis

Foliation, fractures, and faults penetrated in each borehole were delineated from the analysis of OTV and ATV geophysical log analysis. Fractures were classified as small, medium, large, or very large, depending on the apparent aperture or width of the

opening. Measured fracture apertures in the boreholes were considered apparent to account for alterations caused by the drilling process. Small fractures or microfractures have apparent apertures of 0.04 in. (1 mm) or less; medium fractures have apertures of greater than 0.04 to 0.39 in. (greater than 1 to 10 mm); large fractures have apertures greater than 0.39 to 9.8 in. (greater than 10 mm to 25 cm); and very large fractures have apertures greater than 9.8 in. (greater than 25 cm). Borehole-radar analysis was used to (1) verify the assumption that most fractures extend beyond the borehole, (2) detect major fractures or faults as far as 90 ft from the borehole that may not intersect any borehole in the area and would otherwise have been missed, and (3) delineate the orientation (strike and dip) of these distant fractures or faults.

Orientations of each fracture in each borehole were calculated from the ATV and OTV data through standard computer programs (Raax imaging software and WellCAD). Deviation from vertical and magnetic declination of each borehole are included in the final true orientation calculation from apparent orientations. The final, true-corrected orientations of fractures and foliations are listed as dip azimuth and dip angle (dip).

Planar structural features identified in the boreholes are shown as poles to planes on the lower hemispheres of equal area stereonets summarizing these features in each borehole, and as "tadpoles" on the geophysical log suites showing the distribution of these features with depth within each borehole. The "tadpoles" are circles with "tails" plotted with respect to a horizontal scale to indicate the degree of dip angle (inclination) of the structures from 0 to 90°. The tail of each tadpole points to the dip azimuth of the structure. Rockware Inc. stereoplot software was used to create the equal area stereonets. The "tadpole" plots were created with WellCAD software.

The potential tunnel-construction zone (PTCZ) is defined as a zone 100 ft above the bottom of a borehole. The PTCZ was not defined for E12ST-A, ForsythST-B, CatherineST-A, GansST-B, and SouthST-A, since these boreholes were not along any proposed tunnel excavation routes. In three boreholes, conditions including poor visibility, thick sediment on borehole walls, and high borehole-tilt angles, did not provide sufficient data within the PTCZ, so an additional 100 ft was added to the PTCZ at boreholes E30ST-A, Prince ST-A, and W67ST-A (Figs. 4 and 5). A partial collapse of the W67ST-A and W55ST-A boreholes prevented probes from logging the full extent of the open bedrock; therefore, these boreholes are undersampled (Fig. 4). High-angle large fractures above the PTCZ at each of the boreholes, if continuous, could intersect the PTCZ at a distance and therefore are considered to be critical features. For this reason, fracture analysis of the entire borehole is useful for detecting potential intersections with the tunnel away from the borehole. Fracture and foliation data within the PTCZ are useful only at the borehole location.

Foliation

Foliation in each borehole was measured using OTV data. Analysis of the variations in foliation orientations in each borehole and within the study area included tadpole and stereonet plots. A mean foliation orientation was included for the total borehole and the PTCZ.

Fractures

Fracture analysis identifies populations with similar dip azimuths and dip angles. Analysis of the variations in fracture orientations in each borehole and within the study area included tadpole and stereonet plots. A mean fracture orientation was included for the total borehole and the PTCZ, unless multiple fracture populations were detected. Gouge-zones are defined as highly altered or weathered rock zones indicative of either mechanical or chemical weathering or weakening of the bedrock. Gouge-zones which may be large scale faults or highly weathered fracture zones are typically found in the OTV log data and analyzed as fractures in the particular borehole's stereonet analysis.

RQD is a percentage value obtained by dividing the summed lengths of all core pieces equal to or greater than 4 in. long by the cored interval length. The higher the RQD value the lower the number of fractures and the greater the integrity of the bedrock sampled.

Faults

OTV logs were carefully examined for evidence of offset or past movement along a fracture. A fracture is classified as a fault if there is evidence of offset or past movement along it. However, all faults were plotted as fractures "tadpoles" in the geophysical log suite and in the stereonets for a given borehole. Faults were analyzed as a separate group in the structural section of this study.

Ground-Water-Flow Analysis

Fluid-temperature and fluid-specific conductance logs were collected at 31 boreholes during ambient conditions. Flowmeter logs were collected at 8 boreholes (31B-1, W55ST-A, W37ST-A, W34ST-B, W26ST-A, GroveST-A, HudsonST-B, and PrinceST-A) during ambient and pumping conditions (Figs. 4 and 5). Measurements of the drawdown, pumping rate, and total pumping time at 59 bedrock boreholes during specific-capacity pumping tests were applied to a computer program (Bradbury and Rothschild, 1985) to calculate specific capacity and transmissivity of the entire borehole. Similar specific-capacity testing and analysis was completed at the 10 overburden wells (Table 1).

A new geophysical probe called the "QW log" included fluid-temperature, fluid specific conductance (SpC), DO, pH, and redox logs, which were used to help delineate transmissive fractures within the boreholes (Stumm and others, 2004). The conventional fluid temperature and resistivity logs do not always provide information on transmissive fracture locations. Abnormal temperature gradients can be caused by ground-water flow into or out of fractures intersected by the boreholes (Keys, 1990; Williams and Conger, 1990). Changes in water quality also may occur at transmissive fractures and by expanding the measurement parameters, changes in SpC, pH, DO and redox can be detected and more transmissive fractures can be delineated.

The geophysical and hydrologic methods discussed above were applied to a network of 64 bedrock boreholes in southern Manhattan (Figs. 4 and 5). Flowmeter and borehole radar logs were collected at selected boreholes. Faults, fractures, and foliation were interpreted from OTV, ATV, borehole-radar, gamma, SPR, R, MAG and caliper

logs, which are reproduced in the individual borehole summaries that follow in Chapter 2. Anomalies in the gamma log correlating to fractures or lithologic changes are mentioned in the borehole geophysical log description in Chapter 2. SPR and R log responses are variable with depth and correlate to either fracture density or slight lithologic or mineralogical changes in the bedrock. OTV analysis (borehole depth, fracture orientation, and foliation orientation) for all fractures, faults, and foliation in all 31 boreholes. The remaining 33 bedrock boreholes and 10 overburden wells had either specific capacity test, ground-water grab samples, or ground-water level data collected. In some cases all three types of data were collected at a bedrock borehole or overburden well.

Precipitation

Mean annual precipitation measured at Central Park in Manhattan, was 44.63 in. during 1869-2004 (Fig. 7) (NOAA, 2005). During the study period of 1998 through 2004 most precipitation was either slight below or slightly above average, except in 2001, 2003, and 2004. 2001 had below average precipitation with an annual total of 35.92 in.. Both years 2003 and 2004 had above average precipitation totals of 58.56 in. and 51.97 in., respectively.

Ground-Water Levels

Ground-water levels were measured during borehole geophysical logging, water-level synoptics, or specific-capacity tests at all 74 wells (64 bedrock and 10 overburden wells) (Table 2). Water level synoptics of all boreholes were conducted quarterly from

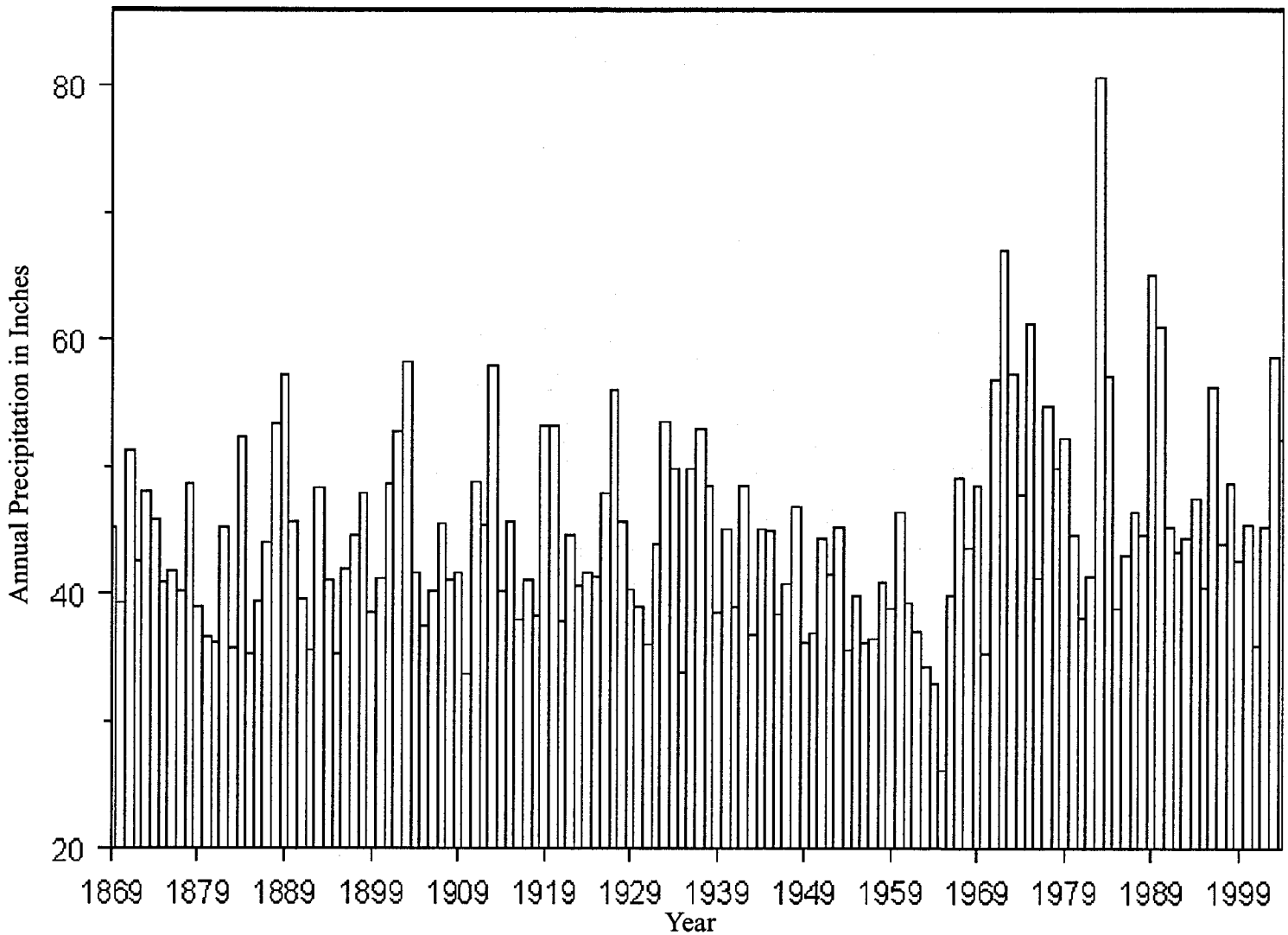

Figure 7. Annual precipitation measured at Central Park from 1869 to 2004, Manhattan, N.Y. (Data from NOAA, 2005).

Hydrogeologic unit	Borehole Name	Water level in feet above mean sea level	Chloride in milligrams per liter	Transmissivity feet squared per day	Stereonet Fracture mean	Stereonet Foliation mean
Fractured-Rock (Bedrock)	31B1	5.42	NA	32	northwest dip	northwest dip
	ALLEN ST-A	2.65	16600	259	NA	NA
	BOND ST-A	5.25	93	3	multiple populations	northwest dip
	BROOME-B	5.67	28	30	NA	NA
	CATHERINE ST-A	0.8	15900	19	624.00	north dip
	CHERRY ST-A	1.54	17600	871	NA	NA
	CROSBY ST-A	2.44	83	341	NA	NA
	DIVISION ST-A	1.61	11500	249	NA	NA
	E12ST-A	17.8	NA	NA	538.00	northwest dip
	E22ST-A	11.19	315	91	NA	NA
	E30ST-A	-2.56	339	31	subhorizontal	northwest dip
	E30ST-B	-42.80	137	131	multiple populations	northwest dip
	E31ST-A	-27.38	32	4	NA	NA
	E33ST-A	-22.10	599	2	multiple populations	northwest dip
	E34ST-B	-15.04	309	4	NA	NA
	E35ST-A	0.8	3470	247	NA	NA
	E35ST-B	-4.81	1130	283	NA	NA
	E35ST-D	-3.84	749	459	multiple populations	west dip
	E35ST-F	-4.76	1550	316	NA	NA
	E39ST-A	10.13	1270	9	multiple populations	northwest dip
	E45ST-A	21.14	184	53	multiple populations	northwest dip
	E48ST-A	12.26	123	11	multiple populations	northwest dip
	E52ST-A	20.69	45	74	multiple populations	northwest dip
	E54ST-A	13.25	423	61	multiple populations	subhorizontal
	E55ST-B	10.75	497	14	multiple populations	subhorizontal

NA indicates that no data was available

Shaded cells indicate an average of historical water levels, all other water levels were measured November 2004.

Table 2. Data from 74 boreholes and wells drilled within the study area, Manhattan Island, N.Y (Part 1 of 3)

Hydrogeologic unit	Borehole Name	Water level in feet above mean sea level	Chloride in milligrams per liter	Transmissivity feet squared per day	Stereonet Fracture mean	Streonet Foliation mean
Fractured-Rock (Bedrock)	E64ST	50.00	NA	NA	NA	NA
	ELDRIDGE ST-A	3.38	15400	189	NA	NA
	ELIZABETH ST-A	4.24	20	32	NA	NA
	ERICSSON PL-A	-0.47	7050	19	multiple populations	southwest dip
	FORSYTH ST-A	3.17	NA	NA	NA	NA
	FORSYTH ST-B	1.27	10450	202	multiple populations	northwest dip
	GRAND ST-B	1.20	132	42	subhorizontal	west dip
	GROVE ST-A	0.4	25	2	multiple populations	northwest dip
	HESTER ST-A	1.11	210	219	NA	NA
	HOUSTON ST-A	-0.88	1200	77	NA	NA
	HUDSON ST-B	-0.90	NA	1	multiple populations	northwest dip
	MADISON ST-A	0.76	14900	58	NA	NA
	MADISON ST-B	1.38	14950	36	NA	NA
	MADISON ST-C	1.35	13000	3	NA	NA
	MONROE ST-1	0.35	16100	32	NA	NA
	MONROE ST-2	0.81	18300	216	NA	NA
	MONROE ST-3	1.42	NA	NA	NA	NA
	MPP-5	-0.19	17400	83	NA	NA
	MULBERRY ST-A	3.56	98	12	NA	NA

NA indicates that no data was available

Shaded cells indicate an average of historical water levels, all other water levels were measured November 2004.

Table 2. Data from 64 boreholes drilled within the study area, Manhattan Island, N.Y (Part 2 of 3)

Hydrogeologic unit	Borehole Name	Water level in feet above mean sea level	Chloride in milligrams per liter	Transmissivity feet squared per day	Stereonet Fracture mean	Stereonet Foliation mean
Fractured-Rock (Bedrock)	PIKE ST-A	1.45	17700	51	NA	NA
	PIKE ST-B	0.99	12250	461	NA	NA
	PRINCE ST-A	4.52	143	109	multiple populations	northwest dip
	SOUTH ST-A	4.39	17800	86	subhorizontal	multiple populations
	ST JAMES-A	0.51	12950	47	NA	NA
	W26ST-A	4.9	2420	35	west dip	northwest dip
	W30ST-A	9.16	195	37	subhorizontal	subhorizontal
	W30ST-C	9.42	820	71	NA	NA
	W34ST-B	10.5	NA	75	northwest dip	southwest dip
	W37ST-A	13.5	NA	360	multiple populations	northwest dip
	W48ST-W	27.19	1940	1	NA	NA
	W55ST-A	29.1	933	11	multiple populations	northwest dip
	W60ST-W	71.60	203	4	NA	NA
	W65ST-A	46.15	NA	NA	subhorizontal	multiple populations
	W67ST-A	64.69	194	25	multiple populations	northwest dip
glacial aquifer	26B-W	3.80	641	359	NA	NA
	28B-2W	-0.34	240	93300	NA	NA
	29B-3W	-0.14	1080	1970	NA	NA
	E35ST-C/W	2.72	1440	2	NA	NA
	E39ST-W	14.70	405	5	NA	NA
	GANS-W	0.91	672	4495	NA	NA
	GRAND ST-W	1.00	331	8228	NA	NA
	MONROE ST-4	NA	15250	648	NA	NA
	PIKE-W	8.65	23	11514	NA	NA
	W13ST-W	0.82	560	4726	NA	NA

NA indicates that no data was available

Shaded cells indicate an average of historical water levels, all other water levels were measured November 2004.

Table 2. Data from 74 boreholes and wells drilled within the study area, Manhattan Island, N.Y (Part 3 of 3)

November 1998 through November 2004. Digital water-level recorders were installed at 13 different fractured-rock boreholes within the study at various lengths of time from October 2003 through February 2005.

Transmissivity

Variations in fracture aperture impact transmissivity at all scales (Caine and others, 2000). The discharge of ground-water is proportional to the fracture width raised to a power of 3 (Freeze and Cherry, 1979). Determination of the aperture of fractures and their 3D orientation is important in assessing the hydraulic characteristics of a fractured-rock ground-water flow system.

The flowmeter logs were analyzed through techniques of Paillet (1998, 2000), whereby differences between flow values at adjacent fracture zones within each borehole were attributed to measurement scatter and a possible net difference in borehole flow. Therefore, flow-log interpretation involves identification of the relative amounts of inflow or outflow occurring at specific depth intervals. Inflow or outflow at several depth intervals at each borehole is measured; each of these intervals coincides with a fracture, or sets of fractures. In accordance with the techniques of Molz and others (1989) and Paillet (2000), the effects of hydraulic-head differences between zones can be eliminated by analyzing flow under ambient and pumping conditions.

Chloride Concentrations

Ground-water grab samples were collected at bedrock boreholes and overburden wells during specific-capacity testing. Typically pumping lasted from 2 to 3 hours.

Water quality parameters such as temperature, pH, and specific conductance were monitored during the specific capacity tests. At the conclusion of the specific-capacity test a ground-water grab sample was obtained. Typically the field water quality parameter data indicate equilibrium was achieved and a generally representative sample obtained.

A chloride ion probe was used to measure the concentration of chloride in the ground-water grab samples. The probe was calibrated using various solutions with laboratory standard concentrations of chloride. Once calibrated the samples were measured and the resulting chloride concentrations recorded. Several boreholes had laboratory analyses of chloride concentrations which were within the accuracy of the chloride probe +/- 10 percent.

2. Fractured-Rock Ground-Water Flow System

A total of 64 bedrock boreholes were drilled within the study area. Of these only 31 bedrock boreholes have had extensive borehole geophysical logging and analysis completed. The geophysical logs and stereonets at 26 of the 31 boreholes have been recently published (Stumm and Chowdhury, 2003, Stumm and others 2001; 2004).

For this dissertation 15 of 31 boreholes were selected based upon the number and types of geophysical probes used, location within the study area, and type of bedrock encountered. The geophysical logs are presented as a suite of logs to emphasize either the physical properties or the fluid properties and hydrology of the bedrock in Appendices 1 through 11. In addition, the fractures and foliation detected with the OTV and or ATV probes are plotted as equal area stereonets also in Appendices 1 through 11. Four boreholes (W34ST-B, E48ST-A, GroveST-A, and PrinceST-A) are presented in this chapter with full geophysical, structural, and hydrologic interpretations as an example of what had been completed at all 31 boreholes. Table 2 lists the hydrologic and structural data of all bedrock boreholes tested.

Structural data on the true strike and dip of fractures, faults, and foliation were measured using advanced borehole geophysical logs. The OTV was used most often and the ATV was sometimes used for quality control and verification of the OTV fracture data and borehole deviation measurements. Bedrock lithologic changes were measured using the Gamma, SPR, R, and MAG logs. Transmissive fractures were sometimes delineated using the gamma and electric logs when conductive clay was associated with the ground-water flow within the fracture. The gamma log was very useful in determining the sediment overburden composition if cores were not available and for

some changes in bedrock lithology such as pegmatite. The electric logs (SPR and R) measured the bedrock resistance and resistivity and indicated a general increase in resistivity of bedrock with increasing depth. This was thought to be due to the regional effect of weathering on the bedrock. This increase in rock resistivity could also be seen in the 60 MHz borehole radar logs as a decrease in attenuation with depth. The MAG log was the most sensitive to changes in lithology due to the variation in the magnetite content common in the bedrock within the study area. Fluid parameter logs such as fluid temperature and fluid resistivity are common logs useful in the delineation of ground-water inflow or outflow in a borehole. However, heat-pulse flowmeter logging of these boreholes revealed the standard fluid parameter logs were sometimes not able to detect moderately to small transmissive zones. One possibility could be the similarity in fluid temperature and fluid resistivity of some fracture ground-water with those of the borehole water column they are in contact with. A new fluid probe the QW log includes fluid temperature, specific conductance, pH, redox, and dissolved oxygen (DO). This new probe produces far superior fluid parameter logs and appears to detect much smaller transmissive fracture zones then the simple fluid-temperature/resistivity logs.

The ATV, OTV, and borehole-radar analysis indicate that all boreholes penetrate moderately fractured rock that contains highly fractured zones. Every borehole contains medium and (or) large open fractures that are transmissive. Structural trends of these geologic deposits and borehole radar logs indicate that most fractures and faults detected in each borehole may extend beyond each borehole. The gamma, SPR, R, fluid-temperature, fluid resistivity, specific conductance, DO, pH, and redox logs detected some of the fracture zones.

Geophysical and Hydrological Analyses

The borehole summaries that follow 1) interpret results of the fault-, fracture-, and foliation-data analysis and describe the ground-water-flow zones for the boreholes; 2) present gamma, SPR, EM, MAG, and caliper logs with tadpole plots of the foliation and fractures from OTV analysis for each borehole geophysically logged; and 3) present stereonet plots of total borehole and PTCZ fractures and foliation (where applicable). These analyses are representative what has been done at all 31 geophysically logged bedrock boreholes in the study area.

W34ST-B

The W34ST-B borehole was selected as an example of a moderately transmissive borehole where heat-pulse flowmeter logging was used to delineate a very large fracture zone. The borehole was drilled to a depth of 625.7 ft BLS (-585.43 ft elevation), with steel casing extending from land surface (40.27 ft elevation) to 8.0 ft BLS (32.27 ft elevation) in the unconsolidated deposits (overburden). The bedrock penetrated by the borehole consists of a sequence of gneiss and schistose gneiss with granite.

Faults, Fractures, and Foliation

The ATV and OTV data indicate a total of 271 small, medium, and large fractures from below the casing to the bottom of the borehole (Fig. 8). Large open fractures were detected at 16, 25, 31, 60, 90, 289, 292, 299, 300, 329, 330 and 332 ft BLS. In addition, four very large open fractures represent a possible fault-gouge zone from 328 to 330 ft BLS (Fig. 8). This gouge zone is highly fractured and has a horizontal diameter of

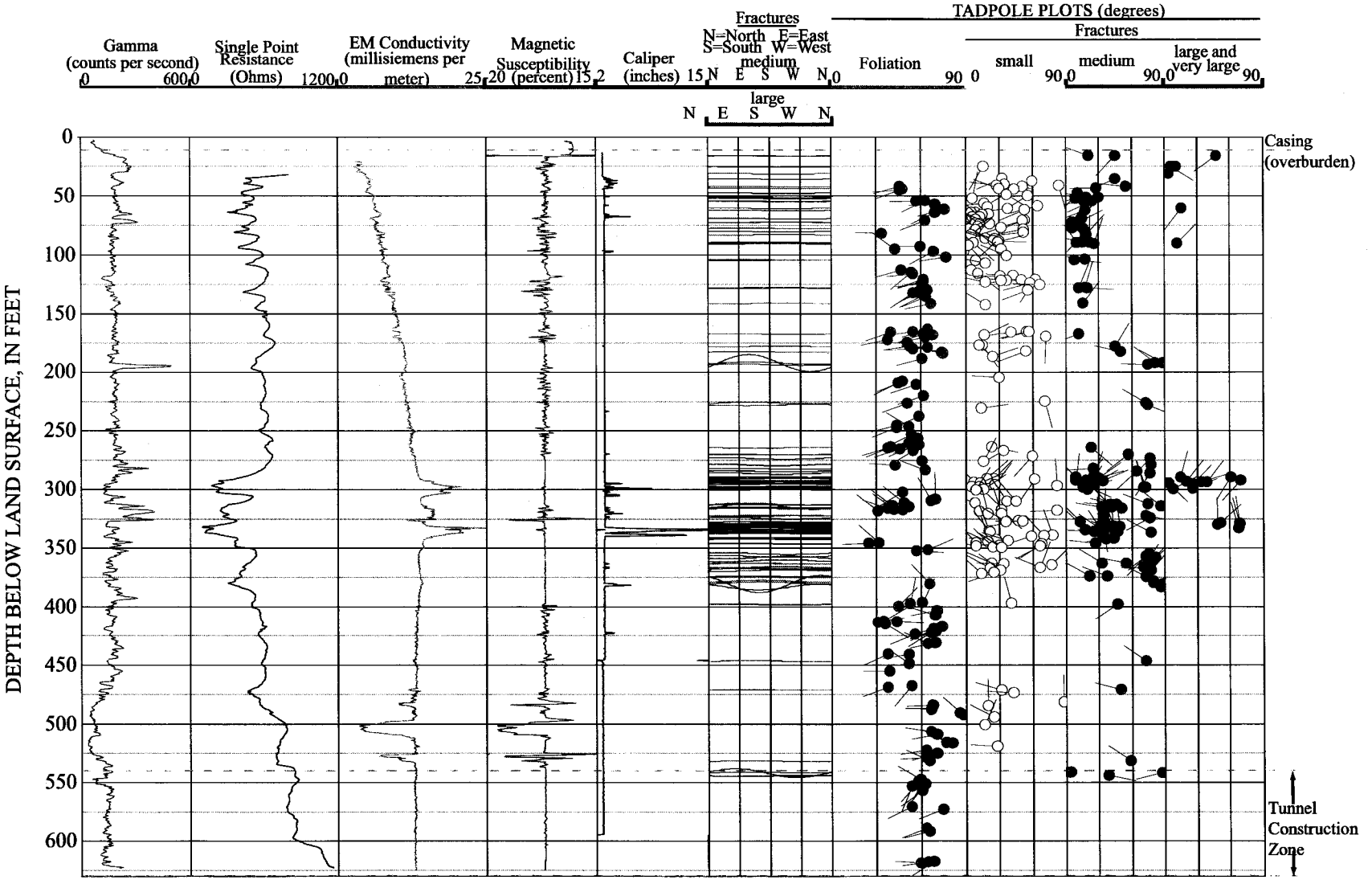

Figure 8. Suite of borehole-geophysical logs from borehole W34ST-B, Manhattan Island, N.Y.

almost 30 in. The tadpole plots of fractures (Fig. 8) indicate a high fracture density at depths from 30 to 125 ft BLS (10.27 to -84.73 ft elevation) and from 275 to 375 ft BLS. The majority of small and large fractures have dip angles less than 45°. No clear pattern of dip azimuth orientations with respect to depth is evident from in the tadpole plots of fractures. The mean fracture orientation for the 271 fractures is N20°E, 17°NW (Fig. 9). About 12 high- angle fractures with dip angles greater than 70° were encountered throughout the length of the borehole. Fractures within the PTCZ, which extends from 540 ft BLS to the bottom of the borehole (Fig. 9), were analyzed. All fractures from 370 ft BLS to the bottom of the borehole were included to provide a statistically significant sample. In all, 24 fractures were detected, 14 of which are medium size. The mean fracture orientation for the PTCZ is N34°E, 39°NW (Fig. 9).

The tadpole plots of foliation (Fig. 8) indicate correlations between foliation, azimuth, dip angle, and depth. The foliation dip azimuth in most of the borehole is southwestward, except in a zone from 350 to 420 ft BLS, where it is northeastward. The foliation dip angle increases slightly with depth. The mean orientation of foliation for the entire borehole is N09°W, 57°SW (Fig. 9). The PTCZ foliation was analyzed from 50 ft above the projected tunnel ceiling (invert) to the bottom of the borehole. The mean PTCZ foliation is N09°W, 65°SW (Fig. 9).

The gamma-log analysis (Fig. 8) indicates fairly uniform gamma counts in the bedrock, except for a few spikes that reflect possible changes in mineralogy. The SPR log (Fig. 8) has conductive spikes at locations that correlate with large fractures; the spikes may indicate chemically weathered zones (clays) and also ground-water in some fractures. The SPR and EM log data indicate the upper 300 ft of the rock to be more

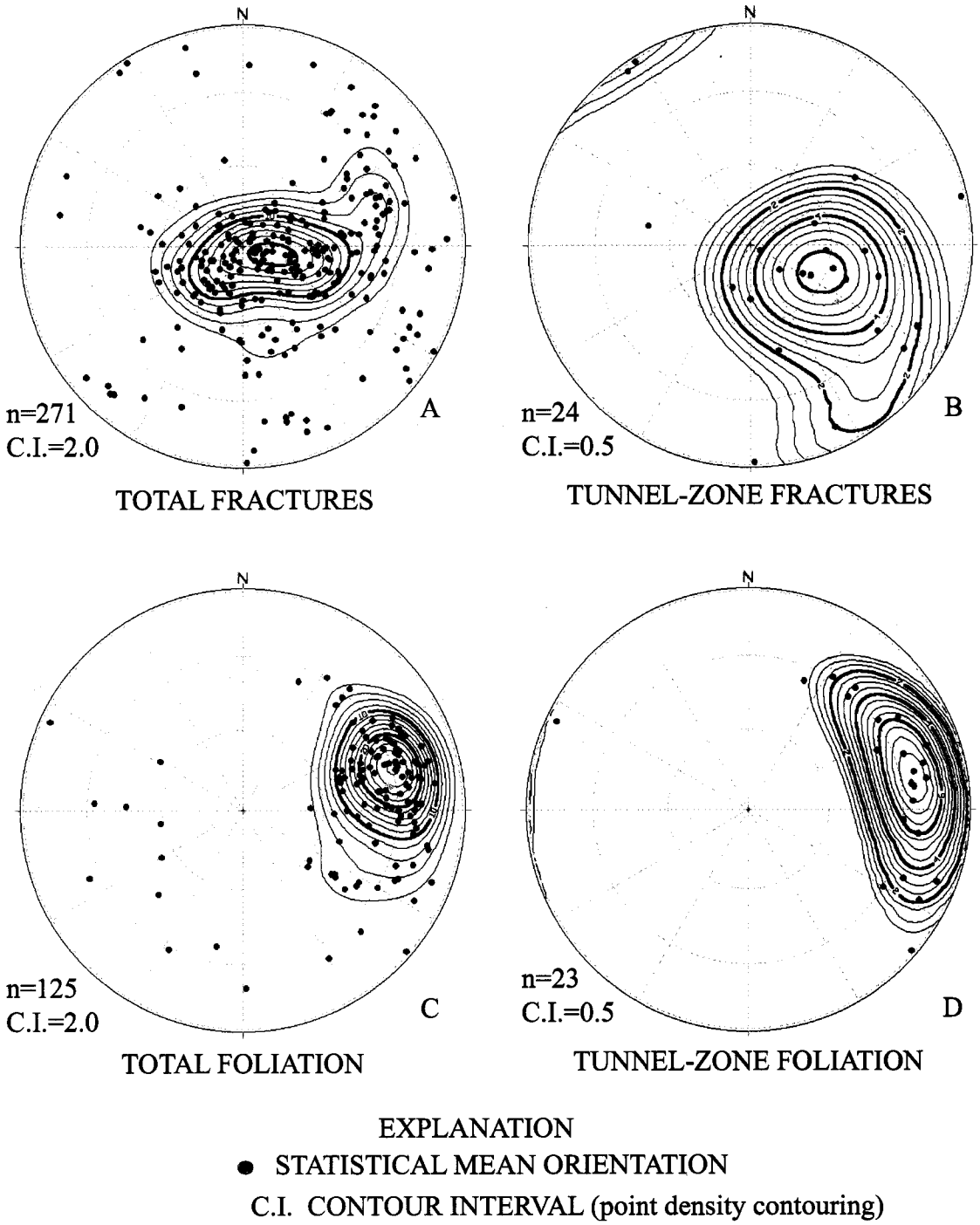

Figure 9. Stereonet plots of borehole W34ST-B, Manhattan Island, N.Y.,: A. Total fractures. B. Tunnel-zone fractures. C. Total foliation. D. Tunnel-zone foliation.

conductive than the rest. Two zones at 290 to 300 ft BLS and 328 to 335 ft BLS have the lowest resistance and the highest EM conductivity in the borehole (Fig. 8) and correlate with two highly fractured transmissive zones. The magnetic-susceptibility log (Fig. 8) shows areas of low response that correlate with granitic zones or other areas containing low concentrations of magnetite. The lowest 85 ft of the borehole is mostly granitic. Borehole radar data indicate six reflectors (possibly fractures) beyond the borehole, with orientations of N156°E, 85°NE; N143°W, 80°SE; N77°E, 53°NW; N77°E 54°NW; N23°W, 75°SW; and N23°W, 88°SW.

Ground-Water Flow Zones

The average hydraulic head at W34ST-B was 10.5 ft elevation. Water-level fluctuations of about 4 ft during successive field visits over 2 months indicate a possible tidal (Hudson River), pumping, or natural recharge effect.

EM-flowmeter, fluid-temperature, fluid-resistance logs from borehole W34ST-B (Fig. 10) indicate several depth intervals at which a deflection or change in slope corresponds to transmissive fractures. Slope changes in these logs are seen at 72, 299, 328 to 330, 355 to 363, and 470 ft BLS (-31.73, -258.73, - 287.73 to -289.73, -314.73 to -322.73, and -429.73 ft elevation, Fig. 10). OTV images of two medium fractures at 72 ft BLS (-31.73 ft elevation) show mineral streaking that suggests ground-water outflow. Small deflections in the fluid-temperature and resistance logs are seen at 72 ft BLS (-31.73 ft elevation, Fig. 10).

Pumping the borehole at a rate of 3 gal/min for 2.88 h produced a drawdown of 11.2 ft, or a specific capacity of 0.27 (gal/min)/ft. Total borehole transmissivity was

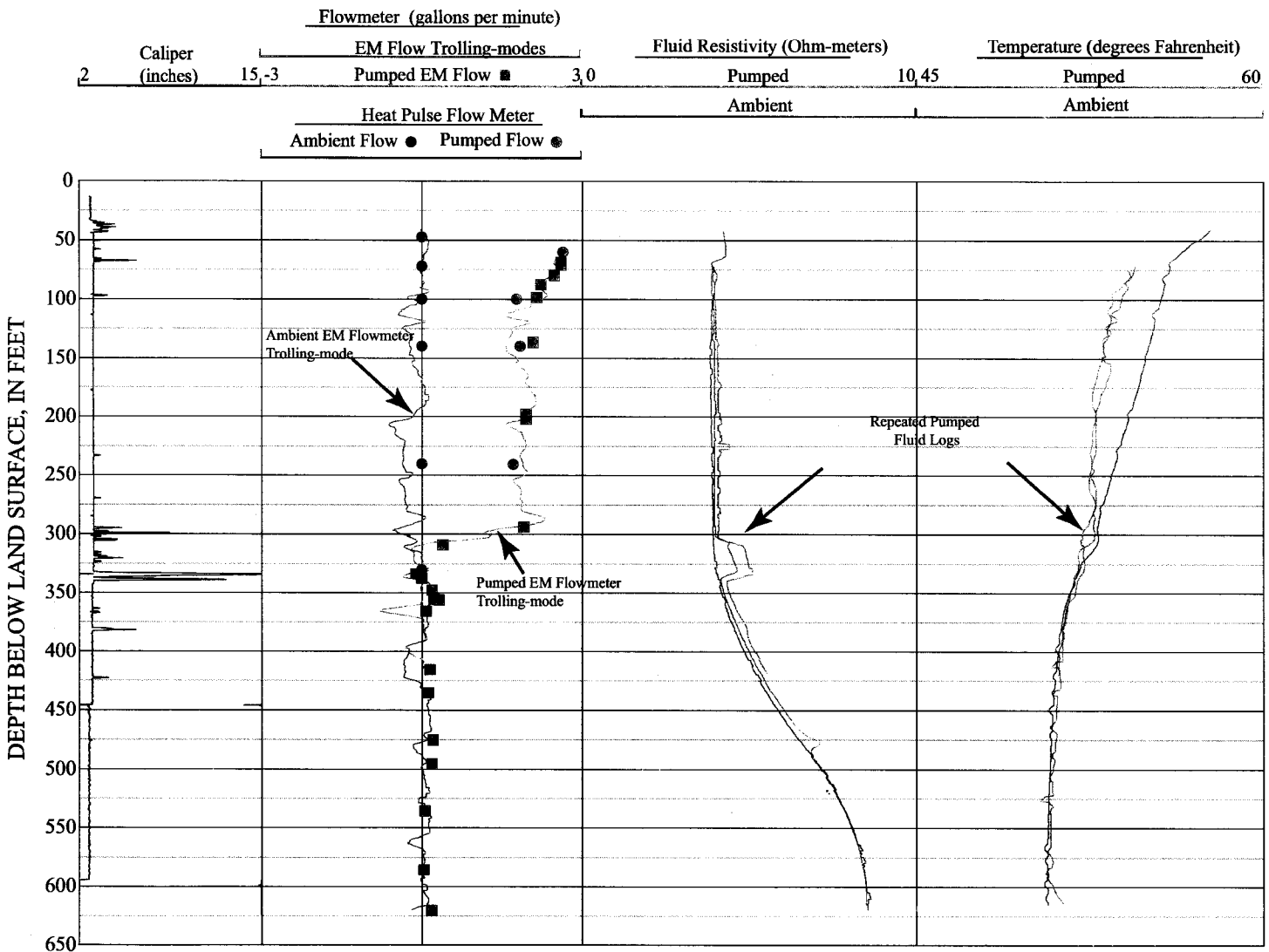

Figure 10. Suite of borehole-geophysical fluid logs from borehole W34ST-B, Manhattan Island, N.Y.

calculated to be 75 ft²/d. EM flowmeter, fluid-temperature, and fluid-resistance logging detected five separate transmissive fracture zones within the borehole at 72, 299, 328 to 330, 355 to 363, and 470 ft BLS (Fig. 10). Although somewhat ambiguous, the analysis of ambient ground-water conditions indicates a small amount of downflow between the 72-ft and 328 to 330 ft BLS fracture zones. Under pumping conditions, 75 percent of the borehole's transmissivity corresponds to the 299-ft BLS zone, and 25 percent to the 72-ft BLS zone. Fluid-log analysis of ambient and pumping conditions also indicates upward ambient flow from the 299-ft BLS zone to the 72-ft BLS zone, and downward flow from the 300-ft BLS zone to the 328- to 330-ft BLS zone. Transmissivity values for the 72-ft and 299-ft BLS fracture zones were 19 and 56 ft²/d, respectively.

If intersected, the 328- to 330-ft BLS fracture zone may result in appreciable quantities of ground water to flow into the tunnel because of high transmissivity and large open fractures. This zone had a reported low RQD during drilling (NYCDEP, oral commun., 1998). Trigonometric analysis of the dip angles and azimuths of the three largest fractures within this zone indicate that all have a northeastward dip that may intersect the proposed tunnel within about 220 ft northeast of borehole W34ST-B. The projection of these high-angle features is speculative but is consistent with the absence of such a major feature at borehole W37ST-A, 875 ft to the northeast. No ground-water grab sample was collected.

E48ST–A

The E48ST-A borehole was selected as an example of a borehole where the heat-pulse flowmeter was not used. However, potentially transmissive fractures were

delineated using the new QW probe. The borehole has 105 ft of casing and extends 490 ft BLS (-463. 1 ft elevation). The borehole is uncased in fractured bedrock which was described as a garnetiferous-hornblende-schistose gneiss with pegmatite.

Fractures and Foliation

OTV and ATV logs detected a total of 308 fractures. Most fractures were small some were medium, and one was large. One fault is detected at 157 ft BLS. Analysis of the borehole radar data indicate that most medium and large fractures extend at least 90 ft away from the borehole. The borehole radar also imaged a possible large fracture or fault that would have been intersected by the borehole had it been drilled to 553 ft BLS. This radar reflector has an orientation of N10°W, 49°NE. Total borehole and PTCZ mean fracture orientations were N11°E, 34°NW and N61°E, 49°NW, respectively (Fig. 11). Total borehole and PTCZ mean foliation orientations were N13°E 03°NW and N16°E, 28°NW, respectively (Fig. 11).

The gamma log was fairly uniform throughout the borehole except when pegmatite was encountered (Fig. 12). The SPR and R logs indicate a large increase in bedrock resistivity from 340 to 420 ft BLS that reflects a lithologic change from gneiss and schist to pegmatite (Fig. 12).

Ground-Water-Flow Zones

Hydraulic head in E48ST-A borehole was 12.26 ft elevation. The fluid parameter logs indicated possible transmissive fractures at 110, 160, 285, 300, and 480 ft BLS, where deflections or slope changes were observed (Fig. 13). The major deflections

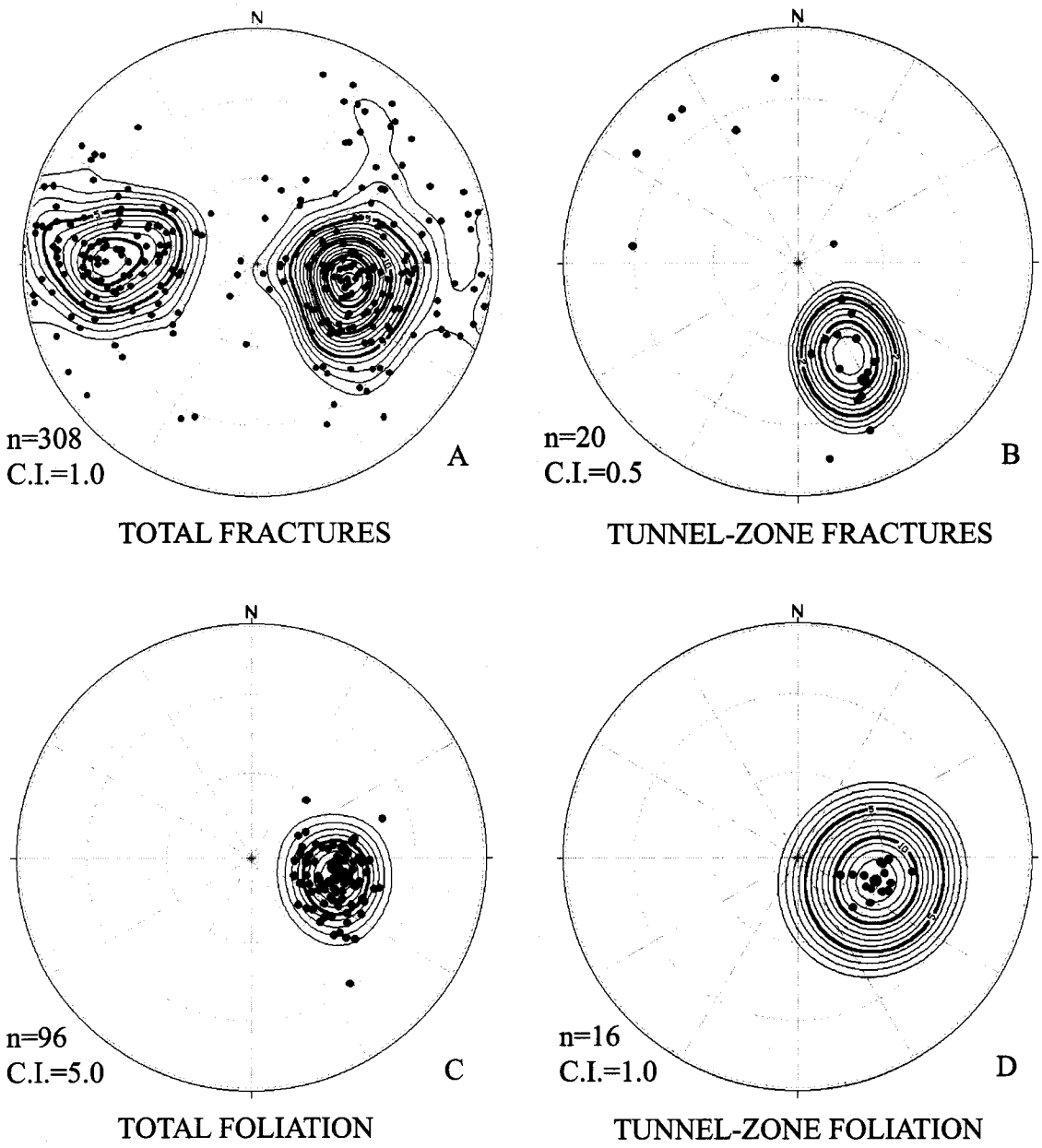

Figure 11. Stereonet plots of borehole E48ST-A, Manhattan Island, N.Y.,: A. Total fractures. B. Tunnel-zone fractures. C. Total foliation. D. Tunnel-zone foliation.

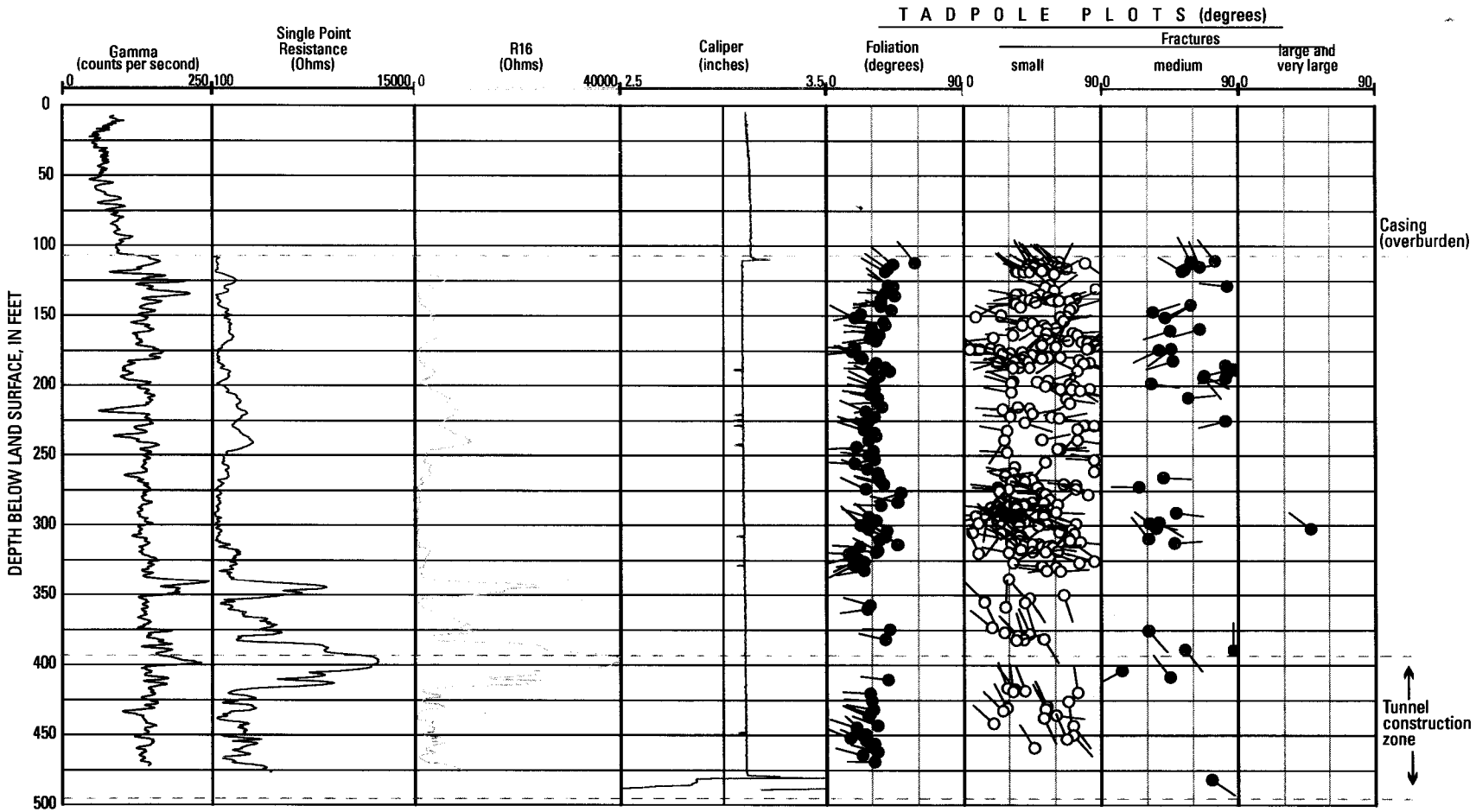

Figure 12. Suite of borehole-geophysical logs from borehole E48ST-A, Manhattan Island, N.Y.

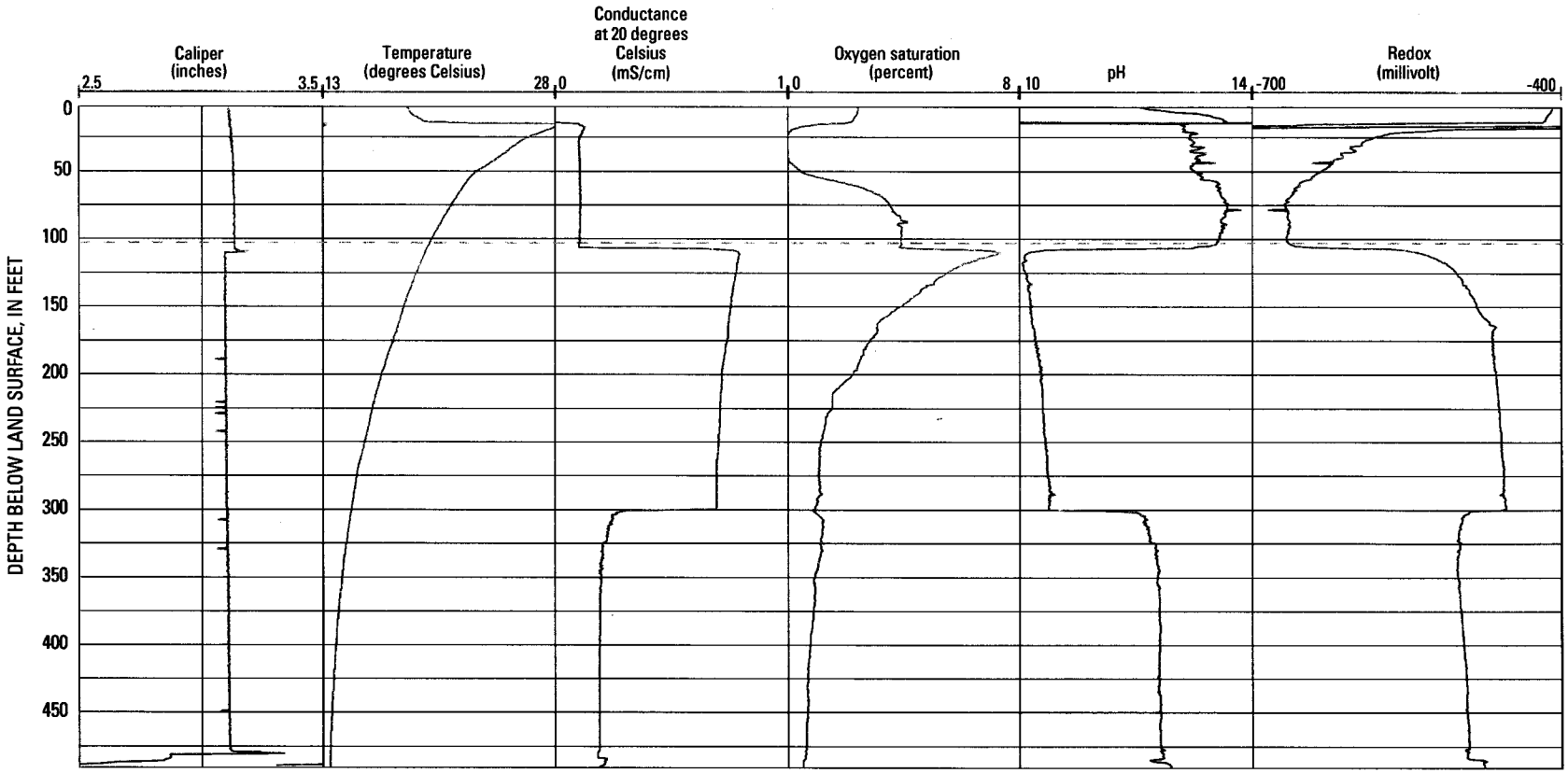

Figure 13. Suite of borehole-geophysical fluid logs from borehole E48ST-A, Manhattan Island, N.Y.

indicated at 110 and 300 ft BLS in the SpC, DO, pH, and Redox logs suggests these two fracture zones are the dominant transmissive fractures in the borehole. The 110 ft BLS and the 300 ft BLS zones correlate to medium and large fractures, respectively (Fig. 13). Analysis of the specific-capacity test data indicated the E48ST-A borehole has a specific capacity of 0.04 (gal/min)/ft and a transmissivity of 11 ft^2/d. The ground-water grab sample obtained during specific capacity testing had a chloride concentration of 123 mg/L.

GroveST-A

The GroveST-A borehole was selected as an example of a borehole with very low transmissivity. The low transmissivity of the fractures illustrates the usefulness of the heat-pulse flowmeter in detecting low range transmissive fractures. The borehole has 71 ft of casing and extends 645 ft BLS (-623.9 ft elevation). The GroveST-A borehole is uncased in bedrock. The bedrock was described as a garnetiferous-muscovite-biotite-hornblende-schist and schistose gneiss.

Fractures and Foliation

ATV and OTV data indicate a total of 247 fractures from below casing to the bottom of the GroveST-A borehole (Fig. 14). The mean orientation for the 247 fractures was N27°E, 25°NW, and N19°E, 67°NW for the foliation (both single clusters) (Fig. 14).

The gamma log is fairly uniform throughout the bedrock except at a 170 ft BLS where a spike appears to correlate with large fractures at that depth (Fig. 15). The SPR and MAG logs indicate slight variations in bedrock lithology. The dramatic decrease in

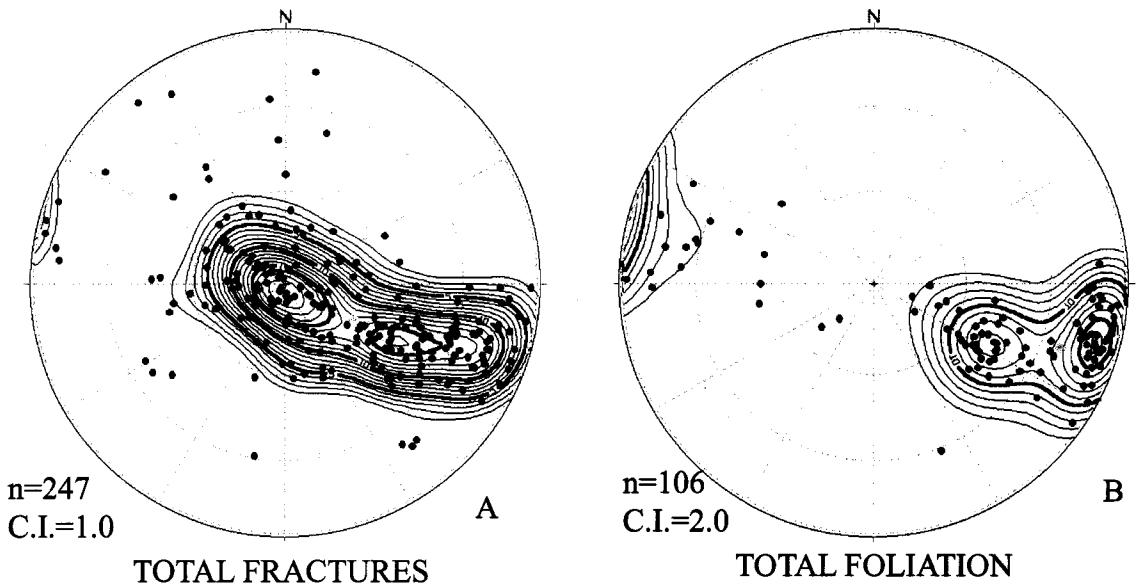

Figure 14. Stereonet plots of borehole GroveST-A, Manhattan Island, N.Y.,: A. Total fractures. B. Total foliation.

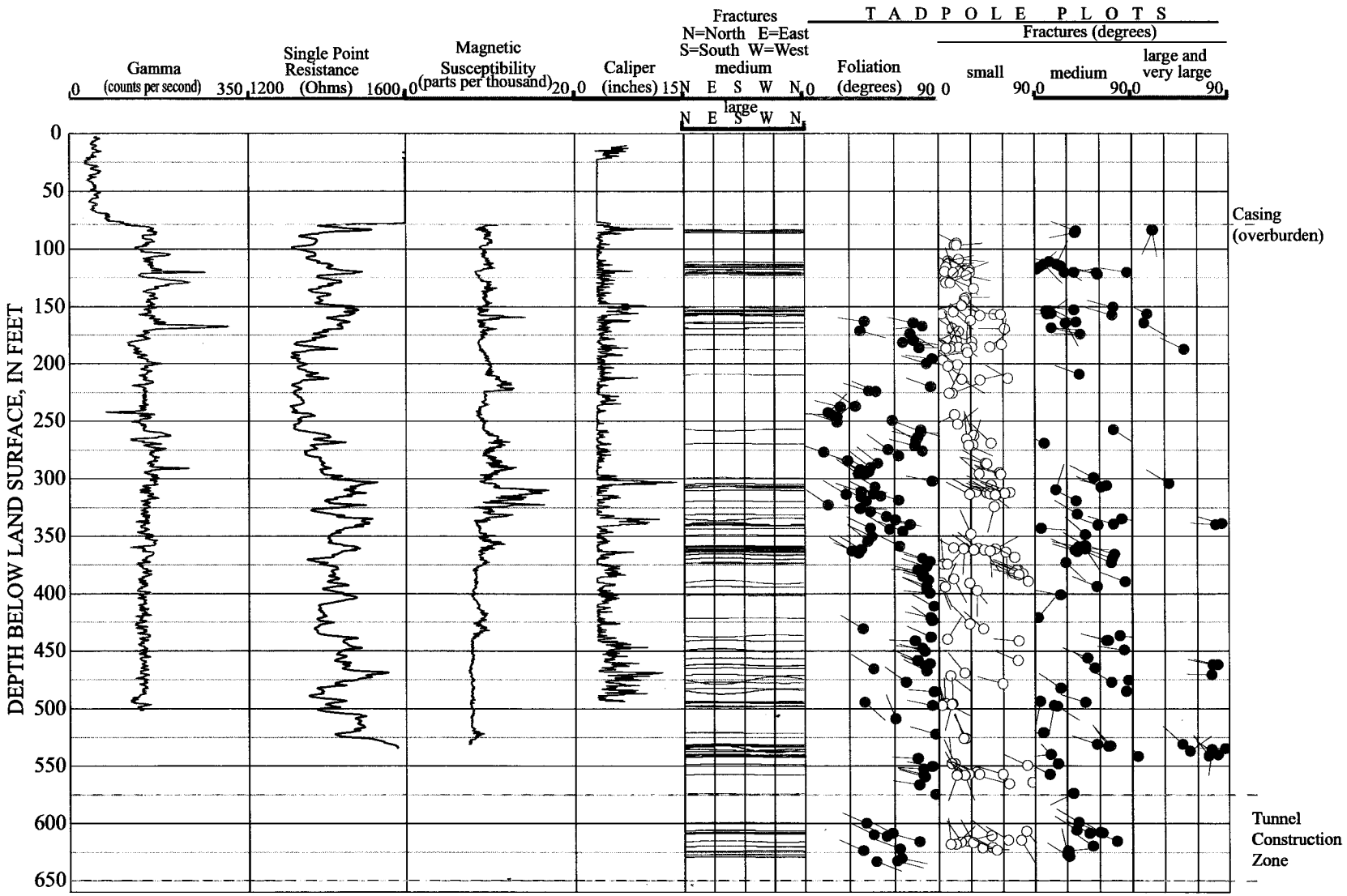

Figure 15. Suite of geophysical logs from borehole GroveST-A, Manhattan Island, N.Y.

MAG log response below about 370 ft BLS correlates with a change in the rock from schist to schistose gneiss (Fig. 15).

Ground-Water Flow Zones

The average hydraulic head at the GroveST-A borehole was -0.03 ft elevation. Heat-pulse flowmeter, fluid-temperature, and fluid-resistivity logs indicate seven possible transmissive fracture zones at 84, 100, 115, 164, 209, 299, and 530 ft BLS (Fig. 16). Pumping the borehole at a rate of 0.5 gal/min for 1.4 h produced a drawdown of 47.3 ft, or a specific capacity of 0.01 (gal/min)/ft. Total borehole transmissivity was calculated to be 2.0 ft^2/d. Under ambient (non-pumping) conditions, a small amount of upflow was detected from 209 ft to 164 ft fracture zones and from the 115 ft to 100 ft fracture zones (Fig. 16). Under pumping conditions, 74 percent of the total borehole transmissivity came from the 164 ft BLS fracture zone. Transmissivity was estimated for the 84, 100, 115, 164, 209, 299, and 503 ft fracture zones to be <0.1, 0.1, 0.2, 1.5, 0.1, 0.1, and <0.1 ft^2/d, respectively. The ground-water grab sample obtained during specific capacity testing had a chloride concentration of 25 mg/L.

PrinceST-A

The PrinceST-A borehole has 120 ft of casing and extends 665 ft BLS (-618 ft elevation). This borehole was selected as an example of highly fractured bedrock with moderate transmissivity in the south-central part of the study area. The PrinceST-A borehole is uncased in fractured bedrock. The bedrock penetrated by the borehole was described as a garnetiferous-biotite-schistose gneiss and mica schist with pegmatite.

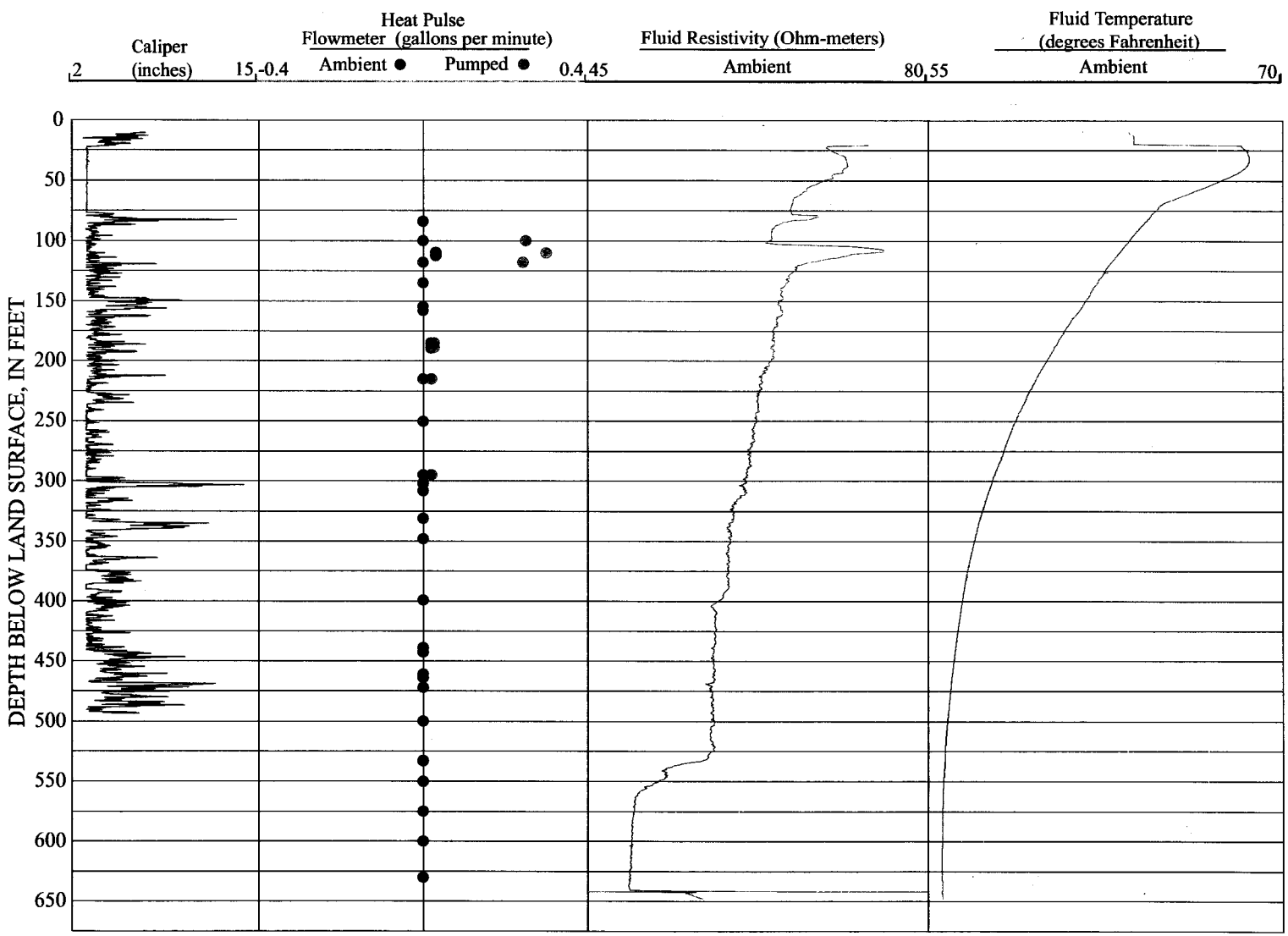

Figure 16. Suite of borehole-geophysical fluid logs from borehole GroveST-A, Manhattan, N.Y.

Fractures and Foliation

Analysis of the OTV and ATV log data indicated 504 fractures were penetrated within the borehole. The majority of the fractures were small and medium in size. A large fracture and gouge zone is detected at 235 ft BLS, with an orientation of N28°E, 39°NW. Two faults were detected at 452 and 479 ft BLS, with orientations of N05°W, 82°E and N04°E, 84°W, respectively. Total borehole and PTCZ fracture mean orientations were N43°E, 30°NW and N42°E, 44°NW, respectively (Fig. 17). Both the total borehole and PTCZ fracture stereonet plots indicate two major population clusters: one shallow dipping toward the southeast and the other moderately dipping toward the northwest.

Borehole radar logging imaged five potentially large fractures or faults away from the borehole. One feature is nearly vertical adjacent to the borehole with an estimated orientation of N10°E, 85°SW. The other four features did not intersect the borehole and have orientations of N30°E, 58°SE; N20°E, 63°SE; N70°E, 67°SE; and N70°W, 53°NE. The total borehole and PTCZ mean foliation orientations were N42°E, 60°NW and N45°E, 57°NW, respectively (Fig. 17).

The overburden sediment has lower gamma response than that of the bedrock below (Fig. 18). A decrease in SPR and R log response below 510 ft BLS correlates to a lithologic change. Most of the large resistivity spikes correlate to pegmatite zones (Fig. 18).

Ground-Water-Flow Zones

The hydraulic head in the PrinceST-A borehole was 4.52 ft elevation in

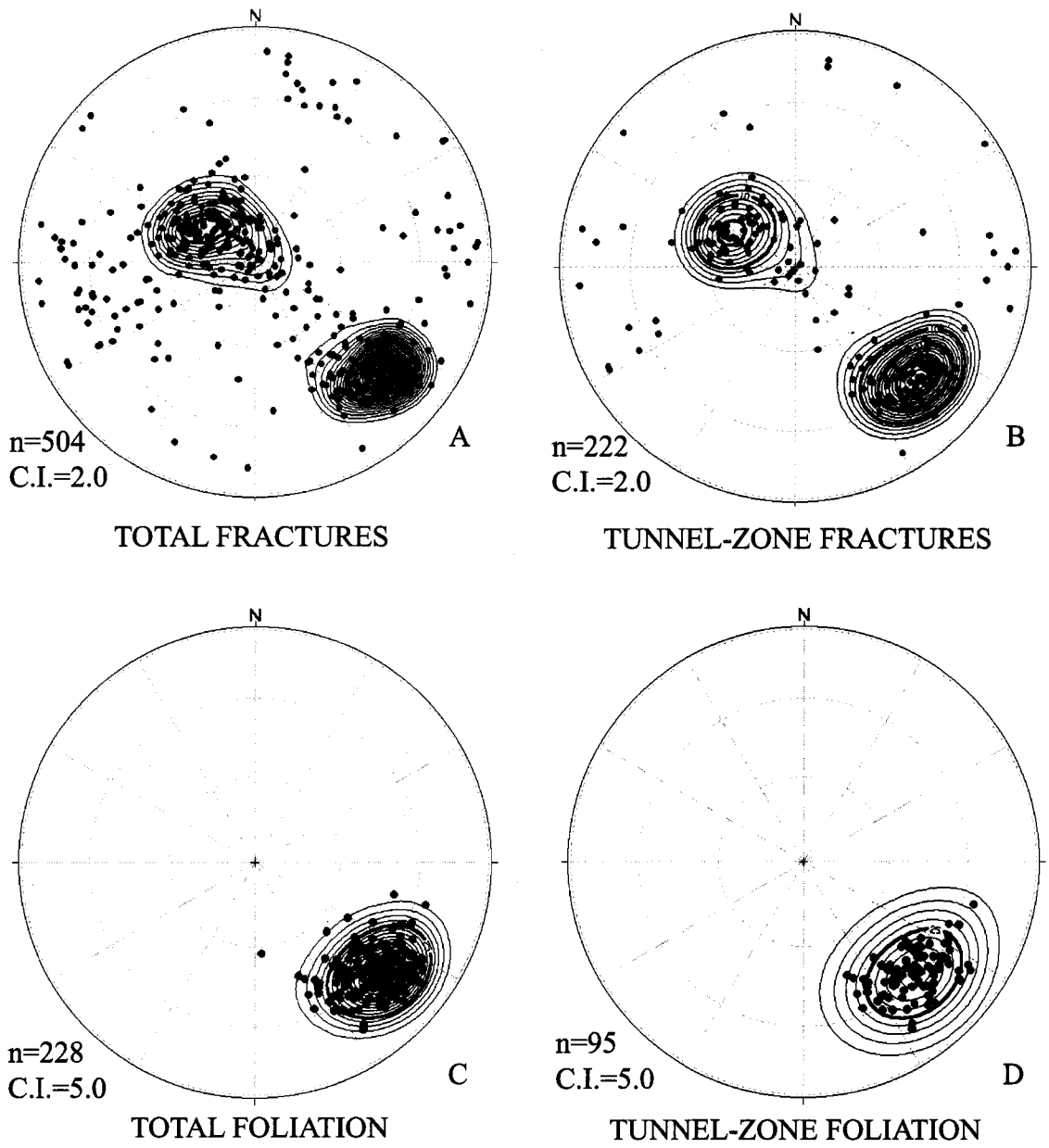

Figure 17. Stereonet plots of borehole PrinceSt-A, Manhattan Island, N.Y.,: A. Total fractures. B. Tunnel-zone fractures. C. Total foliation. D. Tunnel-zone foliation.

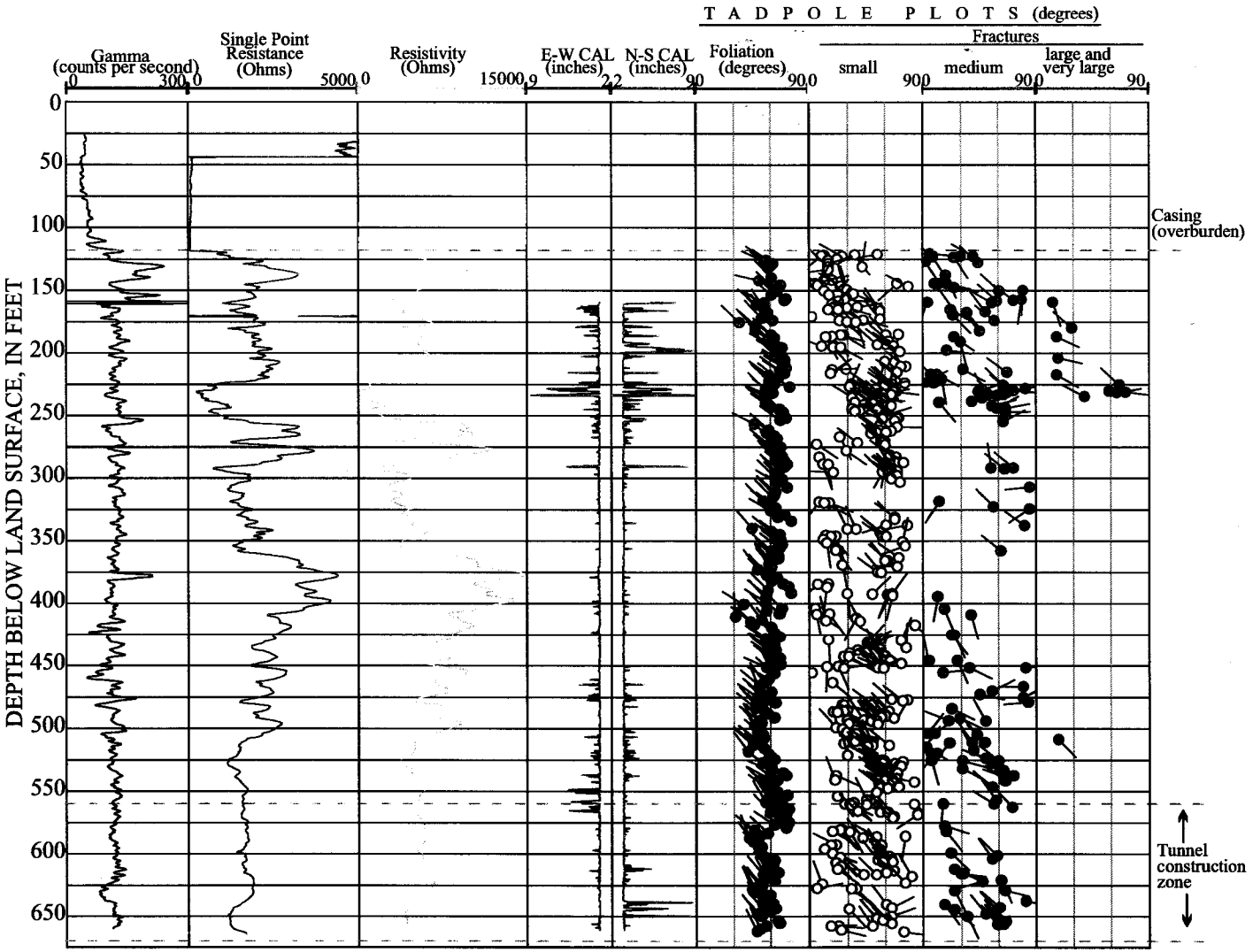

Figure 18. Suite of borehole-geophysical logs from borehole PrinceST-A, Manhattan Island, N.Y.

November 2004. Fluid temperature and fluid resistivity logs have slope changes indicating a possible leaky casing at 100 ft BLS and potentially transmissive fractures at 120, 162, 407, 507, 615, 640, and 650 ft BLS (Fig. 19). Specific-capacity test analysis indicated the PrinceST-A borehole has a specific capacity of 0.32 (gal/min)/ft and a transmissivity of 90 ft^2/d. The ground-water grab sample obtained during specific capacity testing had a chloride concentration of 143 mg/L.

Heat-pulse flowmeter logging within the borehole under ambient and pumping conditions indicated slight ambient upflow from 615 to 162 ft BLS (Fig. 19). Transmissive fractures were delineated with the flowmeter at 162, 230, 407, 507, and 615 ft BLS. Analysis of the ambient and pumping flowmeter data indicate the fractures at 162, 230, 407, and 507 ft BLS have estimated transmissivities of 83, 2, 3, and 2 ft^2/d, respectively. The transmissivity of the zone at 615 ft BLS was not determined and is probably below the detection limit of the flowmeter.

Faults, Fractures, and Foliation

All 31 OTV analyzed borehole stereonets were plotted within the study area. Most of the fractures measured within the study area had subhorizontal population clusters (Figs. 20 and 21). Most of the boreholes also had a secondary population cluster that was moderately dipping toward the northwest, except at E55ST-B, E54ST-A, E52ST-A, and W65ST-A. At these boreholes a smaller population cluster dipped either to the east or southeast (Fig. 20).

A total of 208 large fractures were delineated in the 31 boreholes logged with the OTV. Medium and large fractures combined totaled more than 1,000 fractures.

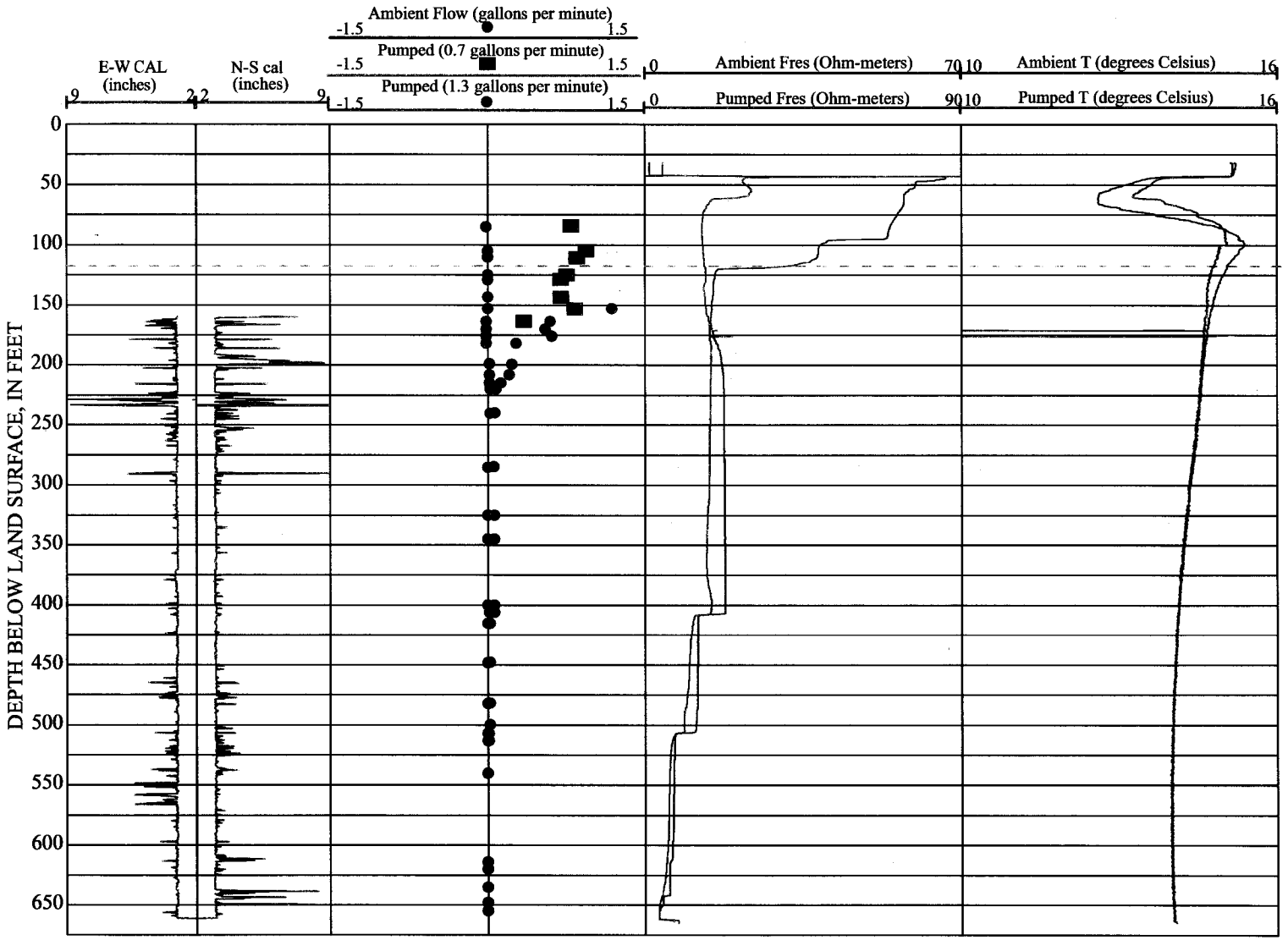

Figure 19. Suite of borehole-geophysical fluid logs from borehole PrinceST-A, Manhattan Island, N.Y.

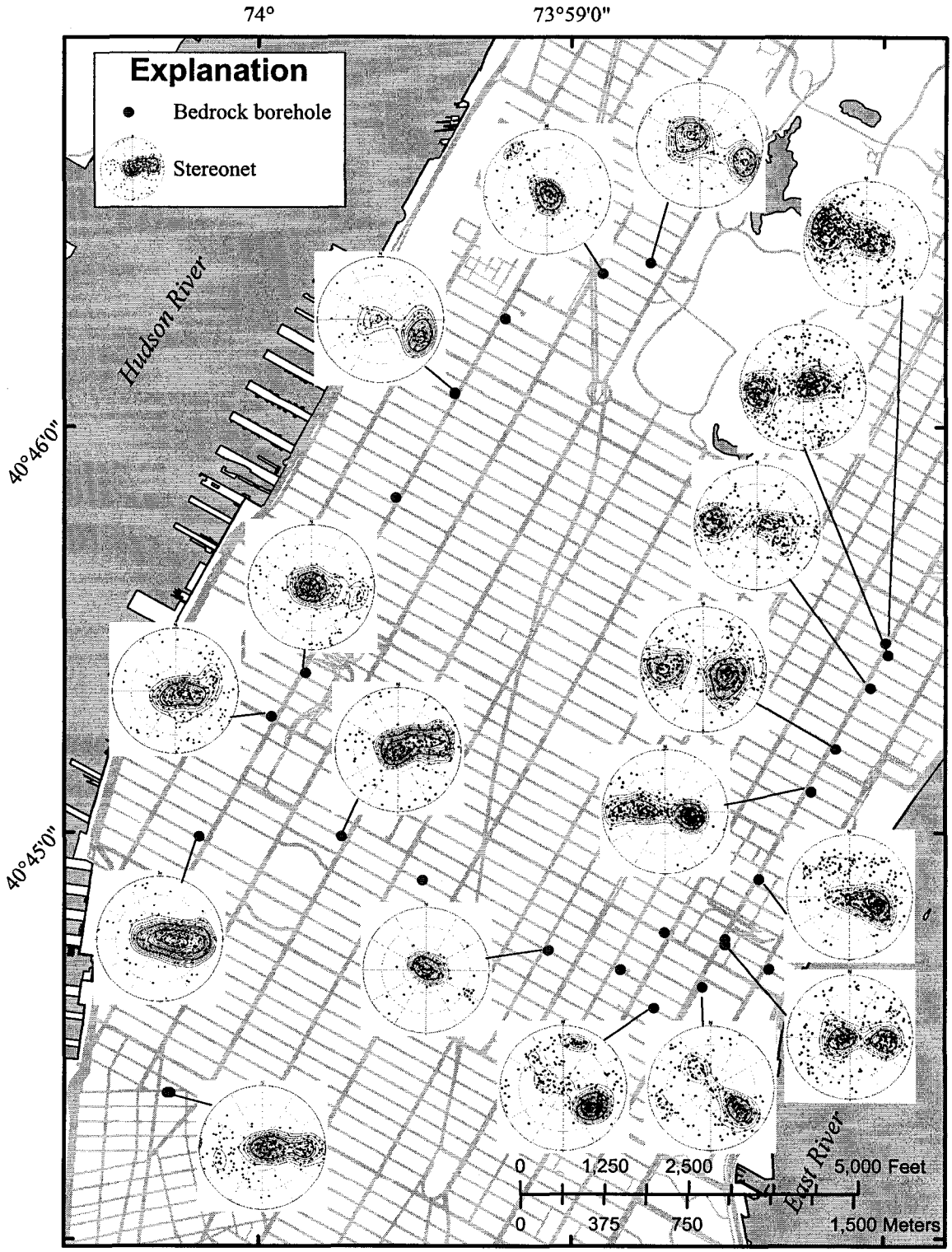

Figure 20. Variation in bedrock borehole fractures, northern detail area, Manhattan Island, N.Y. (Stereonets are plotted as poles to planes).

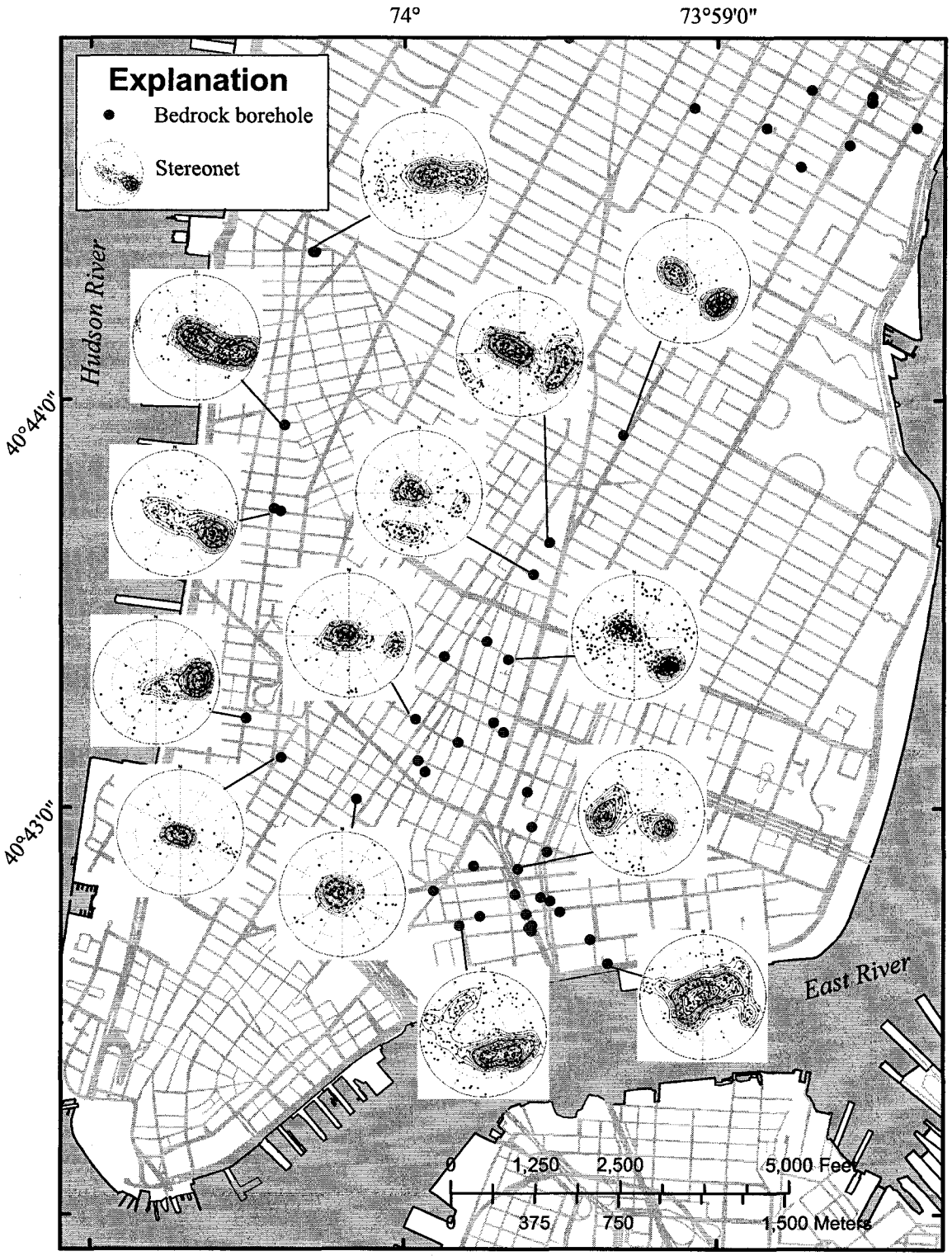

Figure 21. Variation in bedrock borehole fractures, southern detail area, Manhattan Island, N.Y. (Stereonets are plotted as poles to planes).

Stereonet plots of both medium and large fractures produced no clear population cluster. Stereonet analysis of just the 208 large fractures indicates most were part of a subhorizontal population cluster with a mean orientation of N43°E, 07°SE (Fig. 22). A smaller secondary population cluster of large fractures had a moderate to high dip inclination angles toward the northwest.

Several major northwest to southeast trending faults have been mapped within the Island of Manhattan (Berkey, 1910; Baskerville, 1994). A total of 53 faults were delineated in the 31 boreholes analyzed. The majority of these faults were of unknown type. While offsets were detected in OTV logs, the direction of offset was unclear. However, a significant number of faults were determined to be either normal or reverse faults. Most of the offsets detected were only a few inches at most. Baskerville (1994) noted similar small offsets in tunnel excavations within the study area. Stereonet analysis of all faults detected indicated two major population clusters (Fig. 23). One fault population cluster had a mean orientation of N12°W, 66°W and the other N11°W, 70°E. Both fault populations had similar strike azimuths and dip angles but in opposite directions (Fig. 23). The stereonet pattern from detected faults is totally unlike any fracture population analyzed and represents a different mechanism as compared to fractures. The general strike trends of both fault populations were north-northwest. These appear to be roughly parallel to the larger faults mapped on the island of Manhattan (Berkey, 1910; Baskerville, 1994).

Analysis of the foliation data from the 31 boreholes logged with the OTV indicates the foliation within the study area is surprisingly consistent (Figs. 24 and 25). The dominant foliation dip azimuth appears to be northwest to southwest. Foliation

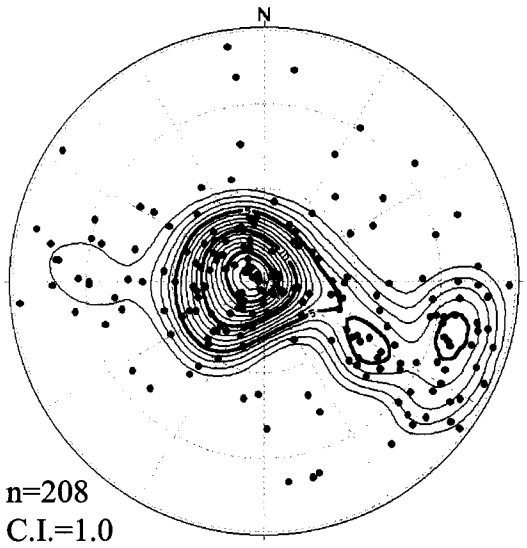

ALL LARGE FRACTURES

EXPLANATION

● STATISTICAL MEAN ORIENTATION

C.I. CONTOUR INTERVAL (point density contouring)

Figure 22. Stereonet plots of all large borehole fractures within the study area, Manhattan Island, N.Y...

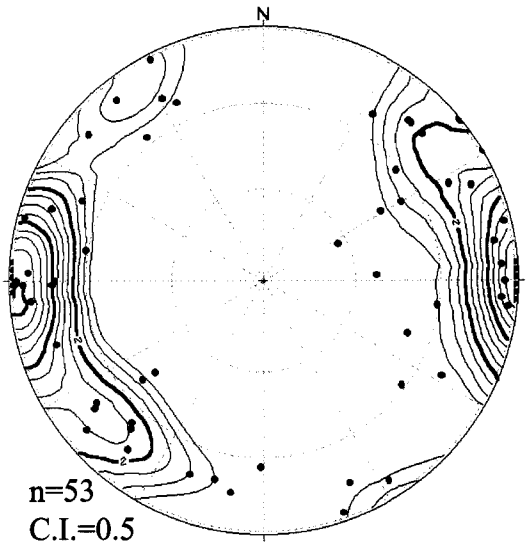

ALL BOREHOLE FAULTS

EXPLANATION

● STATISTICAL MEAN ORIENTATION

C.I. CONTOUR INTERVAL (point density contouring)

Figure 23. Stereonet plots of all borehole faults within the study area, Manhattan Island, N.Y...

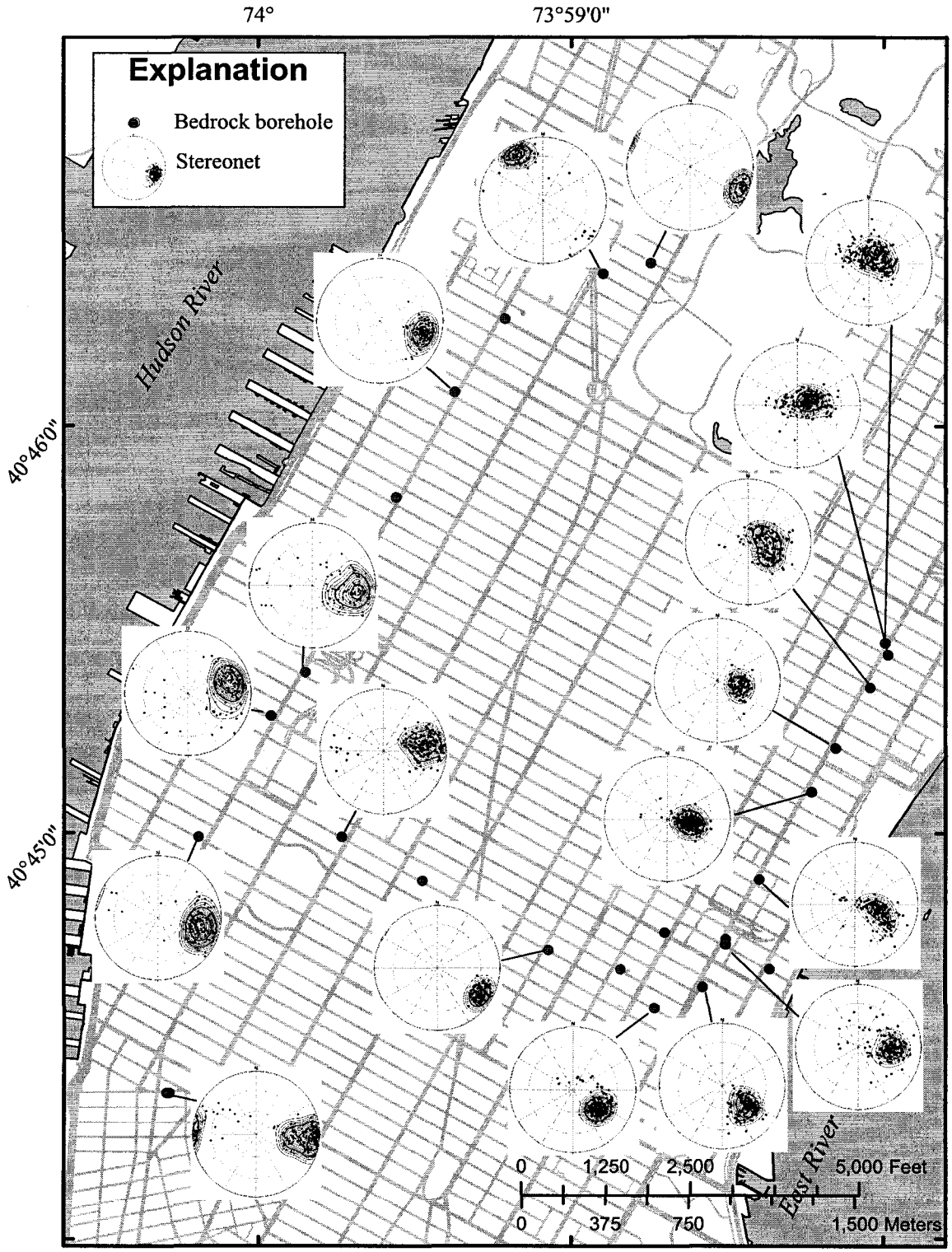

Figure 24. Variation in bedrock borehole foliation, northern detail area, Manhattan Island, N.Y. (Stereonets are plotted as poles to planes).

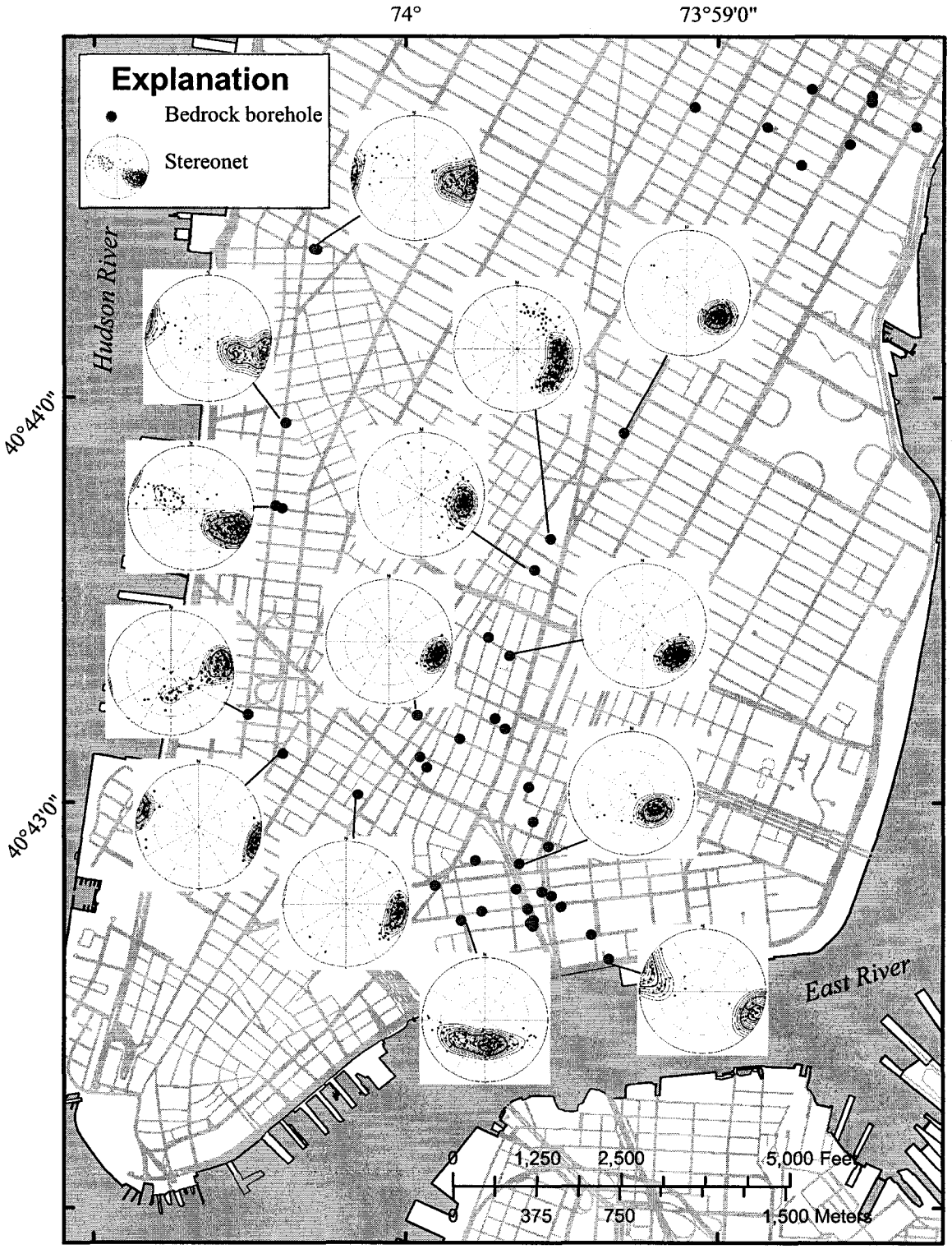

Figure 25. Variation in bedrock borehole foliation, southern detail area, Manhattan Island, N.Y. (Stereonets are plotted as poles to planes).

analyses, grouped by depth, indicate populations with similar dip azimuths and dip angles. Mean foliation dip inclination angles range from subhorizontal at E54ST-A and E55ST-B to nearly vertical at FranklinST-B, W67ST-A, W65ST-A, and SouthST-A (Figs. 24 and 25). In general foliation dip angles were in the 30° to 70° range. Foliation appears to be somewhat horizontal in the northeasternmost part of the study area and gradually increases in dip angle with an azimuth of northwest to southwest (figs. 24 and 25). The exception is at W65ST-A where foliation dips toward the southeast and at CatherineST-A where the foliation of the bedrock (Inwood Marble?) dips northward.

Fractured-Rock Potentiometric-Surface

Ground-water levels were measured at all open boreholes from 1998 to 2005. In November 2004 the largest network of open boreholes was measured during high tide. Only boreholes with chloride concentrations below about 2,000 mg/L were used to contour a potentiometric-surface map. Increasing chloride concentration associated with saltwater intrusion will cause a depression of water elevations as a result of increasing water density. The resulting data were plotted and contoured, producing the first potentiometric-surface map of the bedrock ground-water flow system for southern Manhattan (Fig. 26). The fractured-rock potentiometric surface ranges from 64.7 ft elevation at W67ST-A to -42.8 ft elevation at E30ST-B. In general the fractured-rock ground-water flow system acts like a continuum with ground-water flowing from the recharge area in the northernmost part (the area in the vicinity of Central Park) toward the southern, eastern, and western coastal discharge zones (Fig. 26). Two large cones of

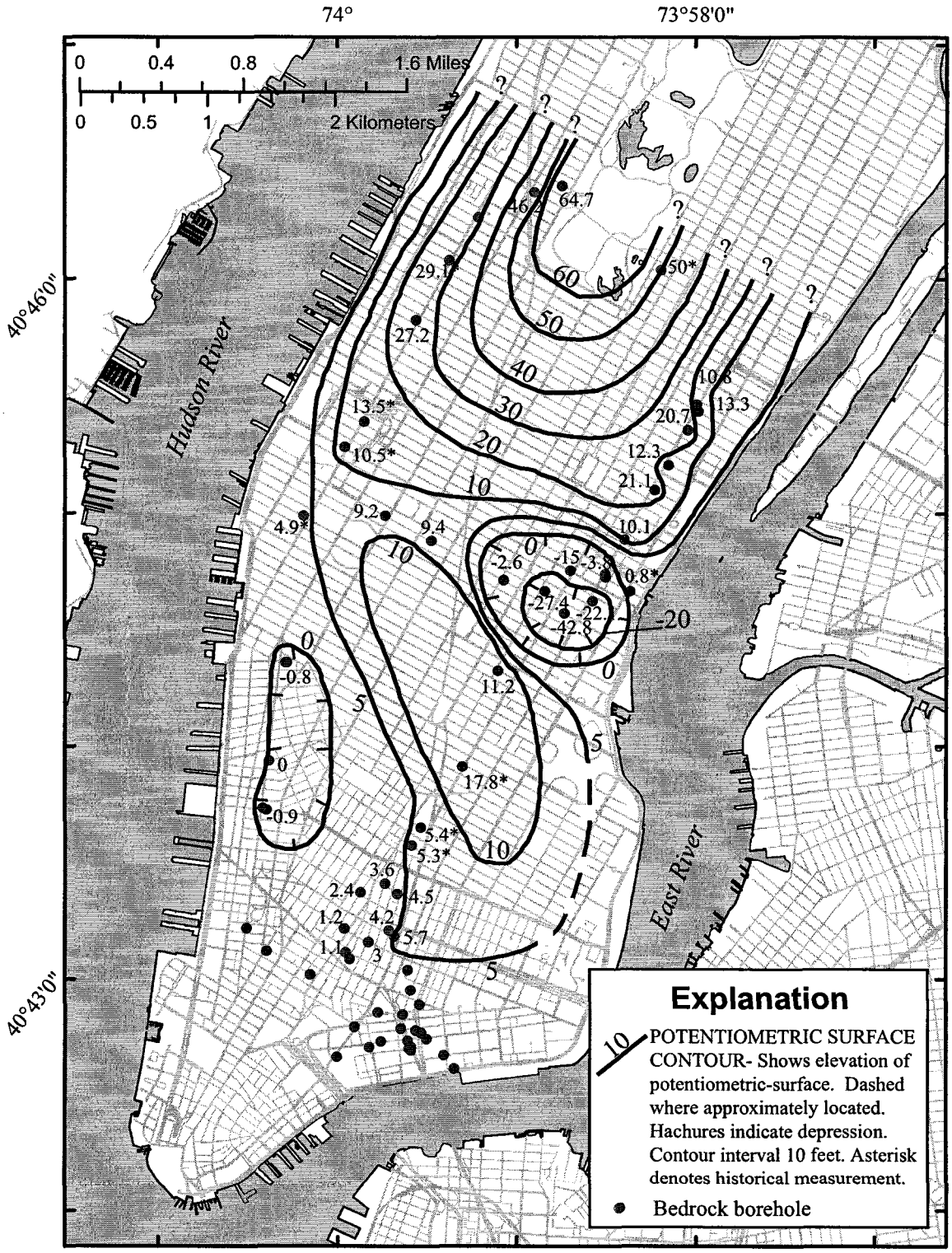

Figure 26. Potentiometric-surface elevation in the bedrock, Manhattan Island, N.Y., November 2004.

depression are indicated on the bedrock potentiometric-surface map (Fig. 26). The largest is on the eastern-midtown part of the study area and includes boreholes E30ST-B, E30ST-A, E31ST-A, E34ST-B, E35ST-D, E35ST-B, E35ST-A, E35ST-F, and E33ST-A (Fig. 4). This cone of depression or midtown cone of depression alters the island's bedrock ground-water flow system, creating a trough that cuts through the central part of the study area as far west as W30ST-A (Fig. 26). The second smaller cone of depression located in south-central part of the study area includes GroveST-A, HudsonST-B, HoustonST-A, GansST-B, and GansST-A (Fig. 5). The cone of depression had a minimum water elevation of -0.9 ft. It is unclear if the cause for this cone of depression is dewatering associated with local subway railways and or the recent excavation of a new water tunnel in this area. The ground-water divide runs somewhat along the central spine of the island except in the central and southern most parts where the two cones of depression have altered the flow system causing the divide to shift eastward (Fig. 26).

Heat-pulse flowmeter logging was completed at 8 boreholes (31B1, PrinceST-A, GroveST-A, W26ST-A, W34ST-A, W37ST-A, and W55ST-A). A result of flowmeter logging is the determination of which fractures or zone of fractures in a borehole are transmissive and an estimate of their transmissivity. A total of 77 transmissive fractures were delineated at the 8 boreholes. Stereonet analysis of these transmissive fractures indicates two population clusters of fractures (Fig. 27). The majority of transmissive fractures was subhorizontal and had a mean orientation of N11°E, 14°SE (Fig. 27). The secondary transmissive fracture population cluster had a mean orientation of N23°E, 57°NW. These data suggest that fractured-rock ground-water flow system in southern Manhattan is dominated by subhorizontal fractures and moderately northwest dipping

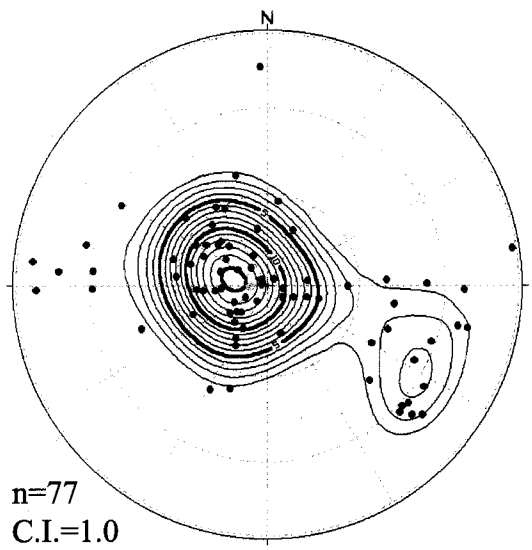

Figure 27. Stereonet plots of all transmissive borehole fractures within the study area, Manhattan Island, N.Y..

fractures. The majority of transmissive fractures delineated (75%) at these 8 boreholes within the study area were medium sized fractures, 20% of the transmissive fractures were large, and only 5% were small.

Bedrock Hydrograph Analyses

Digital water-level recorders were installed at 13 different fractured-rock boreholes within the study at various lengths of time from October 2003 through February 2005. Nine of the 13 boreholes with recorders were selected to show the interconnectivity of the fractured-rock ground-water flow system in the study area. The digital water-level recorders were programmed to record the hydraulic head of each borehole at 15 or 30 minute intervals. The resulting data were plotted as hydrographs. Analysis of the data indicate 1) correlation between increases in water levels and precipitation events, 2) similar variations in water levels at different boreholes indicate a continuum, and 3) tidal fluctuations.

Three boreholes were selected to demonstrate the similar trends and responses to precipitation events in water-levels in the fractured-rock. The three boreholes W67ST-A, E39ST-A, and EricssonPL-A were located in the northwestern, northeastern, and southwestern parts of the study area, respectively. At W67ST-A water elevations ranged from a high of 66.5 ft in January 2004 to a low of 64.5 ft in November 2004 (Fig. 28). Digital water-level recorder data and synoptic water level measurements indicate W67ST-B had the highest ground-water elevation of any bedrock borehole within the study area. From January 2004 through November 2004 there was a gradual decrease in the elevation of the potentiometric-surface punctuated by several spikes which

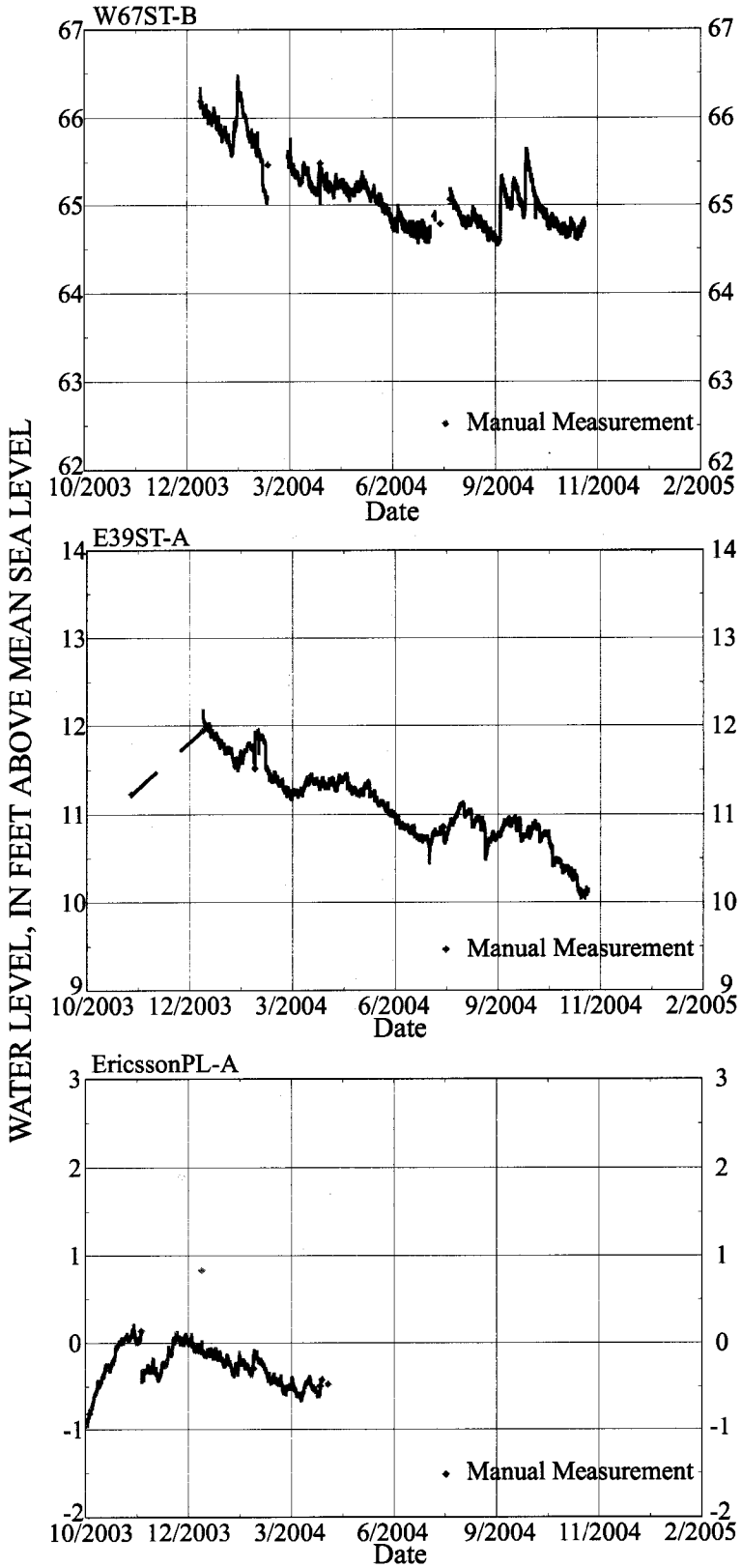

Figure 28. Hydrographs of water-levels in the W67ST-A, E39ST-A, and EricssonPL-A boreholes, Manhattan Island, N.Y.

correspond to precipitation events (recharge). A similar trend in water-levels was seen in the E39ST-A borehole located on the northeastern part of the study area (Fig. 28). Water elevations in the E39ST-A borehole ranged from a high of 12.2 ft in January 2004, to a low of 10.0 ft in November 2004 (Fig. 28). Data indicate a general decrease in the potentiometric-surface during the entire period of record. This correlates to a reduced amount of precipitation in 2004 as compared to 2003. All three boreholes appear to have similar trends and respond to the same precipitation events, in spite of their distances from each other (Fig. 28).

The GroveST-A and HoustonST-A boreholes located nearby each other on the southwestern part of the study area were selected due to the sudden declines in water-levels they experienced in January 2004 (Figs. 5 and 29). At the GroveST-A borehole water elevations ranged from a high of 1.1 ft in January 2004 to -6.4 ft in April 2004 (Fig. 29). This digital water-level recorder was installed from October 2003 to March 2004. The data indicate a gradual increase in the potentiometric-surface from October to January 2003.

Water elevations at the HoustonST-A borehole ranged from a high of -0.5 ft in October 2003 to a low of -2.2 ft in April 2004 (Fig. 29). An increase in the potentiometric-surface at this borehole from October to December 2003 correlates with those measured nearby at GroveST-A to the north.

On January 14, 2003, there was a dramatic decrease in the potentiometric surface of more than 5 ft at the GroveST-A borehole with similar effects seen at the HoustonST-A borehole. Since the GroveST-A borehole was sealed with concrete as the TBM reached this location, the author inferred the dramatic decline in water levels at both

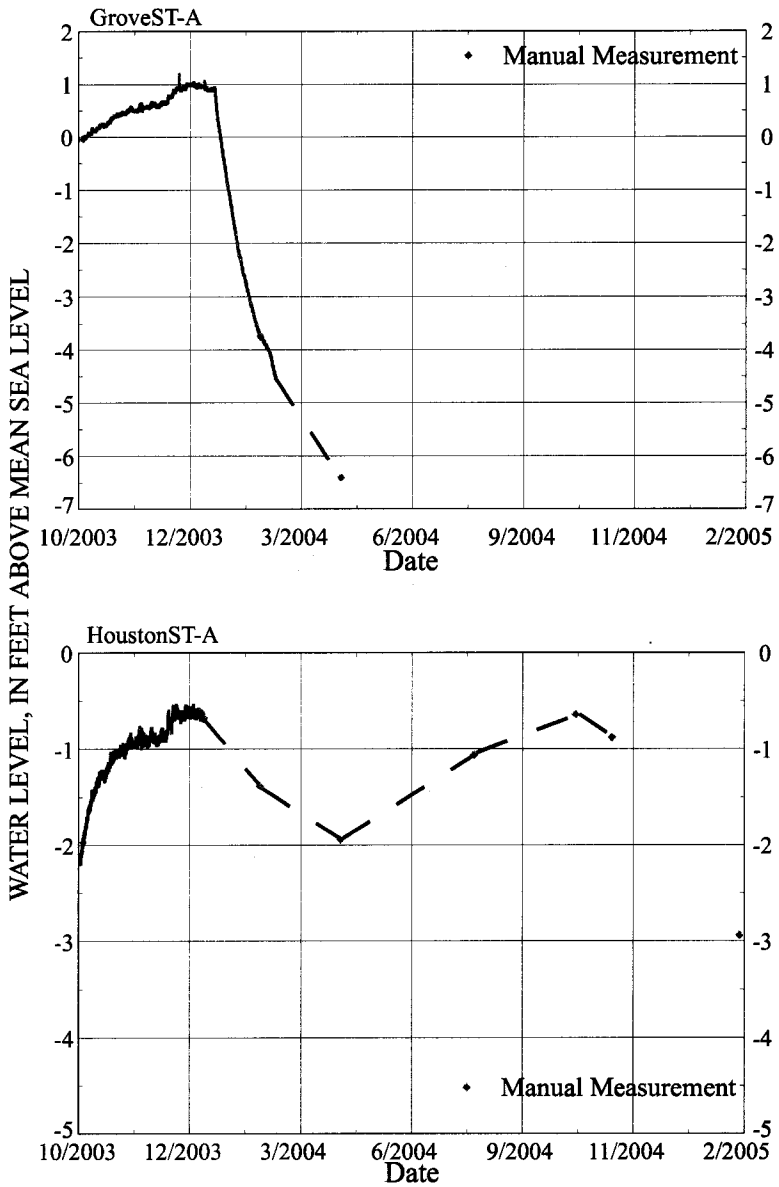

Figure 29. Hydrographs of water-levels in the GroveST-A and HoustonST-A boreholes, Manhattan Island, N.Y.

boreholes was due to the close proximity of the advancing South Water-Tunnel. However, according to NYCDEP South Water-Tunnel excavation records on or about January 14, 2004 the TBM was about 2,500 ft north of the GroveST-A borehole.

Hydrographs from the MPP-5, CatherineST-A, StJamesST-A, and PikeST-B boreholes were selected due to their similar nearly instantaneous declines in water-levels in the southeasternmost part of the study area (Fig. 30). Water levels in most of these boreholes appear to be only slightly affected by the tide fluctuations of the nearby East River. The data from these boreholes are used only to gauge the response of the fractured-rock ground-water flow system and not the absolute water elevations. The chloride concentrations of these boreholes indicate the water elevations are saltwater heads. A dramatic decrease in the potentiometric-surface was indicated in late September to early October with declines of 1 to 5 ft at the four boreholes (Fig. 30). No local explanation for the nearly instantaneous decline in water-levels in this part of the study area could be found. The depth to bedrock in this boreholes ranges from 100 to over 200 ft, ruling out shallow construction or railway dewatering projects. When the author checked the NYCDEP excavation records of the South Water-Tunnel they indicated the TBM was northwest of this area at about the time of the water-level declines. The distance from the boreholes to the TBM excavation line was 2,500, 2,700, 3,100, and 3,200 ft at the MPP-5, CatherineST-A, StJamesST-A, and PikeST-B boreholes, respectively.

The data from MPP-5, CatherineST-A, StJamesST-A, and PikeST-B in the southernmost part and that from GroveST-A and HudsonST-B in the southwestern parts of the study area suggest an interconnected network of transmissive fractures may exist

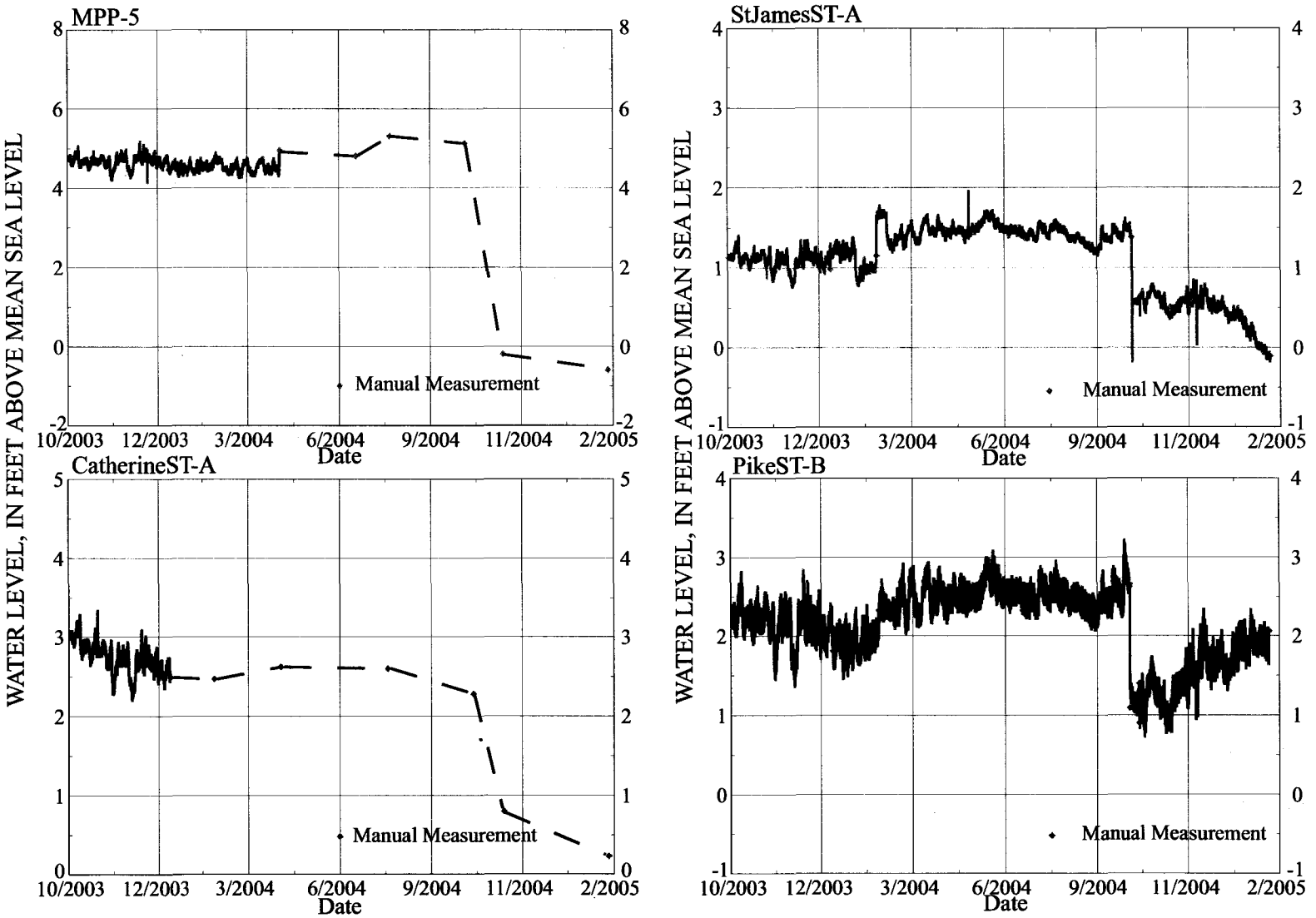

Figure 30. Hydrographs of water-levels in the MPP-5, CatherineST-A, StJamesST-A, and PikeST-B boreholes, Manhattan Island, N.Y.

within the study area. The potentiometric-surface map also provides additional evidence for the interconnectivity of transmissive fractures.

Bedrock Transmissivity

A total of 59 bedrock boreholes had specific-capacity test data analyzed for total borehole transmissivity. The bedrock transmissivity ranged from 0.7 to 871 ft^2/d within the study area (Table 2). The majority of boreholes (69%) had transmissivities less than 100 ft^2/d. Only 15% of the bedrock boreholes had transmissivities greater than 250 ft^2/d. Figure 31 shows the spatial distribution of bedrock transmissivity within the study area. Two areas of elevated bedrock transmissivity were indicated, one on the central-east coastal area and the second on the southernmost coastal area. The highest transmissivities were found within the southernmost coastal area (Fig. 31). This area of high transmissivity in the bedrock maybe associated with a structural discontinuity or plane of weakness (fault?).

Saltwater Intrusion of the Bedrock

Fifty-seven bedrock boreholes had chloride concentrations measured from ground-water grab samples obtained during specific capacity testing. The chloride concentrations were measured using a calibrated chloride ion probe. Chloride concentrations of the bedrock ground-water flow system ranged from 25 mg/L at GroveST-A to 17,800 mg/L at SouthST-A (Table 2). The majority of the bedrock boreholes tested had chloride concentrations less than 100 mg/L in the north-central and

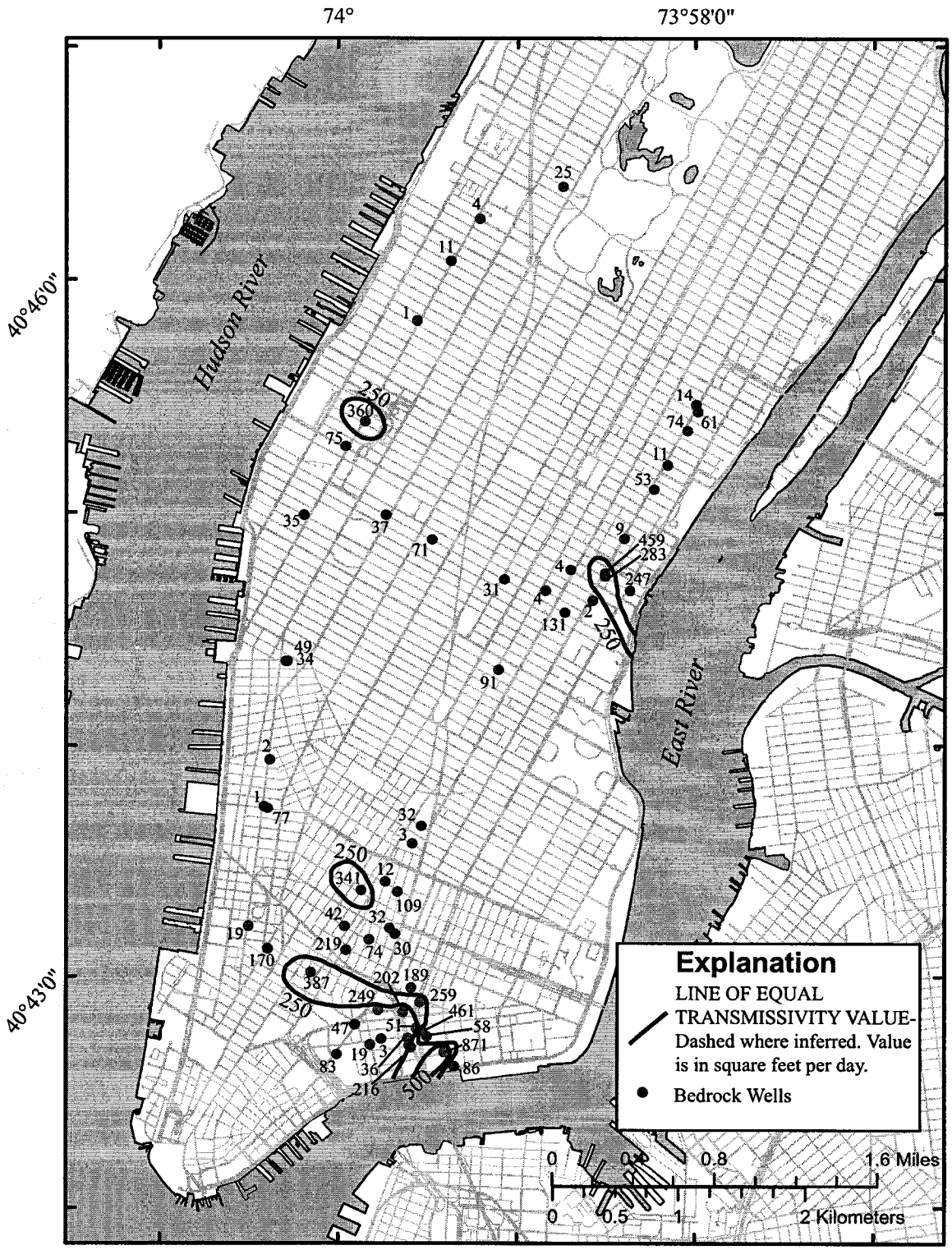

Figure 31. Transmissivity values of the total borehole in bedrock, Manhattan Island, N.Y.

south-central parts of the study area (Fig. 32). These low chloride regions are truncated at 30th Street by a trough of higher chloride concentrations which extends across the island from the Hudson to the East River (Fig. 32).

Three areas of saltwater intrusion in the bedrock ground-water flow system were designated areas A, B, and C. An area of very high chloride concentrations was found in the southernmost part of the study area designated area A in Figure 33. This area includes EricssonPL-A to the west and EldridgeST-A to the east and all boreholes south of these boreholes. This group of saltwater intruded boreholes includes 19 boreholes. There appears to be a very narrow transition zone or freshwater-saltwater interface. The extent of saltwater intrusion indicates a highly interconnected network of transmissive fractures within this part of the study area. Most of the 19 boreholes in this area had chloride concentrations above 10,000 mg/L (Fig. 33).

A second area of saltwater intrusion in the fractured-rock ground-water flow system designated area B is along the northwestern coastal area of the study area (Fig. 32). This area of saltwater intrusion includes W55ST-A, W48ST-W, W26ST-A, and W30ST-C. Chloride concentrations ranged from 820 to 2,420 mg/L.

A third area of saltwater intrusion is designated area C in the central-eastern coastal part of the study area (Fig. 32). The saltwater intrusion in the area includes E39ST-A, E35ST-A, E35ST-B, E35ST-D, E35ST-F, and E33ST-A. The chloride concentrations in area C ranged from 599 to 3,470 mg/L. Saltwater intrusion areas B and C appear to be associated with the dewatering operation that has created the midtown cone of depression.

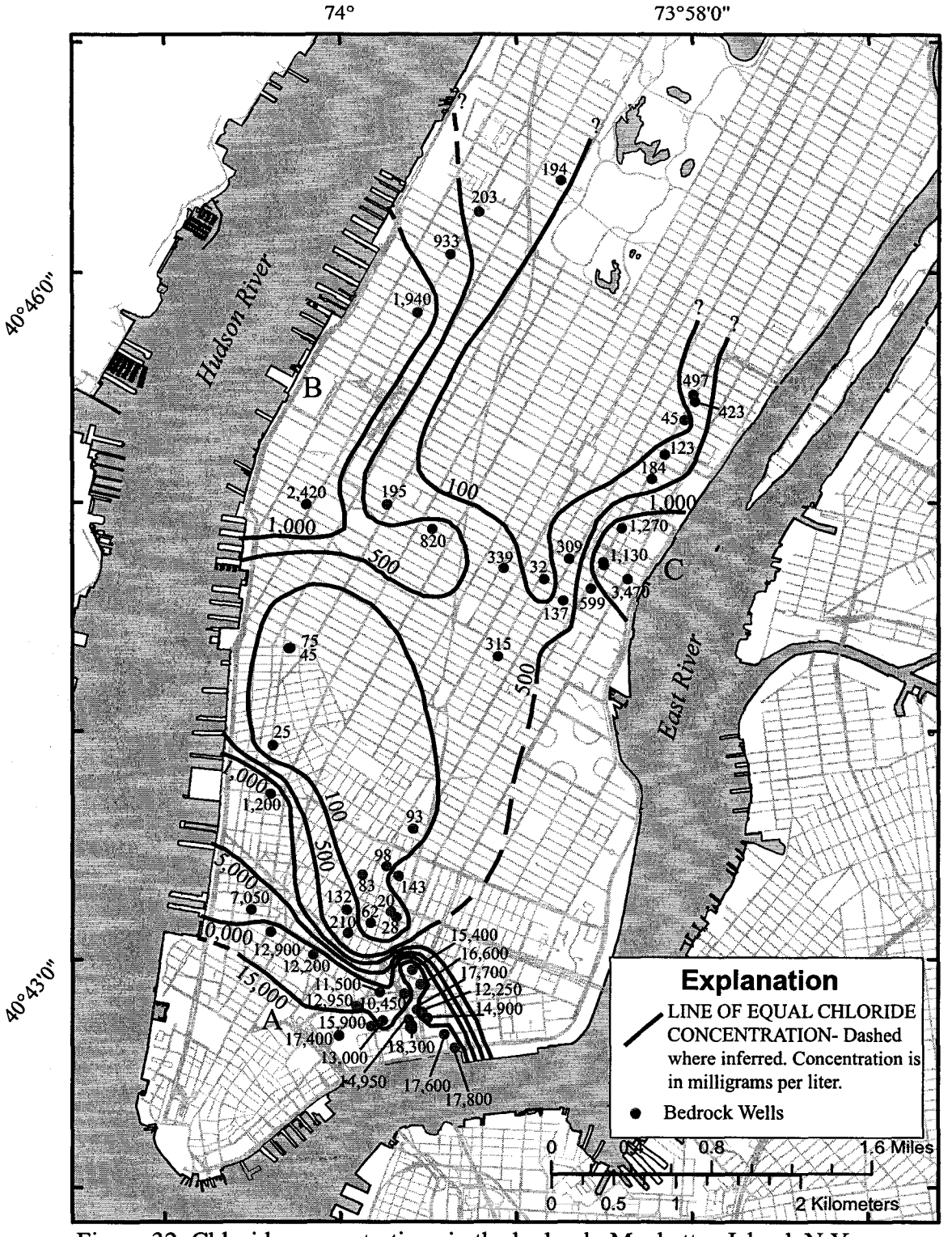

Figure 32. Chloride concentrations in the bedrock, Manhattan Island, N.Y., saltwater intrusion areas A, B, and C shown.

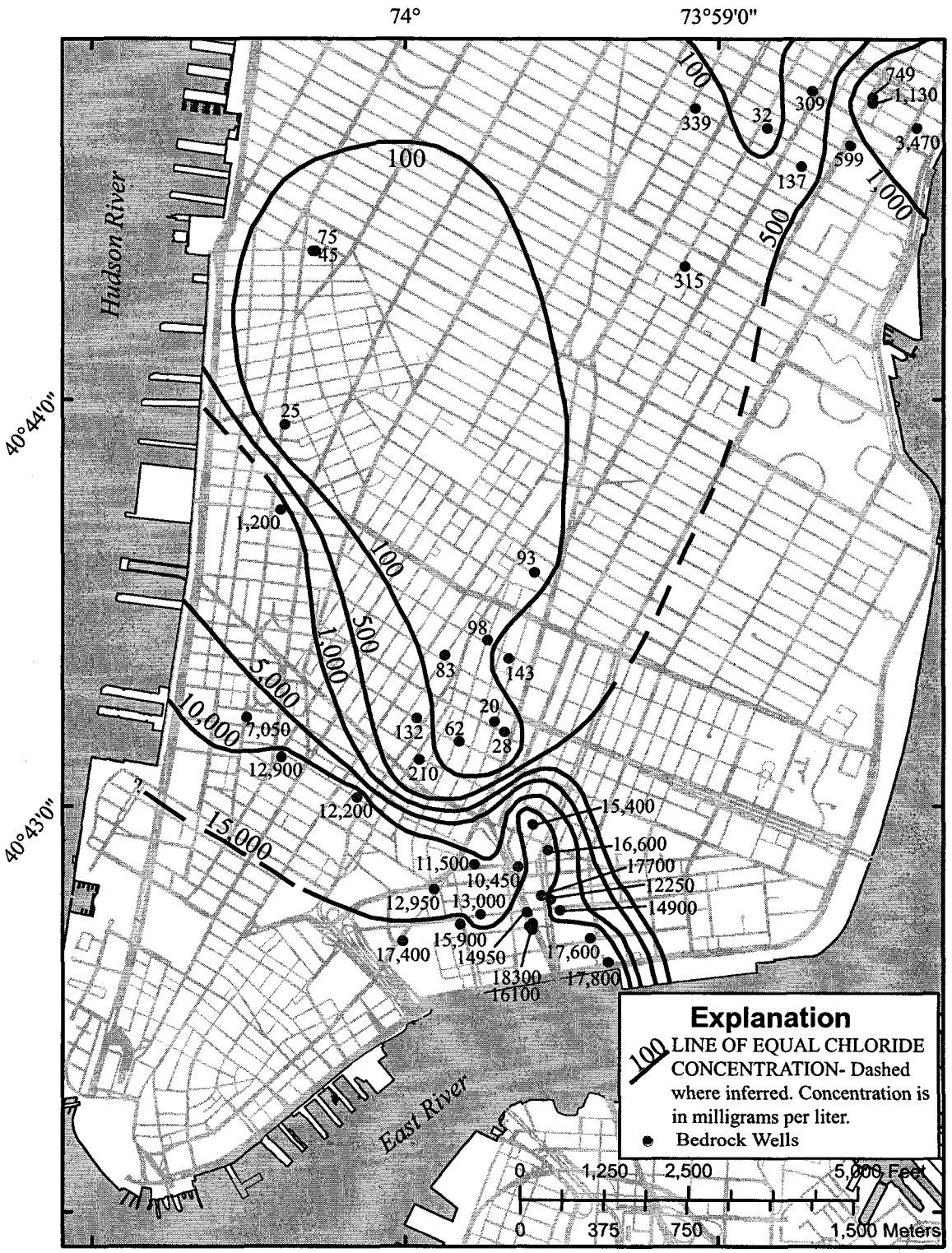

Figure 33. Chloride concentrations in the bedrock within the southern detail area, Manhattan Island, N.Y., (Data from chloride probe analysis).

Discussion

The gamma, SPR, R, and MAG logs were useful in delineating changes in bedrock lithology and in some cases transmissive fractures. The OTV log was most useful in delineating the strike and dip of fractures and foliation. The ATV log was used as a quality control for fracture orientations and deviation of boreholes. Fluid-temperature and fluid-resistivity logs were sometimes useful in delineating transmissive fractures. However, the new QW probe provided far superior fluid parameter logs and appears to detect smaller transmissive fractures than the simple temperature/resistivity logs. The heat-pulse flowmeter log was most useful in delineating specific fractures that were transmissive. When collected under both ambient and pumping conditions the heat-pulse flowmeter allowed the determination of transmissivity to individual fractures or fracture zones.

All boreholes penetrated moderately fractured bedrock that contained medium and large fractures. Most fractures delineated by the OTV log were subhorizontal within the study area. A total of 208 large fractures were delineated in the 31 boreholes. Stereonet analysis indicates two large fracture population clusters, one subhorizontal the second moderately dipping to the northwest. Fifty-three faults were delineated in the 31 boreholes. Stereonet analysis indicates two population clusters with similar strikes and dip inclination angles with mean orientations of N12°W, 66°W and the N11°W, 70°E. Foliation was fairly consistent throughout the study area with dip azimuths ranging from northwest to southwest and dip inclination angles ranging from 30° to 70°.

The first potentiometric-surface map of the bedrock in southern Manhattan indicates water elevations ranged from 64.7 ft at W67ST-A to -42.8 ft at E30ST-B. The

potentiometric-surface map indicates ground-water flows from a recharge area in the northernmost part (vicinity of Central Park) to the south, western, and eastern coastal discharge zones. Two cones of depression alter the local ground-water flow system. Overall, the data suggests the fractured-rock ground-water flow system acts like a continuum.

Heat-pulse flowmeter logging in 8 boreholes delineated 77 transmissive fractures in the study area. Stereonet analysis indicates transmissive fractures in the study area are either subhorizontal with a mean orientation of N11°E, 14°SE, or northwest dipping with a mean of N23°E, 57°NW.

Hydrograph analysis of boreholes W67ST-A, E39ST-A, and EricssonPL-A indicate all have similar trends and respond to the same precipitation events. The boreholes are located in the northwestern, northeastern, and southwestern parts of the study. Hydrograph analysis of boreholes GroveST-A and HoustonST-A and NYCDEP excavation records indicate both responded to hydraulic stresses induced by the South Water-Tunnel TBM while it was 2,500 feet away. Similar responses were discovered at boreholes MPP-5, CatherineST-A, StJamesST-A, and PikeST-B in the southeastern part of the study area.

The bedrock transmissivity ranged from 0.7 to 871 ft^2/d within the study area. Two areas of elevated bedrock transmissivity were indicated, one on the central-east coastal area and the second on the southernmost coastal area. Bedrock transmissivity was highest in the southernmost part of the study area.

The first chloride concentration or isochor map of the bedrock in southern Manhattan indicates chloride concentrations ranged from 25 mg/L at GroveST-A to

17,800 mg/L at SouthST-A. The majority of the bedrock boreholes tested had chloride concentrations less than 100 mg/L in the north-central and south-central parts of the study area. Three areas of saltwater intrusion in the bedrock ground-water flow system were designated areas A, B, and C. An area of very high chloride concentrations was found in the southernmost part of the study area designated area A. This area includes EricssonPL-A to the west and EldridgeST-A to the east and all boreholes south of these boreholes. This group of saltwater intruded boreholes includes 19 boreholes. A second area of saltwater intrusion in the fractured-rock ground-water flow system designated area B is along the northwestern coastal area of the study area. This area of saltwater intrusion includes W55ST-A, W48ST-W, W26ST-A, and W30ST-C. A third area of saltwater intrusion is designated area C in the central-eastern coastal part of the study area.

3. Unconsolidated Overburden Ground-Water Flow System

Ten overburden wells screened in this aquifer were used to determine the hydraulic properties and distribution of chloride concentration (Tables 1 and 2). The glacial aquifer has a limited extent in the northern part of the study. A lack of wells in the central part of the glacial aquifer limited the certainty of the extent of the aquifer, the maximum hydraulic head values, and the chloride concentration in that part of the aquifer. Future drilling in the central part of this aquifer will provide valuable information on the distribution of chloride concentration, hydraulic head, and transmissivity.

Extent and Thickness of the Glacial Aquifer

The surface topography of the study area has been significantly altered when the present topographic surface is compared with pre-development maps. The northern part of the study area's topography is dominated by the bedrock outcrops and a shallow veneer of soils above them. A narrow ridge runs along the spine of the island. Subtraction of the surface topography and the new bedrock surface elevation maps using ArcMap GIS software produced a sediment thickness map. While this is only an approximation it provides useful information on the thickness of the glacial aquifer within the study area (Fig. 34). Drilling data indicate the sediment thins to less than 20 feet in a large part of the northern study area above 30th Street. The sediment thickness map indicates several areas with thicknesses of 50 ft and more in isolated pockets in the northern part of the study area (north of 30th Street). The deep southern buried valley contains the thickest sediment deposits of up to 250 ft (Fig. 34).

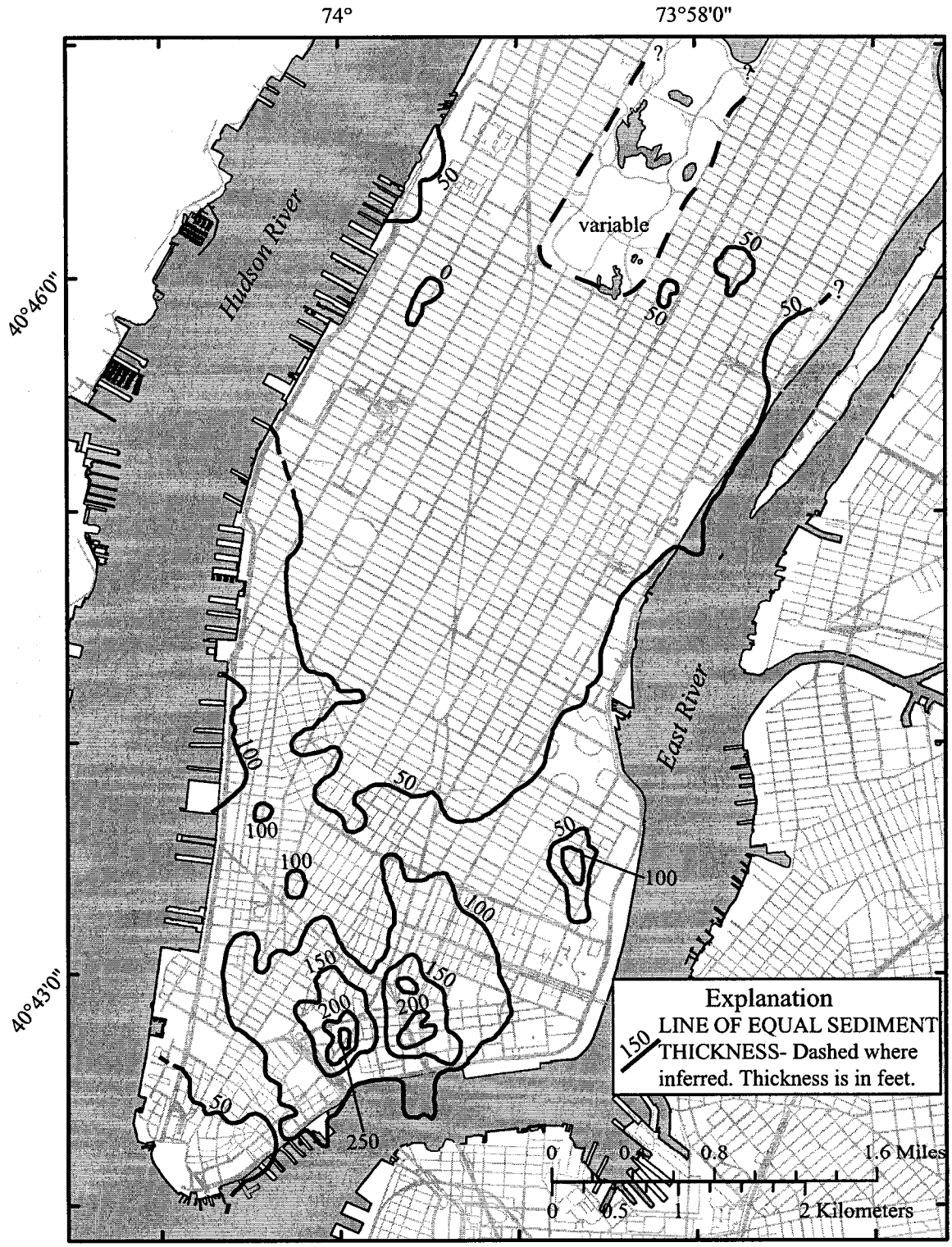

Figure 34. Thickness of the unconsolidated overburden within the study area, Manhattan Island, N.Y.

Based upon driller's and engineering logs of wells drilled within the study area the glacial aquifer does not appear to extend north of 30th Street, except in isolated locations (small buried stream valleys). Bedrock boreholes found within this northern zone have unsaturated zones as opposed to all other boreholes where there are no unsaturated zones indicated.

Glacial Aquifer Water-Table

This study presents the first water-table map ever constructed for southern Manhattan. It indicates that ground-water in the glacial aquifer appears to be unconfined with water level elevations ranging from 14.7 ft at E39ST-W to -0.3 ft at 28B-W (Table 2). The highest water levels occur in the central part of the study area which appears to be the recharge zone for the aquifer (Fig. 35). Ground-water flows from the central part of the study area toward the south, west, and east coastal discharge zones. The ground-water divide in the glacial aquifer appears to follow the central spine of the island, but is slightly altered to the east (Fig. 35). This same shift was seen in the bedrock potentiometric-surface ground-water divide. Leakage from water mains and sewers probably contributes significant amounts of recharge to the glacial aquifer.

The E35ST-W overburden well is screened within unconsolidated sediments of the glacial aquifer overlying the bedrock. The E35ST-W well is at the same location as bedrock boreholes E35ST-D and E35ST-F. Pumping of both bedrock boreholes during specific-capacity testing had no effect on the water levels in well E35ST-W, indicating the glacial aquifer is not hydraulically connected to the transmissive bedrock fractures at this site.

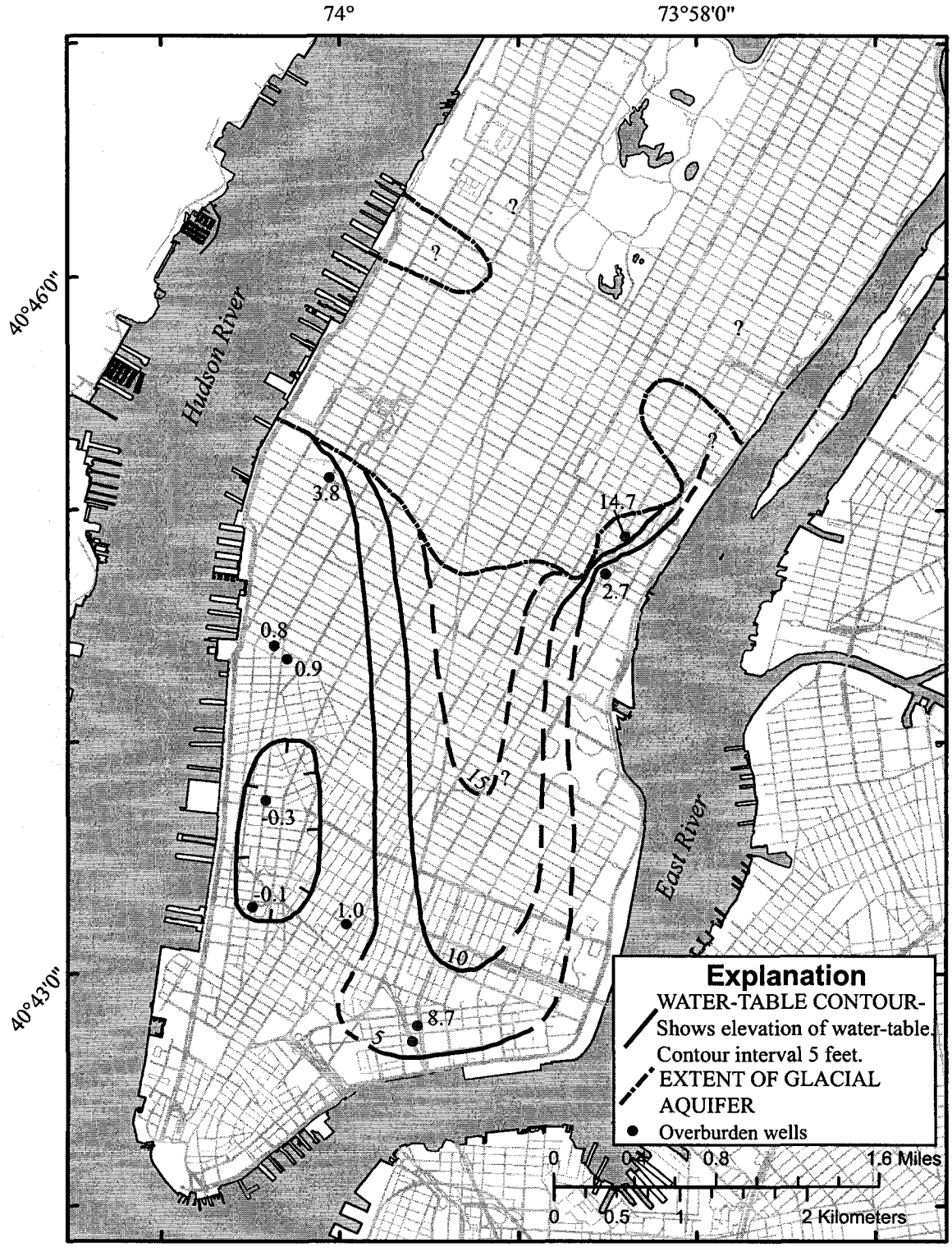

Figure 35. Water-table elevation in the glacial aquifer, Manhattan Island, N.Y., November 2004.

A cone of depression along the southwest part of the study area was indicated in the water-table map (Fig. 35) and includes wells 28B-W and 29B-W. Dewatering of the glacial aquifer in the area for subway railways is a possible explanation. Of interest is the fact that below this cone of depression the bedrock potentiometric-surface also has a cone of depression in the same general location (Figs. 26 and 35). This may indicate a possible interconnection between the overlying glacial aquifer and the fractured-rock system below in that area.

Glacial Aquifer Transmissivity

Specific-capacity tests of the 10 glacial aquifer wells indicate a wide range of aquifer transmissivity. The glacial aquifer transmissivity ranged from 2 to 93,000 ft^2/d (Table 2). The first transmissivity map of the glacial aquifer in southern Manhattan indicates lower permeable sediments near the northern extent of the aquifer (Fig. 36). The highest transmissivity was measured at well 28B-W. In general the southern part of the glacial aquifer has the higher transmissivity (Fig. 36). These high transmissivities are correlated with the southern Manhattan buried valley.

Saltwater Intrusion of the Glacial Aquifer

The only comprehensive study on the unconsolidated sediments in Manhattan was completed by Perlmutter and Arnow (1953). In that report they listed the location, depth, and chloride concentration of private wells within the study area. Examination of these data indicate 36 private wells were sampled for chloride concentration from 1940 to 1950 within the study area (Figs. 4 and 6). All of these wells were screened in the glacial

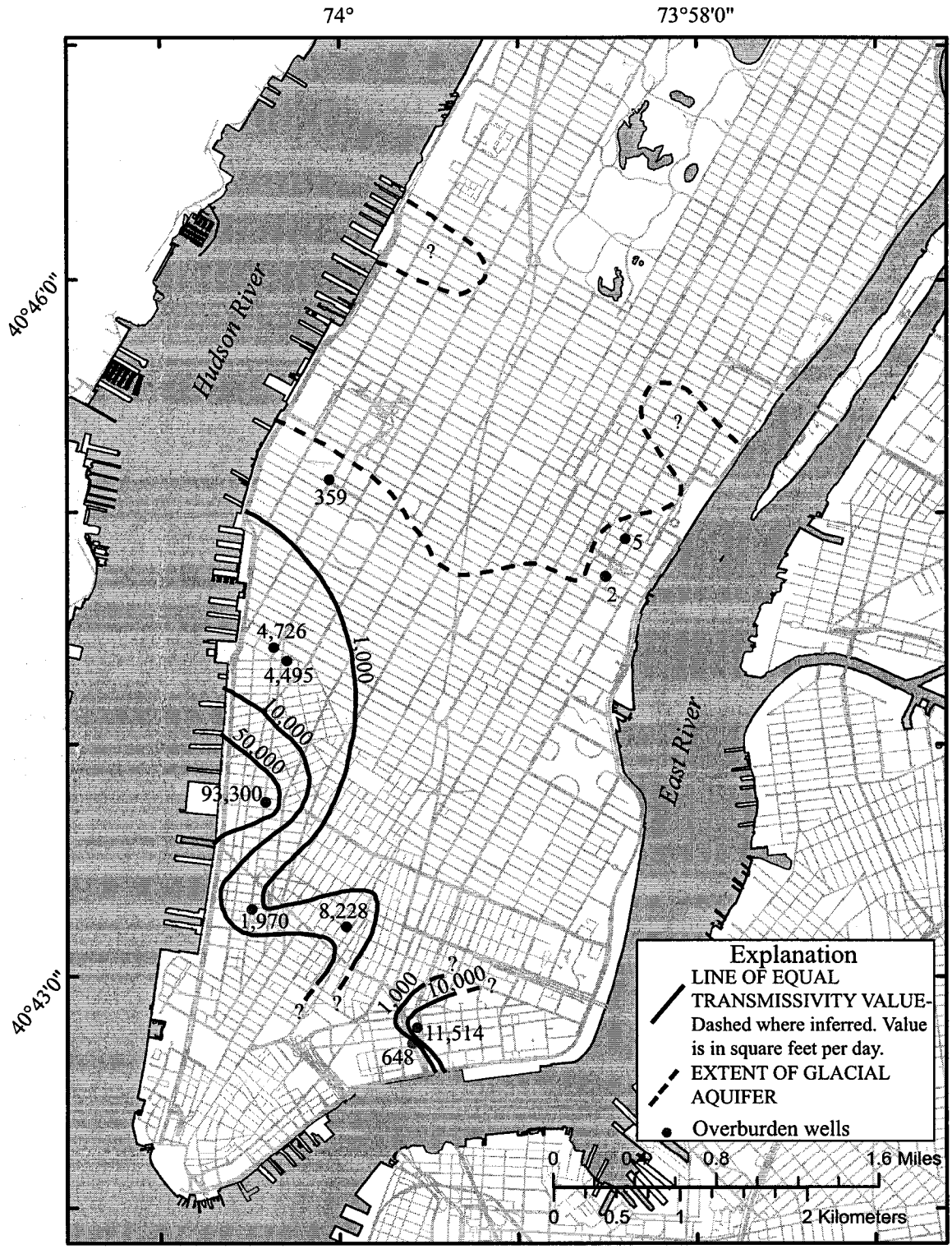

Figure 36. Transmissivity values of the glacial aquifer, Manhattan Island, N.Y.

aquifer. No chloride concentration or isochlor map of the glacial aquifer has ever been made. When these historical chloride concentrations are plotted as a historic chloride concentration map several wedges of saltwater intrusion are evident (Fig. 37). Industrial pumpage in southern Manhattan during the 1940's to 1950's was documented to be as high as 5 million gallons per day (Perlmutter and Arnow, 1953). This appears to be the leading cause for the saltwater intrusion of the glacial aquifer during that time. The limited recharge capability of this aquifer due to impervious surfaces and the extreme pumpage created a severe stress on this system. The majority of the study area appears to have had chloride concentrations less than 100 mg/L during 1940 to 1950 (Fig. 37). Three areas of historical saltwater intrusion are indicated and designated wedges A, B, and C (Fig. 37). The first historic saltwater wedge A in the southernmost part of the study area had a peak chloride concentration of 10,150 mg/L in well NY-61 (Fig. 37). This wedge of saltwater intrusion extended to well NY-101 and indicates water from the salty East River had intruded this part of the glacial aquifer in 1940 to 1950 (Figs. 6 and 37). The second historic saltwater wedge is west of saltwater wedge B along the Hudson coastline (Fig. 37). The peak chloride concentration of this wedge was 2,800 mg/L at well NY-35. The wedge is smaller than wedge A and indicates salty water from the Hudson River had intruded this part of the glacial aquifer in 1940 to 1950. A third wedge of historical saltwater intrusion wedge C was indicated along the northwesternmost part of the glacial aquifer (Fig. 37). Peak chloride concentration at well NY-83 was 2,350 mg/L.

Current chloride concentration data from these private wells is not available, many of these wells have been destroyed or abandoned. Ground-water grab samples

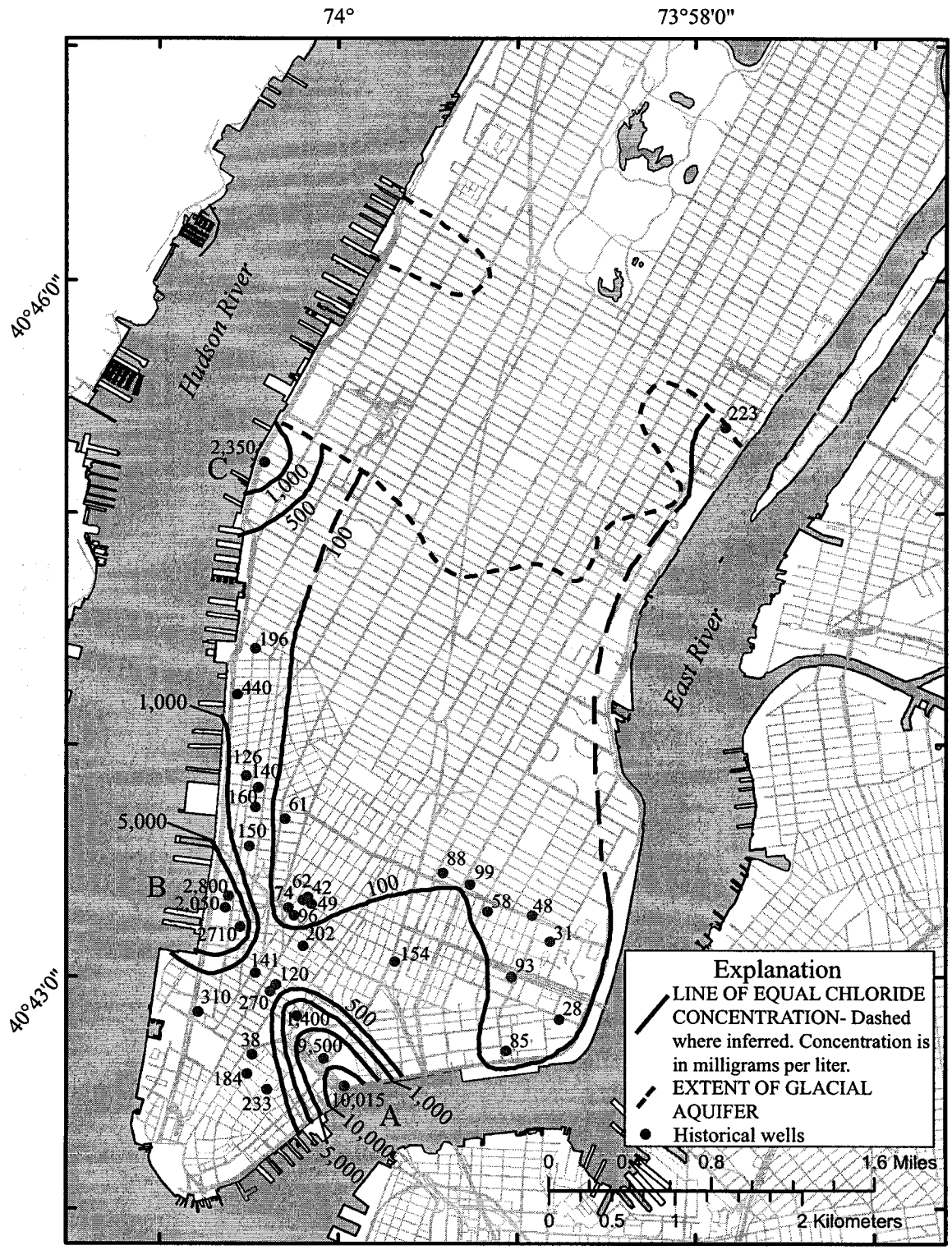

Figure 37. Chloride concentrations in the glacial aquifer from 1940-50, Manhattan Island, N.Y., saltwater wedges A, B, and C shown (Data from Perlmutter and Arnow, 1953).

were obtained from the 10 recently installed observation wells screened in the glacial aquifer during specific-capacity testing in 2004. Figure 38 is the first chloride concentration or isochlor map of the glacial aquifer in southern Manhattan. The map includes chloride data collected in 2004. Chloride concentrations in the glacial aquifer ranged from 28 mg/L at well PikeST-W (35 ft deep) and 15,250 mg/L at well Monroe-4 (185 ft deep) (Figs. 6 and 38). The majority of the central part of the glacial aquifer appears to have less than 100 mg/L chloride concentrations. However, given the lack of observation wells in this area this is uncertain. The majority of the 10 glacial aquifer wells were located along the coastal areas. Three areas of saltwater intrusion were indicated and designated saltwater wedges A, B, and C (Fig. 38). Saltwater wedge A appears to be a remnant of the historical saltwater wedge in this same area more than 50 years ago (Fig. 38). Peak chloride concentration was 15, 250 mg/L at the Monroe-4 well.

EM logs of three bedrock boreholes (SouthST-A, PikeST-A, and EldridgeST-A) and one glacial aquifer well (Monroe-4) cased in PVC facilitated the delineation of saltwater wedge A in the glacial aquifer (Fig. 39). EM logs of these wells indicate the highest concentrations are found at Monroe-4 and PikeST-A. SouthSt-A while closest to the coastline is probably northeast of saltwater wedge A's peak concentration area. EldridgeST-A had the lowest concentrations and the thinnest saltwater wedge indicating this borehole is at the toe of saltwater wedge A. The EldridgeST-A borehole is also located near the northern extent of saltwater intrusion area A in the bedrock (Figs. 32, 33, and 39). Using the peak EM log response at Monroe-4 and the measured chloride concentration of that zone a conversion factor was calculated for the glacial aquifer. This conversion factor technique has been used to estimate the chloride concentration of

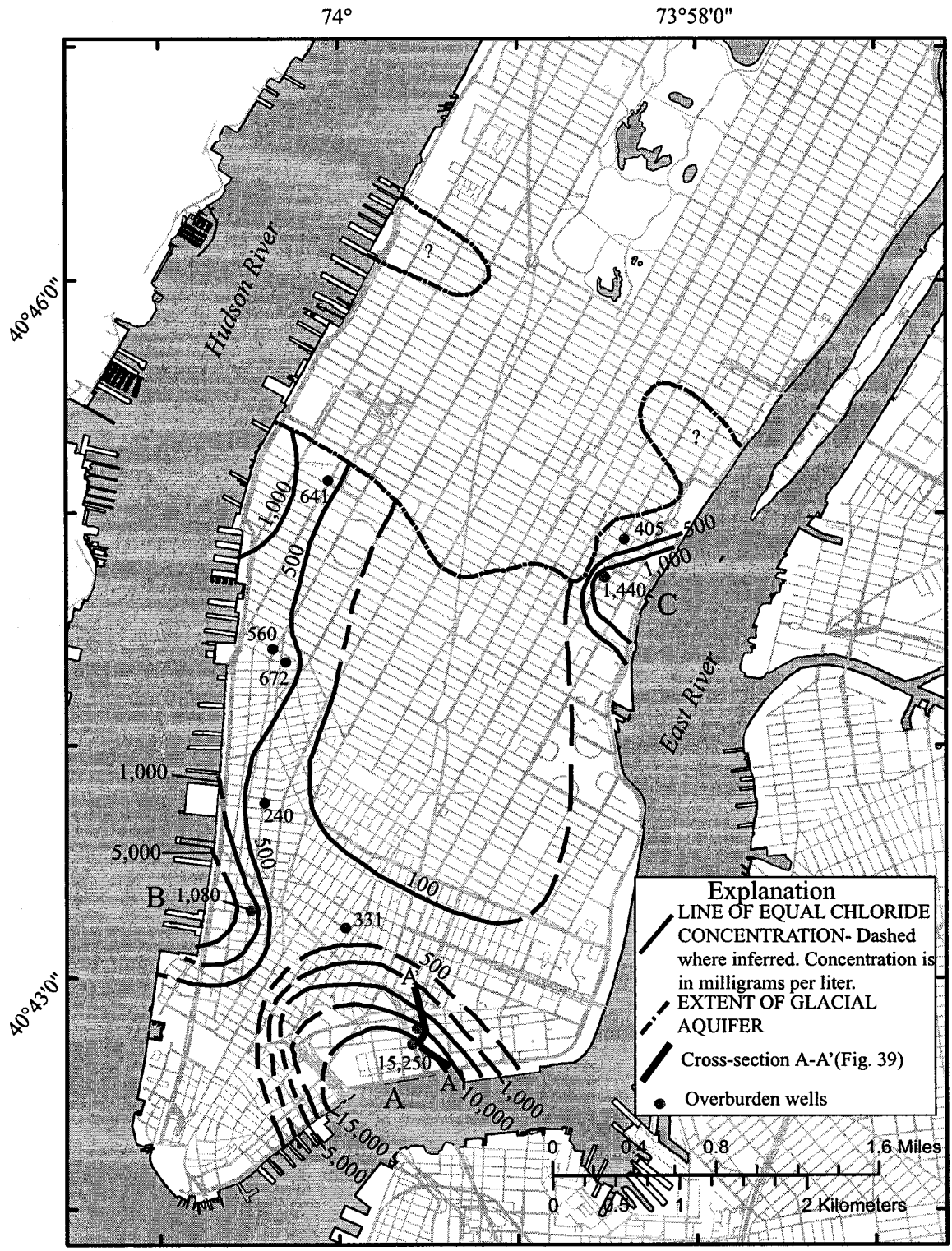

Figure 38. Chloride concentrations in the glacial aquifer in 2004, Manhattan Island, N.Y., (saltwater wedges A, B, and C shown).

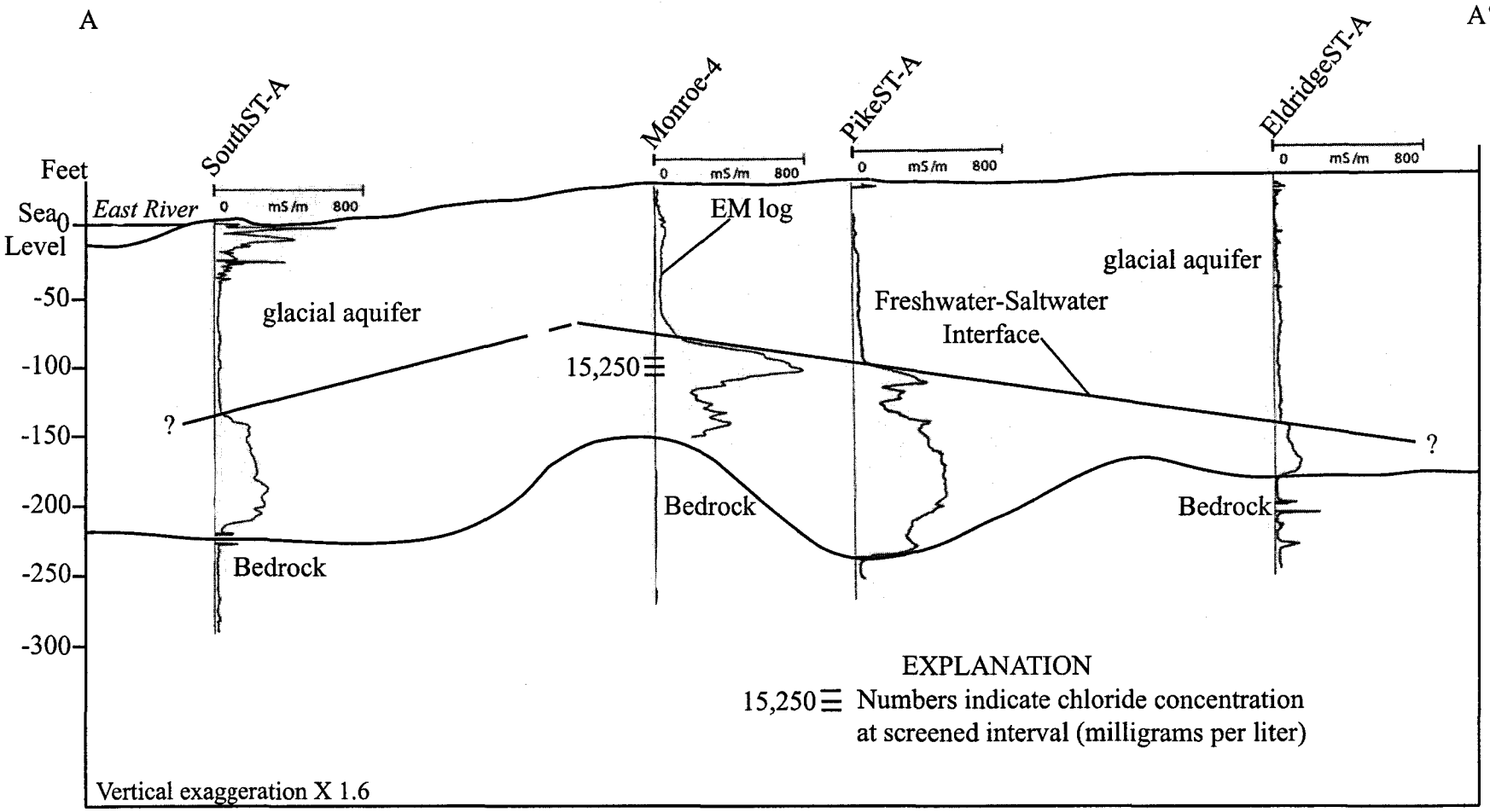

Figure 39. Hydrogeologic section showing the extent of saltwater wedge A, Manhattan Island, N.Y. (location shown in Fig. 38).

saltwater wedges using peak EM log responses in aquifers on Long Island (Stumm, 2001c; Stumm and others, 2002). The peak EM response at Monroe-4 was 777 mS/m which correlates to a chloride concentration of 15,250 mg/L (Fig. 39). The saltwater wedge is 84 ft thick with a freshwater-saltwater interface 91 ft BLS (-62 ft elevation). Using this relation the peak EM responses at SouthST-A, PikeST-A, and EldridgeST-A were used to estimate peak chloride concentrations. SouthST-A had a peak EM response of 280 mS/m which correlates to an estimated chloride concentration of 5,500 mg/L (Fig. 39). Saltwater wedge A is 75 ft thick and the freshwater-saltwater interface is a sharp contact at 141 ft BLS (-135 ft elevation). At PikeST-A the peak EM log response was 470 mS/m which correlates to an estimated chloride concentration of 9,200 mg/L (Fig. 39). Saltwater wedge A is 138 ft thick at this borehole with a sharp freshwater-saltwater interface 131 ft BLS (-96 ft elevation). The farthest inland borehole
that was EM logged was EldridgeST-A. The saltwater wedge A is 38 ft thick with an estimated peak chloride concentration of 2,800 mg/L (Fig. 39). The freshwater-saltwater interface is a sharp contact 175 ft BLS (-131 ft elevation).

The saltwater wedge B is located on the southwestern coastal area of the study area (Fig. 38). Saltwater wedge B appears to be another remnant of a historical saltwater wedge documented in that area in 1940 to 1950 (Perlmutter and Arnow, 1953). Well 29B-W is located within saltwater wedge B, had a chloride concentration of 1,080 mg/L. Another saltwater wedge C was indicated along the central-eastern coastline (Fig. 38). Wells E35ST-W and E39ST-W had chloride concentrations of 1,440 and 405 mg/L, respectively.

Discussion

The first water-table map in southern Manhattan indicates ground-water in the glacial aquifer appears to be unconfined with water level elevations ranging from 14.7 ft at E39ST-W to -0.3 ft at 28B-W. The highest water levels occur in the central part of the study area which appears to be the recharge zone for the aquifer. Ground-water flows from the central part of the study area toward the south, west, and east coastal discharge zones. A cone of depression along the southwest part of the study area was indicated in the water-table map and includes wells 28B-W and 29B-W. Dewatering of the glacial aquifer in the area for subway railways is a possible explanation. This may indicate a possible interconnection between the overlying glacial aquifer and the fractured-rock system below in that area of southern Manhattan.

Specific-capacity tests of the 10 glacial aquifer wells indicate a wide range of aquifer transmissivity from 2 to 93,000 ft^2/d. The first transmissivity map of the glacial aquifer in southern Manhattan indicates lower permeable sediments near the northern extent of the aquifer.

Historical chloride data indicate 36 private wells were sampled for chloride concentration from 1940 to 1950 within the study area. No chloride concentration or isochlor map of the glacial aquifer had ever been made. A historic chloride concentration map presented in this chapter indicated three wedges of historical saltwater intrusion are indicated and designated wedges A, B, and C. The majority of the study area appears to have had chloride concentrations less than 100 mg/L during 1940 to 1950. The first historic saltwater wedge A in the southernmost part of the study area had a peak chloride concentration of 10,150 mg/L in well NY-61. This wedge of saltwater intrusion extended

to well NY-101 and indicates water from the salty East River had intruded this part of the glacial aquifer in 1940 to 1950. The second historic saltwater wedge is west of saltwater wedge B along the Hudson coastline had a peak chloride concentration of 2,800 mg/L at well NY-35. A third wedge of historical saltwater intrusion wedge C was indicated along the northwesternmost part of the glacial aquifer and had a peak chloride concentration at well NY-83 of 2,350 mg/L.

The first chloride concentration or isochlor map of the glacial aquifer in southern Manhattan was presented in this chapter. The map includes chloride data collected in 2004. Chloride concentrations in the glacial aquifer ranged from 28 mg/L at well PikeST-W (35 ft deep) and 15,250 mg/L at well Monroe-4 (185 ft deep). The majority of the central part of the glacial aquifer appears to have less than 100 mg/L chloride concentrations. Three areas of saltwater intrusion were indicated and designated saltwater wedges A, B, and C. Saltwater wedge A appears to be a remnant of the historical saltwater wedge in this same area more than 50 years ago. Peak chloride concentration was 15, 250 mg/L at the Monroe-4 well.

EM logs of three bedrock boreholes (SouthST-A, PikeST-A, and EldridgeST-A) and one glacial aquifer well (Monroe-4) cased in PVC were used to delineate saltwater wedge A in the glacial aquifer. EM logs of these wells indicate the highest concentrations are found at Monroe-4 and PikeST-A. Estimated chloride concentrations using EM log responses in the PVC cased overburden parts of boreholes SouthST-A, PikeST-A, and EldridgeST-A were 5,500, 9,200, and 2,800 mg/L, respectively.

EldridgeST-A had the lowest concentrations and the thinnest saltwater wedge indicating this borehole is at the toe of saltwater wedge A. The EldridgeST-A borehole is also located near the northern extent of saltwater intrusion area A in the bedrock.

The saltwater wedge B is located on the southwestern coastal area of the study area and appears to be another remnant of a historical saltwater wedge documented in that area in 1940 to 1950. Well 29B-W is located within saltwater wedge B, had a chloride concentration of 1,080 mg/L. Another saltwater wedge C was indicated along the central-eastern coastline had a peak chloride concentration of 1,440 mg/L at well E35ST-W.

4. Discussion

A total of 64 bedrock boreholes and 10 glacial aquifer wells were installed from 1998 to 2004 in southern Manhattan. Advanced borehole geophysical and hydrologic techniques were applied at the boreholes and wells to delineate the fractured-rock and unconsolidated overburden ground-water flow systems. The study was a unique opportunity to characterize both ground-water flow systems in a highly urbanized environment.

Fractured-Rock (Bedrock)

ATV, OTV, and borehole radar data indicate all boreholes penetrate moderately fractured bedrock with medium and large transmissive fractures. Stereonet analyses of the fractures delineated in all 31 geophysically logged boreholes indicate the majority of fractures were subhorizontal with a secondary population of fractures dipping toward the northwest. Similar findings were made when all large fractures were plotted and analyzed using stereonets. Fifty-three faults were delineated in the 31 boreholes using the OTV. Stereonet analysis of the faults indicate two population clusters with mean orientations of N12°W, 66°W and the other N11°W, 70°E. The strike trends of both of these fault populations are roughly subparallel to large scale northwest trending faults mapped in the area (Berkey, 1910 and Baskerville, 1994). Foliation was fairly consistent throughout the study area with the majority of boreholes indicating northwest to southwest dip azimuths and dip inclination angles in the 30° to 70° range.

The first potentiometric-surface map of southern Manhattan indicates a ground-water recharge area in the vicinity of Central Park and ground-water discharge areas

along the southern, western, and eastern coastlines. Two large cones of depression were also indicated. Heat-pulse flowmeter logging of 8 boreholes in the study area delineated 77 transmissive fractures. Stereonet analysis indicated the fractured-rock ground-water flow system in southern Manhattan consists of subhorizontal fractures and cross-cutting northwest dipping fractures. The presence of the northwest dipping transmissive fractures may explain the fairly even distribution of hydraulic head found in most boreholes. The relatively small amount of ambient flow detected by heat-pulse flowmeter logging suggests small differences in hydraulic head of fractures encountered in the boreholes.

Specific-capacity test data from 59 boreholes indicate the total borehole transmissivity ranged from 0.7 to 871 ft^2/d. The first bedrock transmissivity map of southern Manhattan indicates two areas of elevated transmissivity, one in the southernmost part, and the second in the northeastern part of the study area.

Chloride concentrations measured at 57 bedrock boreholes indicate three areas of saltwater intrusion in the fractured-rock ground-water flow system in southern Manhattan. Chloride concentrations ranged from 25 mg/L at GroveST-A to 17,800 mg/L at SouthST-A. Three areas of saltwater intrusion were designated areas A, B, and C in the bedrock. Saltwater intrusion area A had the highest chloride concentrations and is located in the southernmost part of the study area. The freshwater-saltwater interface appears to be very narrow suggesting a highly interconnected transmissive fracture network. Within this saltwater intrusion area several boreholes had the highest chloride concentrations of any borehole tested. In addition, these same boreholes had the highest transmissivity values as well. This suggests an interconnected network of highly

transmissive fractures in this area. It was uncertain how extensively the bedrock fractures were interconnected.

The TBM Ultimate Pump Test

In the summer of 2003 the South Water-Tunnel TBM began excavating a new tunnel toward the southern part of the study area at 600 ft below land surface. Analysis of the potentiometric-surface map, chloride concentration map, and transmissivity map of the bedrock suggested the fractured-rock ground-water flow system acted like a continuum with fracture interconnections. However, it was still unclear how extensive such interconnections were in southern Manhattan. Unbeknownst to the author the approaching TBM was about to provide the ultimate pump test for a fractured-rock ground-water investigation and verify the major hypothesis for this dissertation.

Digital and manual measurements of the water levels at the GroveST-A and HoustonSt-A boreholes indicated that on or near January 14, 2004 there was a sudden and almost instantaneous decline in water levels. The GroveST-A borehole located in the southwestern part of the study area had a 5 ft decline in water levels. Shortly thereafter the GroveST-A borehole was sealed in anticipation of the nearby arrival of the TBM. The author inferred that the declines in water levels at both wells was due to the close proximity of the advancing TBM. However, examination of the NYCDEP excavation records for the TBM indicated it was actually 2,500 ft north of the GroveST-A borehole on or about January 14, 2004. This indicates that when the TBM encountered a specific set of transmissive fractures, 600 ft below the land surface, the resulting hydraulic stress (depressurization of the fractures) was measured on January 14, 2004 as a rapid decline

in water levels in the GroveST-A borehole 2,500 ft to the south. This was an extraordinary piece of evidence that the bedrock was a continuum of interconnected transmissive fractures.

A second TBM ultimate pump test occurred nine months later in late September to early October, 2004 in the southernmost part of the study area. Hydrographs from MPP-5, CatherineST-A, StJamesST-A, and PikeST-B indicated sudden nearly instantaneous declines in water levels from 1 to 5 ft. Digital water-level recorders at StJamesST-A and PikeST-B indicated sudden declines on or about late September to early October, 2004. At that time the TBM had already completed a wide turn toward the east near FranklinST-A and FranklinST-B and was then heading north toward 31B-1. This explains why the decline was first measured at StJamesST-A and later at PikeST-B (StJamesST-A is slightly farther south than PikeST-B). No local explanation for the nearly instantaneous declines in water levels could be found. The depth to bedrock in this area ranges from 100 to over 200 ft below sea level. When NYCDEP excavation records were analyzed by the author the TBM was northwest of the boreholes at that time. The distance from the boreholes to the TBM excavation line was 2,500, 2,700, 3,100, and 3,200 ft at the MPP-5, CatherineST-A, StJamesST-A, and PikeST-B boreholes, respectively. This indicates that when the TBM encountered a specific set of transmissive fractures, 600 ft below the land surface, the resulting hydraulic stress (depressurization of the fractures) was measured at the end of September to early October, 2004 up to 3,200 ft away in these boreholes. This is another independent verification that the fractured-rock ground-water flow system in southern Manhattan is a continuum of interconnected transmissive fractures.

Both TBM ultimate pump test examples provide definitive evidence of transmissive fracture interconnections in the bedrock that extend at least 3,200 ft. It is unclear how much a delay occurred between the TBM encounter of specific transmissive fractures and the measurable response in these boreholes. However, these data combined with the chloride concentration, transmissivity, and potentiometric-surface data verify the hypothesis that the fractured-rock ground-water flow system in southern Manhattan is a continuum.

Glacial Aquifer

The glacial aquifer appears to be limited in its northern extent north of 30th Street. North of 30th Street within the study area the sediments appear to be mostly unsaturated except in isolated areas.

The first-ever water-table map of the glacial aquifer presented in Chapter 3 indicates an unconfined system with a recharge zone in the central-northern part and discharge zones along the sooth, west, and east coastal areas. Transmissivity of the glacial aquifer ranged from 2 to 93,000 ft^2/d. The first transmissivity map of the glacial aquifer indicates the highest transmissivity values were in the southern parts of the study area and lowest in the northern parts.

Historical chloride data collected by Perlmutter and Arnow (1953) from 1940 to 1950 in 36 private glacial wells was contoured. Three wedges of saltwater intrusion designated wedges A, B, and C were indicated in the glacial aquifer at that time. The highest chloride concentrations were found within saltwater wedge A in the southernmost part of the study area. The limited recharge capability of the aquifer due to impervious

surfaces and the 5 million gallons per day of reported industrial pumpage was probably the cause for the saltwater intrusion of the glacial aquifer.

In 2004 chloride concentrations from the 10 glacial aquifer wells indicated three saltwater wedges. Two of the saltwater wedges designated A and B appear to be remnants of the historical saltwater intrusion wedges delineated earlier. Industrial pumpage appears to have ceased in the glacial aquifer probably due to current regulations and elevated chloride concentrations and dissolved solids. EM logs provided a unique opportunity to delineate the thickness and concentration of saltwater wedge A. The EM logs indicate the freshwater-saltwater interface is still very sharp or narrow. In spite of the cessation of industrial pumpage 55 years ago the freshwater head in the glacial aquifer has been unable to push the saltwater interface to any measurable degree back to its source. This suggests the glacial aquifer is not in equilibrium and may not have recovered from the extensive pumpage or the lack of recharge.

Aquifer Interconnections

The extent of hydraulic interconnection between the bedrock and glacial aquifers is unclear. One indication of some areas with little or no hydraulic interconnection was the specific-capacity pump tests at E35ST-D and E35ST-F. Both pump tests failed to lower water levels in a nearby glacial well E35ST-W. It is possible that the specific-capacity tests were not long enough or of a large enough stress to cause a decline in the overlying glacial aquifer. Other possibilities might be that the bedrock in this part of the study area contains fewer northwest dipping transmissive fractures that crop out at the

bedrock surface, or the bedrock surface could be more saprolitic in this area. Saprolite consists of significant amounts of clay which would impede ground-water flow.

Comparison of the bedrock potentiometric-surface and glacial aquifer water-table maps indicates overlapping ground-water divides and similar head values in the southern part of the study area. This suggests a possible interconnection between the two ground-water flow systems. Another possible line of evidence for interconnection is the nearly identical location of saltwater intrusion areas and wedges in both the fractured-rock and glacial aquifer maps. Both chloride concentration maps of the bedrock and glacial aquifer indicate the highest chloride concentrations occurred in the same southernmost part of the study area. Similar overlap in the locations of two other saltwater intrusion areas in both ground-water flow systems were also indicated. In addition, both saltwater intrusion areas in this part of the study area had narrow or sharp freshwater-saltwater interfaces. The EldrigeST-A borehole was at the northern toe of both the glacial aquifer saltwater wedge and the bedrock saltwater intrusion area. This suggests hydraulic interconnection between both ground-water flow systems may exist in this area.

A cone of depression in the southwestern part of the study is indicated in the same location in both the glacial aquifer and fractured-rock water-level maps. One possible mechanism may be the cropping out of transmissive fractures at the bedrock surface. These fractures would be in direct hydraulic connection with the overlying glacial aquifer. Dewatering in the southwestern part of the study area in the glacial aquifer may have lowered heads in transmissive fractures of the bedrock below. If glacial scouring of the bedrock surface removed saprolite from the bedrock surface in parts of the study area it could provide a potential hydraulic interconnection.

Based upon the similarities in the ground-water divide locations, saltwater intrusion locations, and a cone of depression location in both ground-water flow systems there appears to be possible bedrock and glacial aquifer hydraulic interconnection in parts of the study area. This indicates that one of the dissertation hypotheses that the fractured-rock and glacial aquifer ground-water flow systems are separate systems may be somewhat incorrect. It might be more accurate to describe the two ground-water flow systems as separate systems with some indications of hydraulic interconnection.

5. Conclusions

This study has accomplished all of the objectives outlined at the beginning of this investigation. The author has delineated the fractured-rock and unconsolidated overburden ground-water flow systems in southern Manhattan through the use of advanced borehole geophysical techniques. Using a toolbox approach of multiple geophysical probes and techniques the initial hypotheses have been verified. 1) There are definite structural patterns to the major population orientations of both fractures and foliation, 2) there are patterns to the distribution of hydraulic head in both the bedrock boreholes and fractures indicating a continuum or inter-connectivity of transmissive fractures and there are recharge areas in the center of the island and discharge zones along the coastlines, and 3) transmissive fractures have similar structural trends or orientations in southern Manhattan. The fourth hypothesis that the unconsolidated overburden is a separate ground-water flow system from the bedrock may be too restrictive.

Sixty-four boreholes were drilled by the NYCDEP during 1998-2004 to identify the type of rock and its degree of fracturing in the boreholes at the proposed tunnel depths. Ten overburden wells were also utilized to delineate the hydraulic head, transmissivity, and chloride concentration of the overburden sediment ground-water flow system.

The first objective of this dissertation was to determine the spatial distribution of fractures and foliation. This was accomplished by analyzing the OTV and ATV data. Stereonet analysis of the fractures delineated in all 31 boreholes indicate a majority of the fractures were subhorizontal with a secondary population that dip toward the northwest.

A similar grouping was found when all 208 large fractures were analyzed. Foliation data from all 31 boreholes indicates a fairly consistent dip azimuth between northwest and southwest throughout the study area. In general the foliation dip inclination was lowest in the northeastern part of the study area and gradually increased to about 70° in the rest of the study area. The hypothesis that there are structural patterns to the major population orientations of both foliation and fractures was verified.

The second and third objectives of this study were to determine which fractures were transmissive and to determine their orientations. Both of these objectives were accomplished using a toolbox approach with advanced borehole geophysical techniques. The OTV, fluid parameter logs, and the heat-pulse flowmeter were most instrumental in delineating the transmissive fractures. Seventy-seven transmissive fractures were delineated from the 8 boreholes logged with the heat-pulse flowmeter and other probes. Stereonet analysis indicated two population clusters of transmissive fractures in southern Manhattan. The first was subhorizontal with a mean orientation of N11°E, 14°SE and the second was northwest dipping with a mean orientation of N23°E, 57°NW. These data verify the hypothesis that transmissive fractures have similar structural trends or orientations in southern Manhattan.

Another objective of this study was to determine if an interconnection of fracture networks exists. This was the most important objective and it was accomplished using the TBM, the potentiometric-surface map, the chloride concentration map, and the transmissivity map. Two TBM ultimate pump tests provided definitive evidence of a highly interconnected network of transmissive fractures. Boreholes as far as 3,200 ft away from the TBM had declines in water-levels due to hydraulic stresses induced by the

TBM. These data combined with the head distributions, cones of depression, and high transmissivity/chloride concentration boreholes verified the most important hypothesis in this dissertation, that the fractured-rock ground-water flow system is a continuum of interconnected transmissive fractures.

The final hypothesis of this dissertation, that the unconsolidated overburden aquifer is a separate ground-water system from the bedrock requires some modification based upon the data obtained during the study. At first glance the two ground-water flow systems are separate and different. The glacial aquifer is an unconsolidated porous ground-water flow system that is unconfined. The bedrock is a fractured-rock ground-water flow system that depends on transmissive fractures to transmit ground water. However, comparison of the potentiometric-surface and water-table maps indicates overlapping locations of the ground-water divide, similar locations of a cone of depression, and similar head values in the southern part of the study area. In addition, the locations of saltwater intrusion areas and wedges in both ground-water flow systems coincide with each other. These data suggest that transmissive fractures may crop out at the bedrock surface and could be in hydraulic connection with the glacial aquifer above. The final hypothesis should be modified to state that while the fractured-rock and unconsolidated overburden ground-water flow systems are separate and different there appears to be hydraulic interconnections between the two systems in parts of the study area.

This dissertation produced a number of unique data sets and maps for the fractured-rock and overburden sediment for first time in this study area. This study was the first to accomplish the following in southern Manhattan:

1. Delineate the orientation and spatial distribution of fractures from boreholes.
2. Delineate the orientation and spatial distribution of foliation from boreholes.
3. Map the potentiometric-surface of the bedrock on this scale.
4. Determine the orientation of transmissive fracture populations.
5. Demonstrate hydraulic interconnection of fractures as far as 3,200 ft from a TBM.
6. Determine the spatial distribution of bedrock transmissivity.
7. Determine the spatial distribution of chloride concentrations in bedrock.
8. Delineate three saltwater intrusion areas in the bedrock.
9. Delineate the extent of the glacial aquifer.
10. Map the water-table of the glacial aquifer on this scale.
11. Determine the spatial distribution of transmissivity in the glacial aquifer.
12. Determine the spatial distribution of chloride concentrations in the glacial aquifer from 1940 to 1950.
13. Determine the spatial distribution of chloride concentrations in the glacial aquifer in 2004.
14. Delineate the thickness and chloride concentration throughout a saltwater wedge in the glacial aquifer using EM logs.

6. Appendices 1 through 11

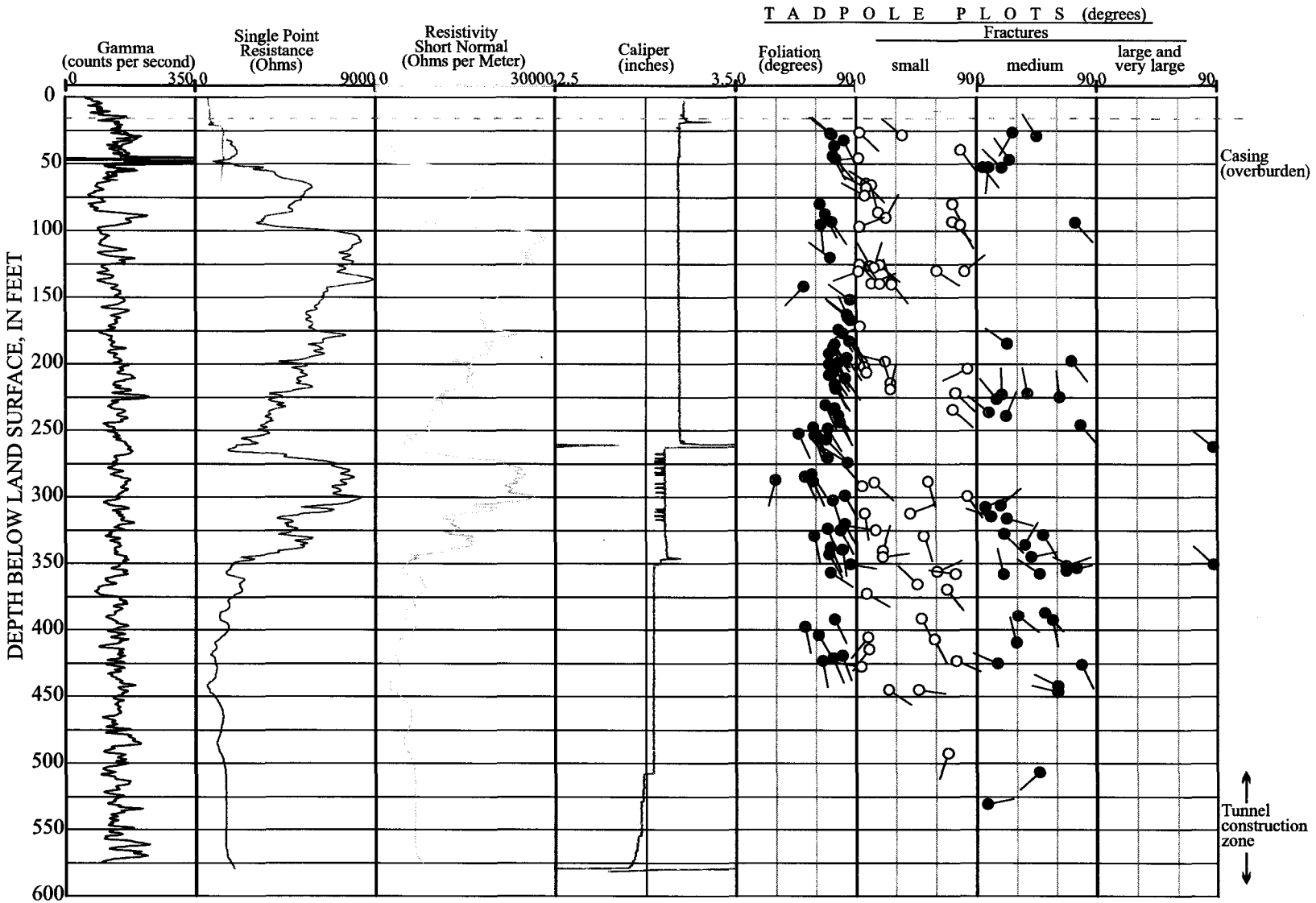

Appendix 1a. Suite of borehole-geophysical logs from borehole W65ST-A, Manhattan Island, N.Y.,.

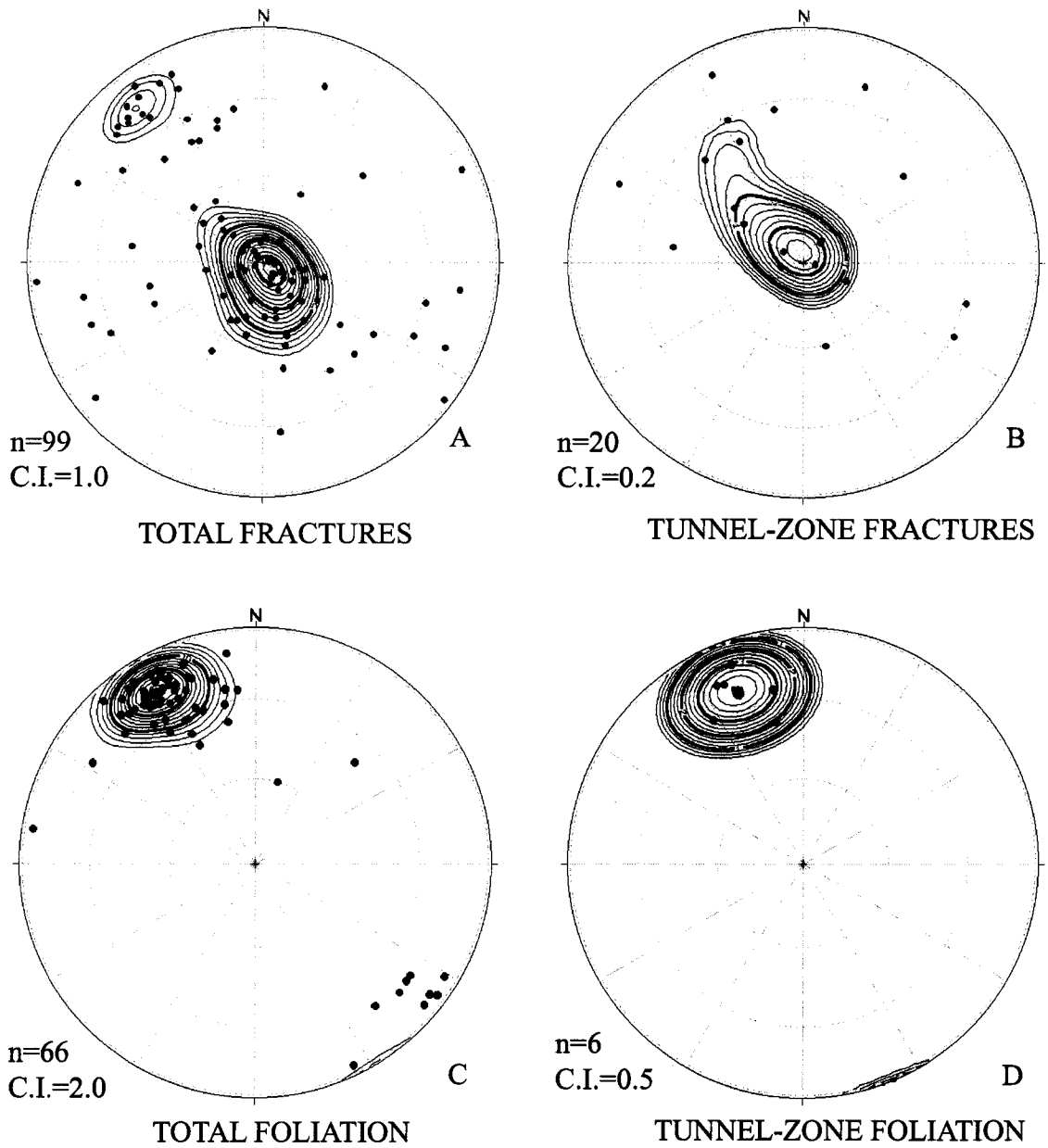

Appendix 1b. Stereonet plots of borehole W65ST-A, Manhattan Island, N.Y.,: A. Total fractures. B. Tunnel-zone fractures. C. Total foliation. D. Tunnel-zone foliation.

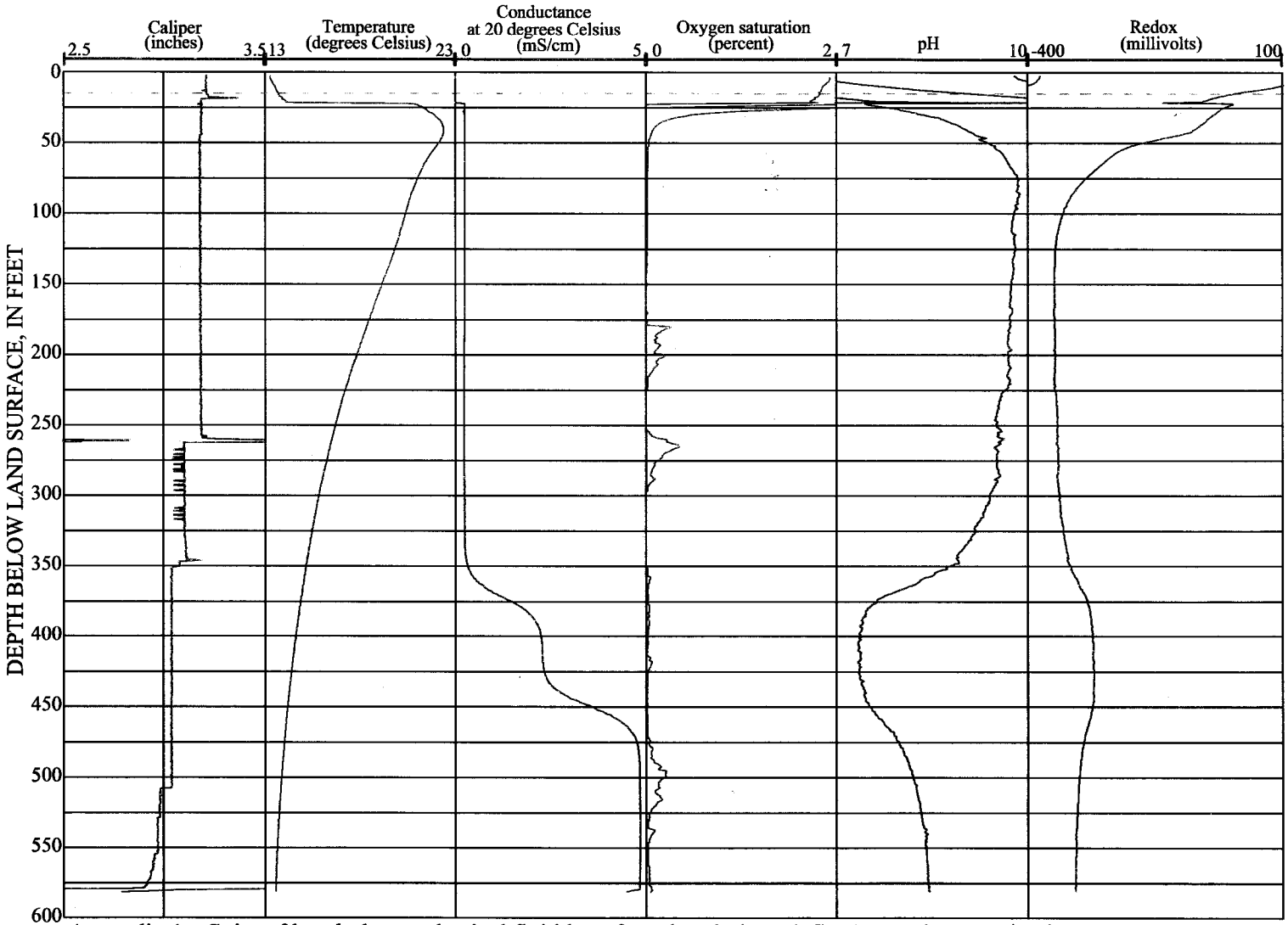

Appendix 1c. Suite of borehole-geophysical fluid logs from borehole W65ST-A, Manhattan Island, N.Y.,

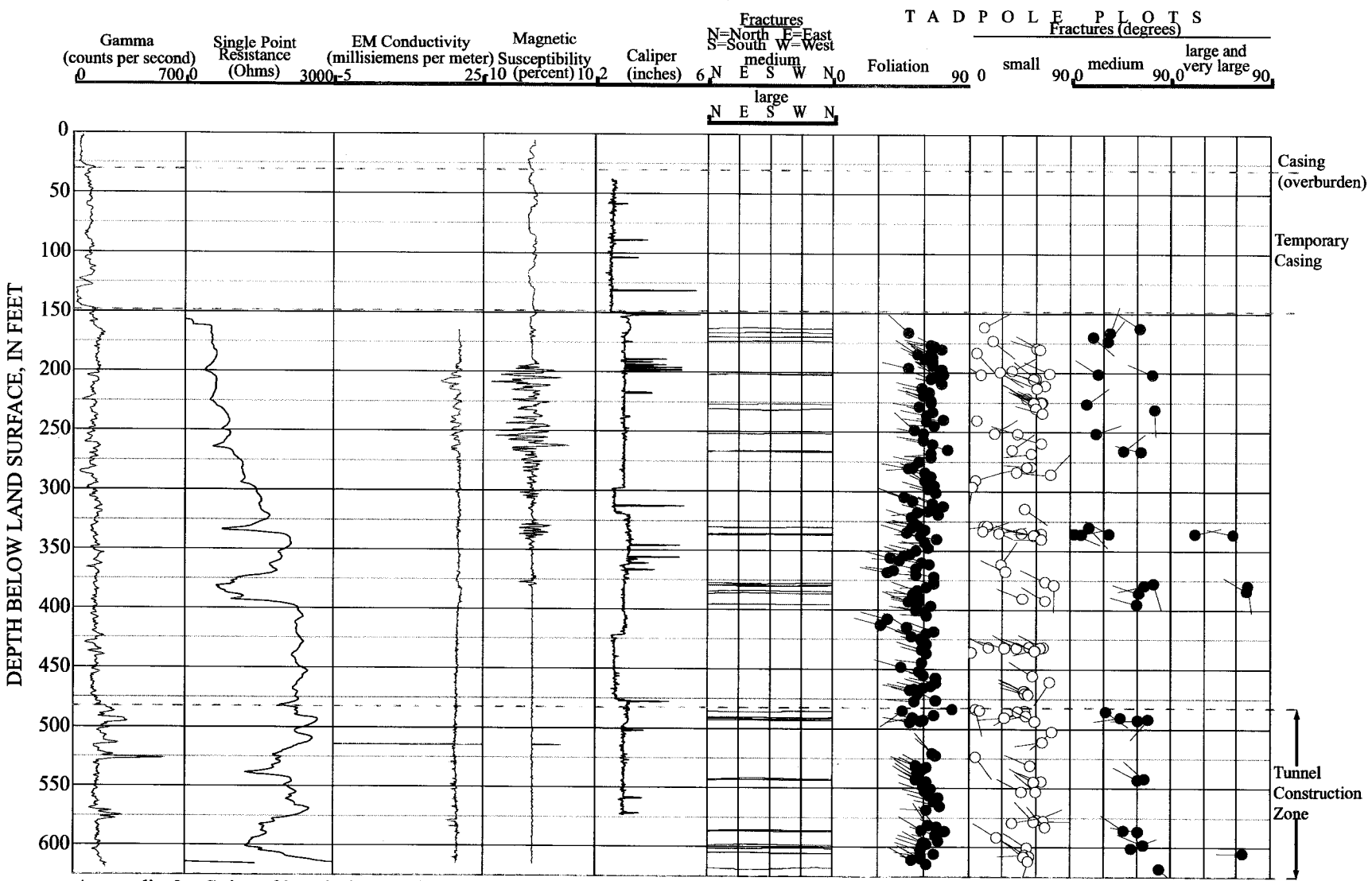

Appendix 2a. Suite of borehole-geophysical logs from borehole W55ST-A, Manhattan Island, N.Y.

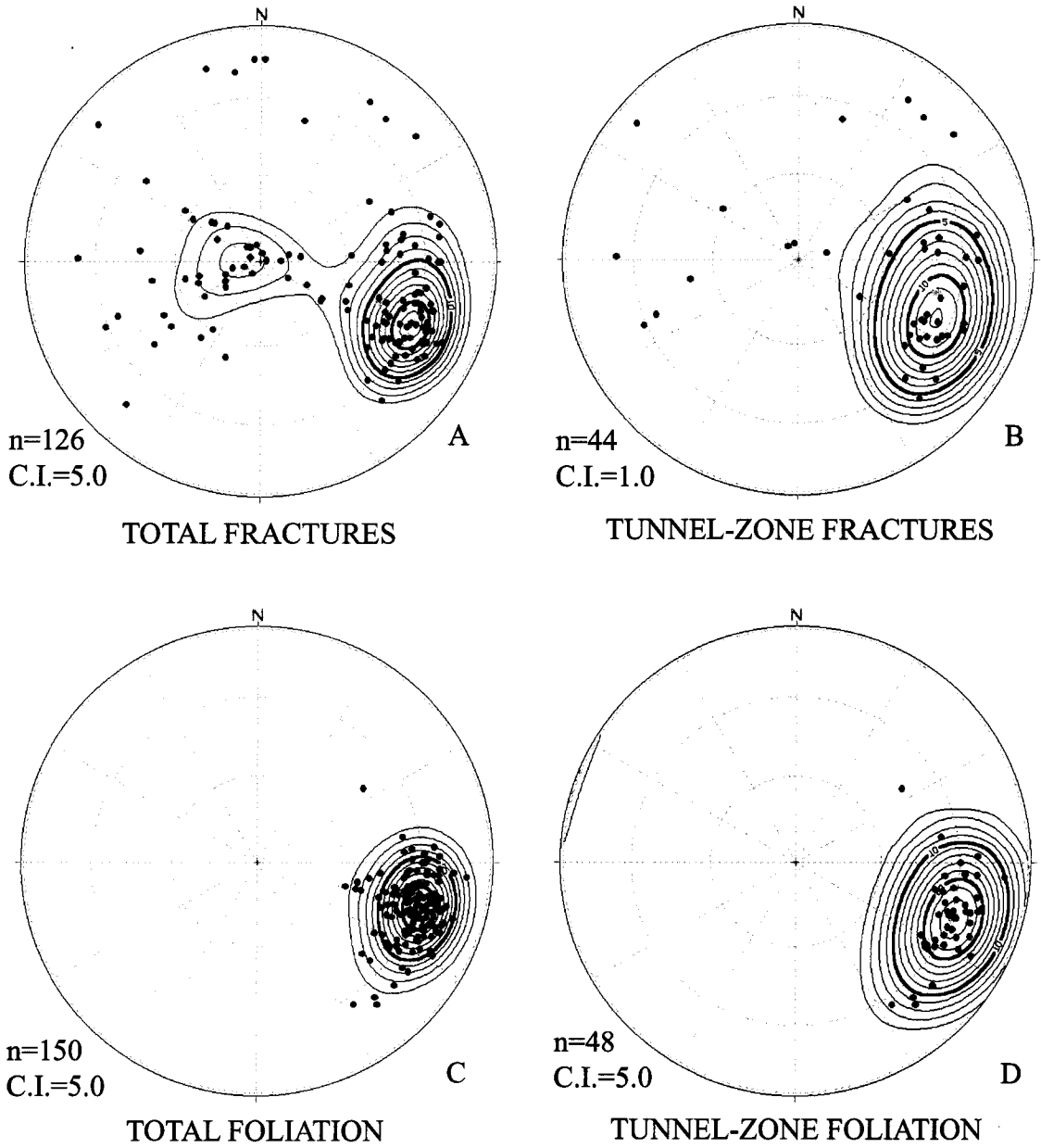

Appendix 2b. Stereonet plots of borehole W55ST-A, Manhattan Island, N.Y.,: A. Total fractures. B. Tunnel-zone fractures. C. Total foliation. D. Tunnel-zone foliation.

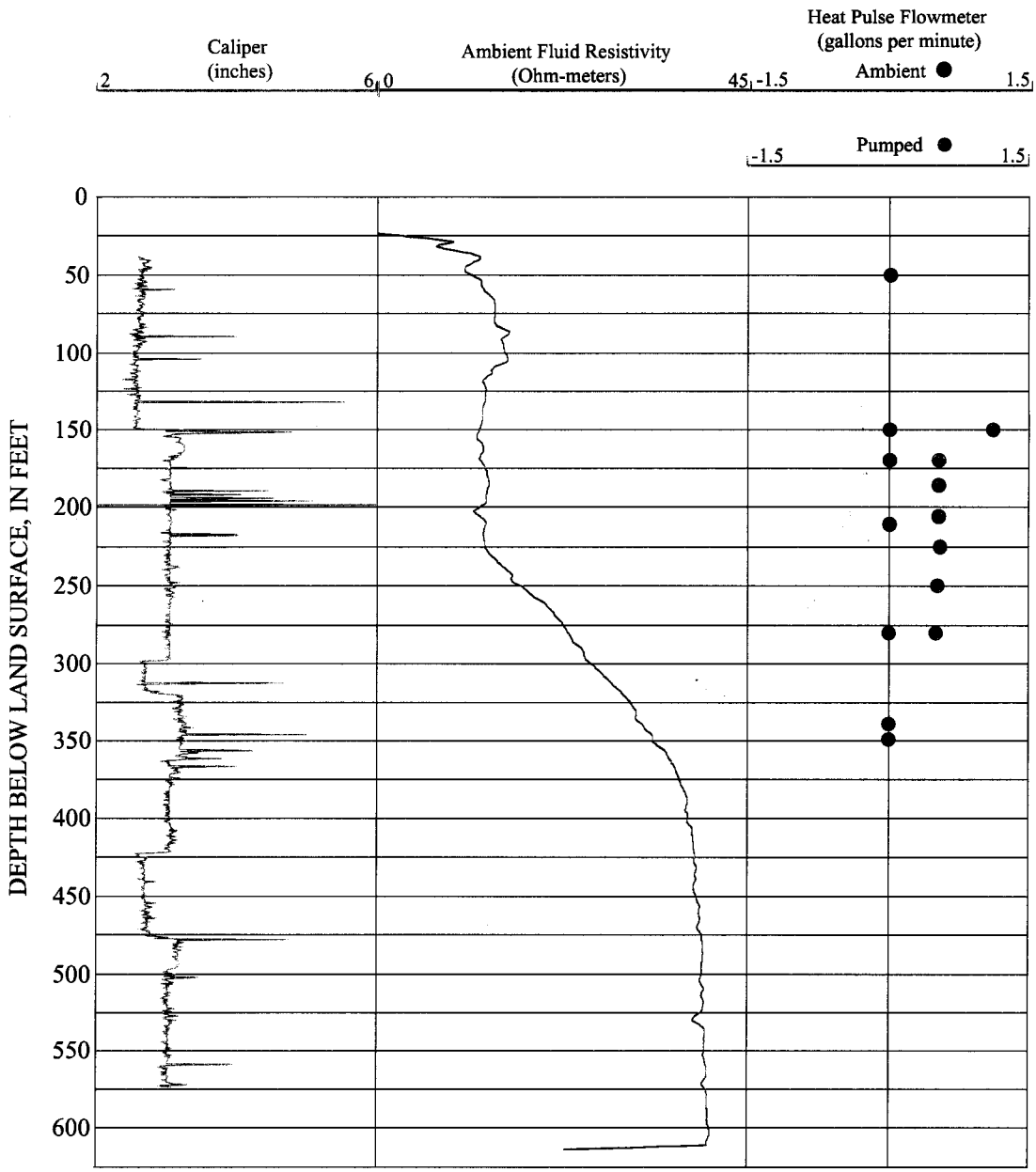

Appendix 2c. Suite of borehole-geophysical fluid logs from borehole W55ST-A, Manhattan Island, N.Y.

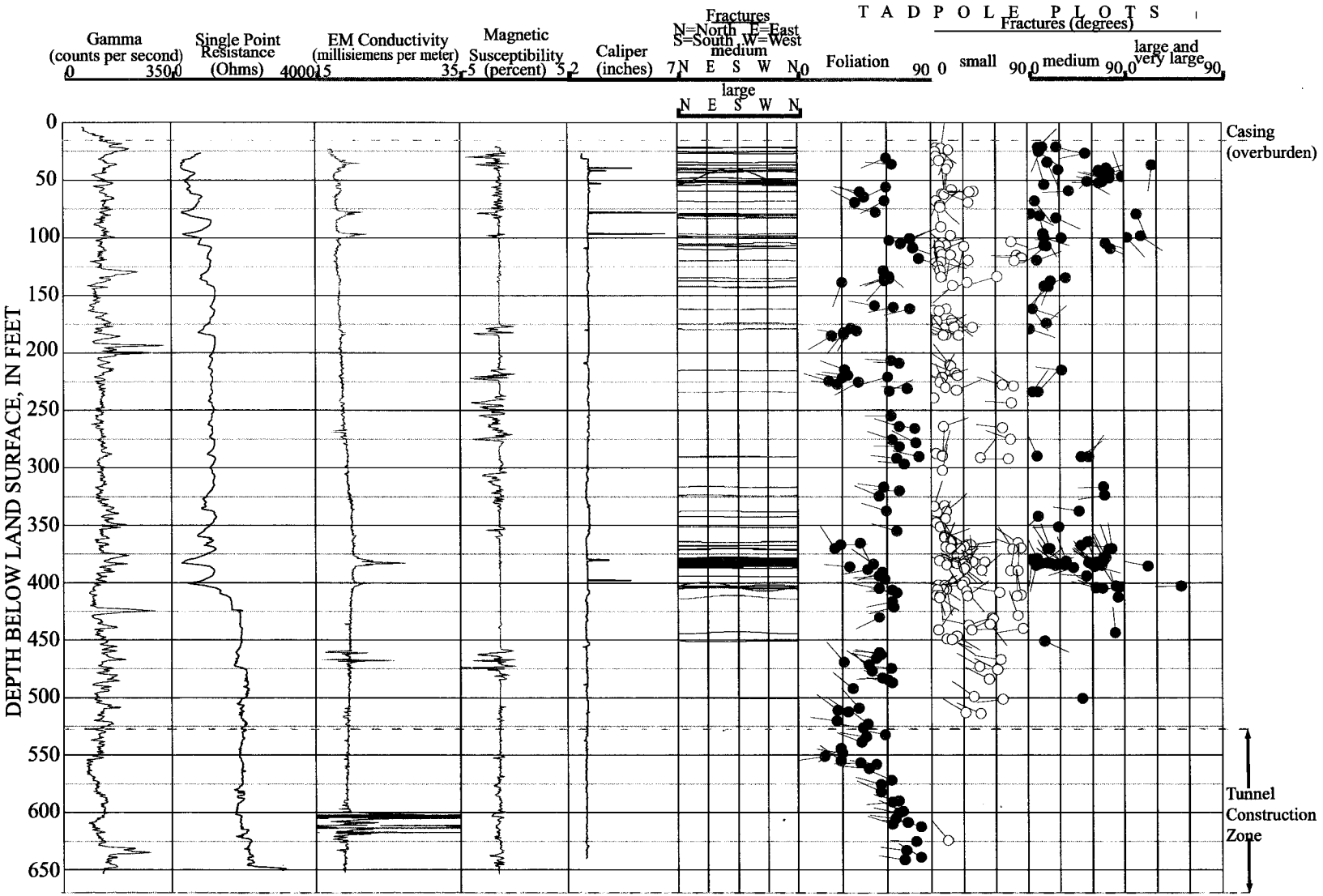

Appendix 3a. Suite of borehole-geophysical logs from borehole W37ST-A, Manhattan Island, N.Y.

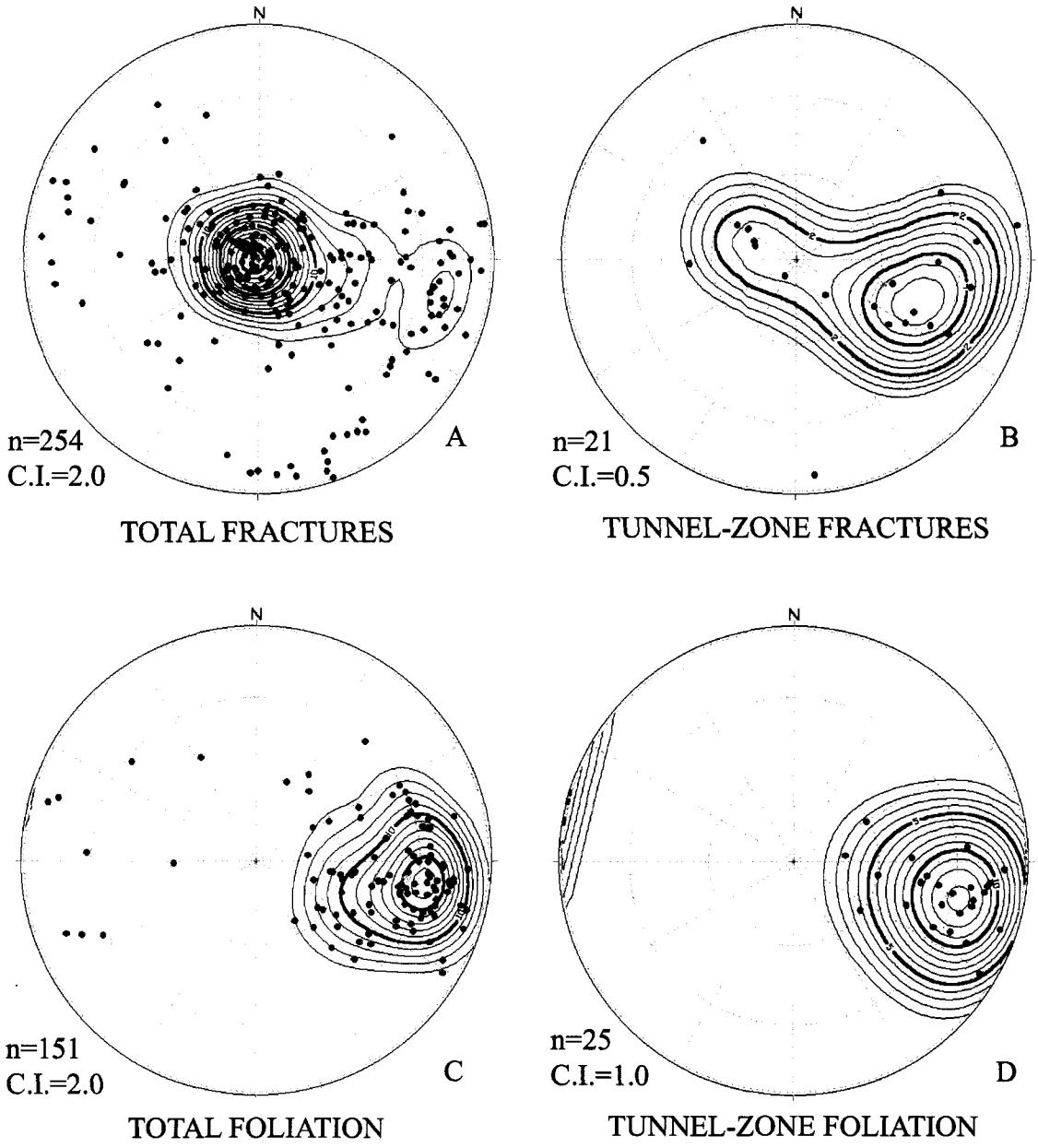

Appendix 3b. Stereonet plots of borehole W37ST-A, Manhattan Island, N.Y.,: A. Total fractures. B. Tunnel-zone fractures. C. Total foliation. D. Tunnel-zone foliation.

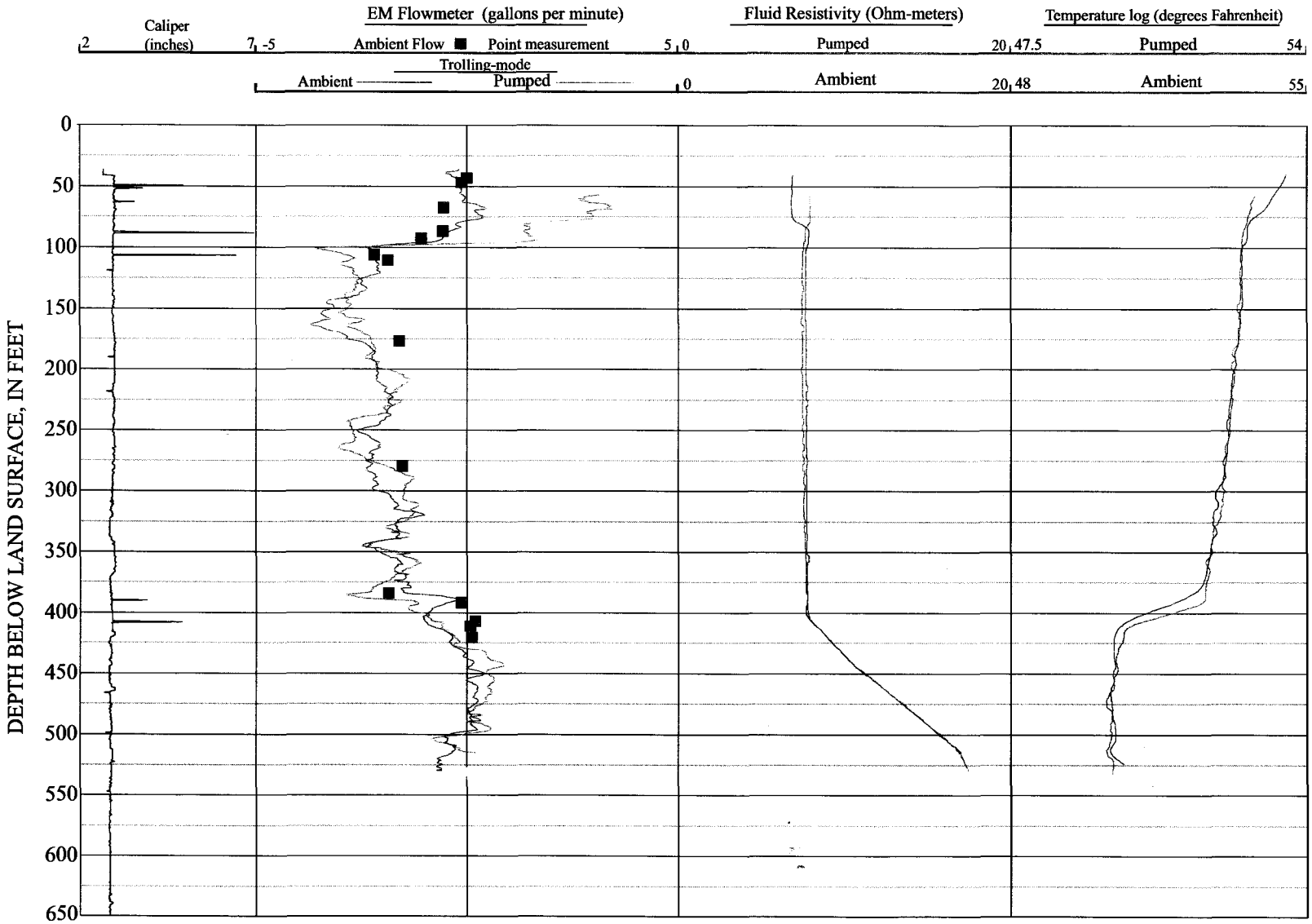

Appendix 3c. Suite of borehole-geophysical fluid logs from borehole W37ST-A, Manhattan Island, N.Y.

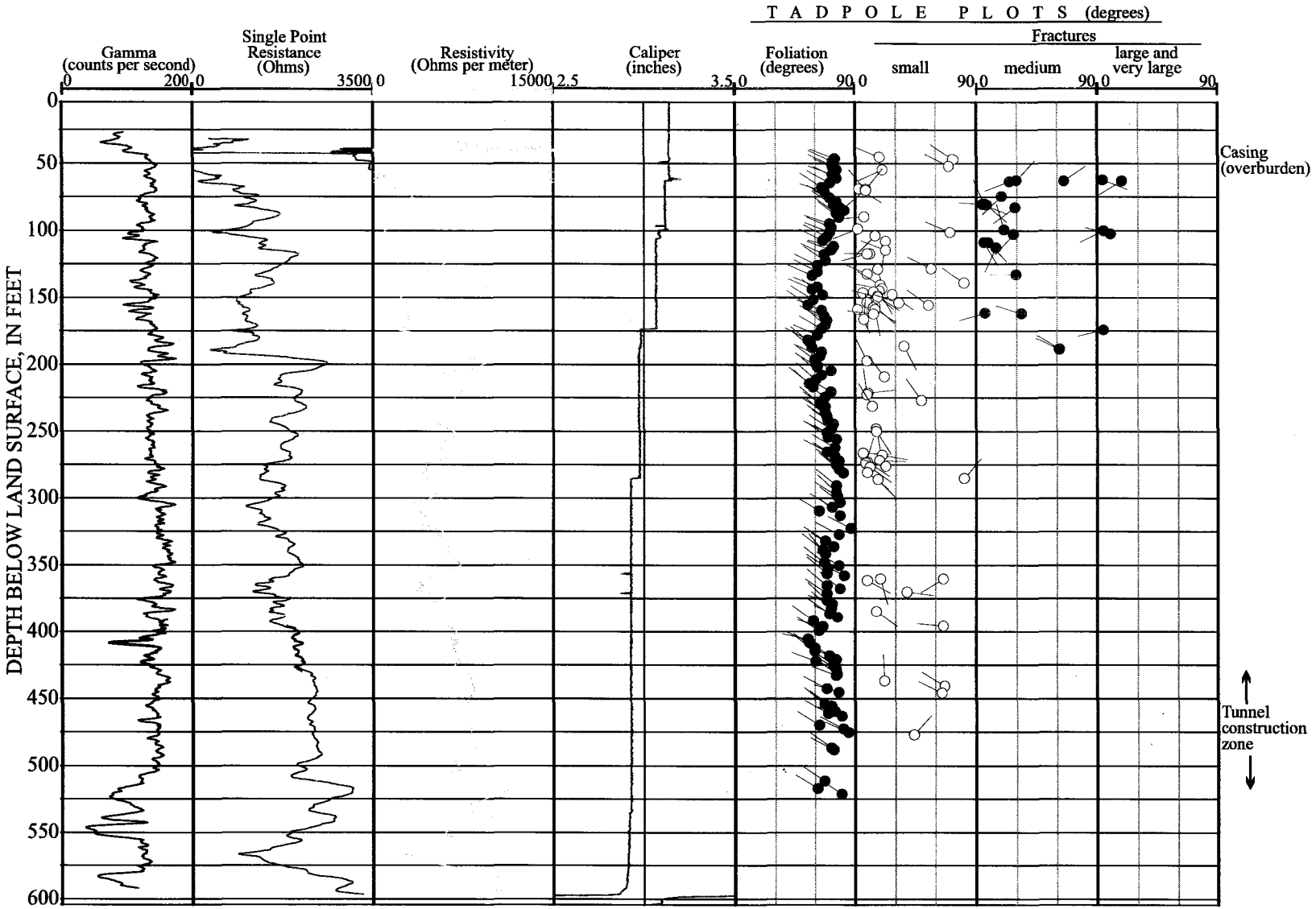

Appendix 4a. Suite of borehole-geophysical logs from borehole E30ST-A, Manhattan Island, N.Y.

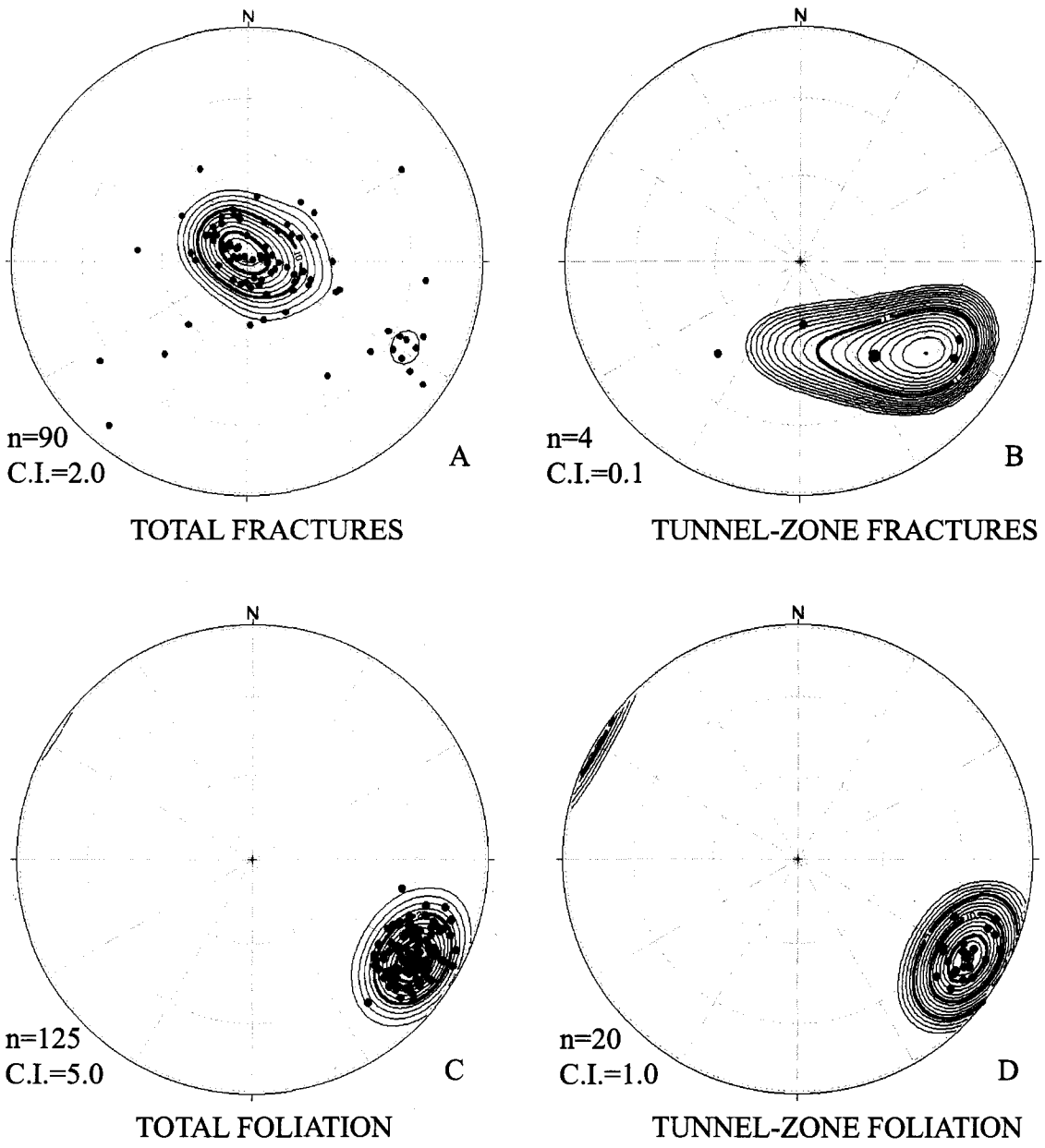

Appendix 4b. Stereonet plots of borehole E30ST-A, Manhattan Island, N.Y.,: A. Total fractures. B. Tunnel-zone fractures. C. Total foliation. D. Tunnel-zone foliation.

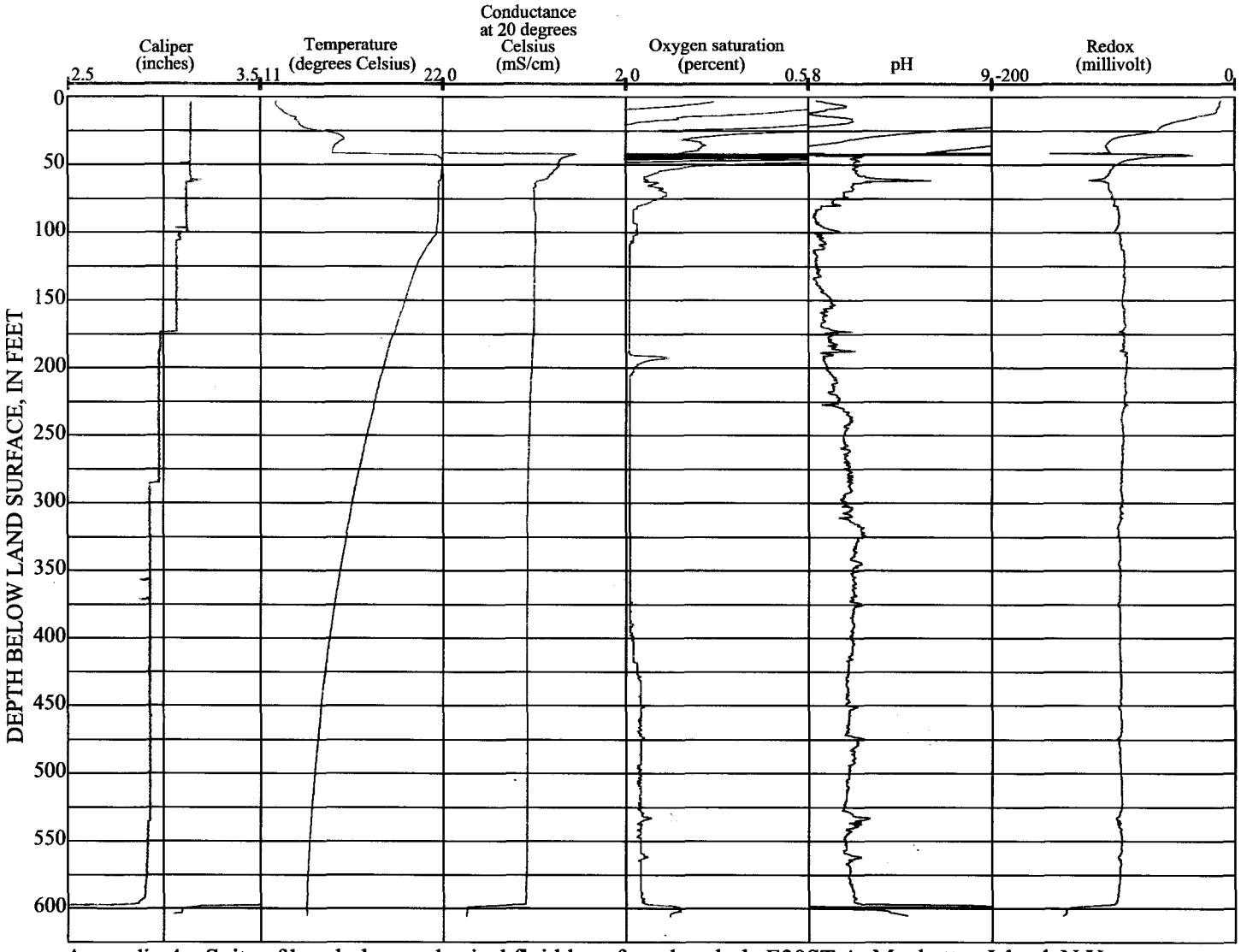

Appendix 4c. Suite of borehole-geophysical fluid logs from borehole E30ST-A, Manhattan Island, N.Y.

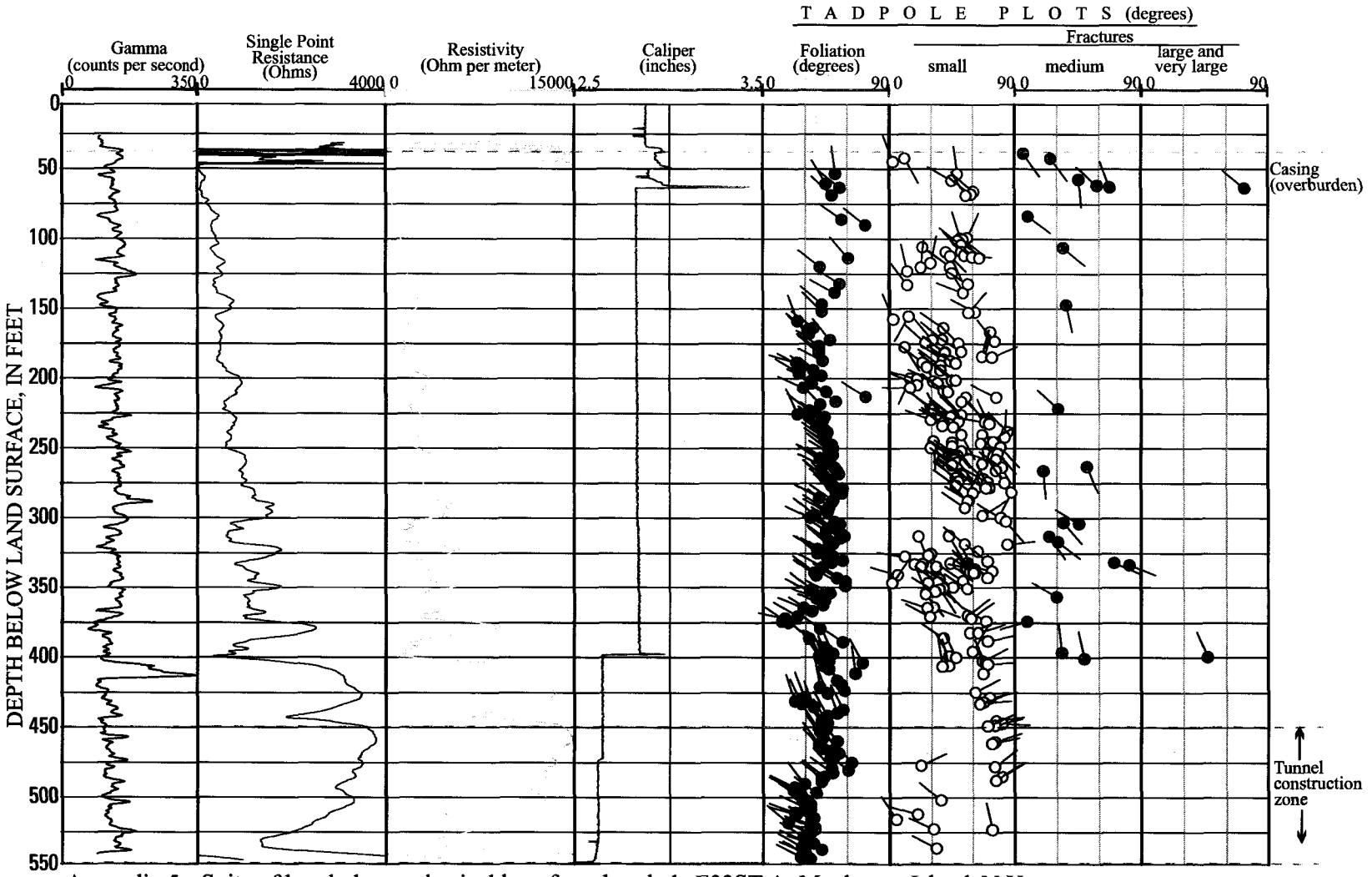

Appendix 5a. Suite of borehole-geophysical logs from borehole E33ST-A, Manhattan Island, N.Y.

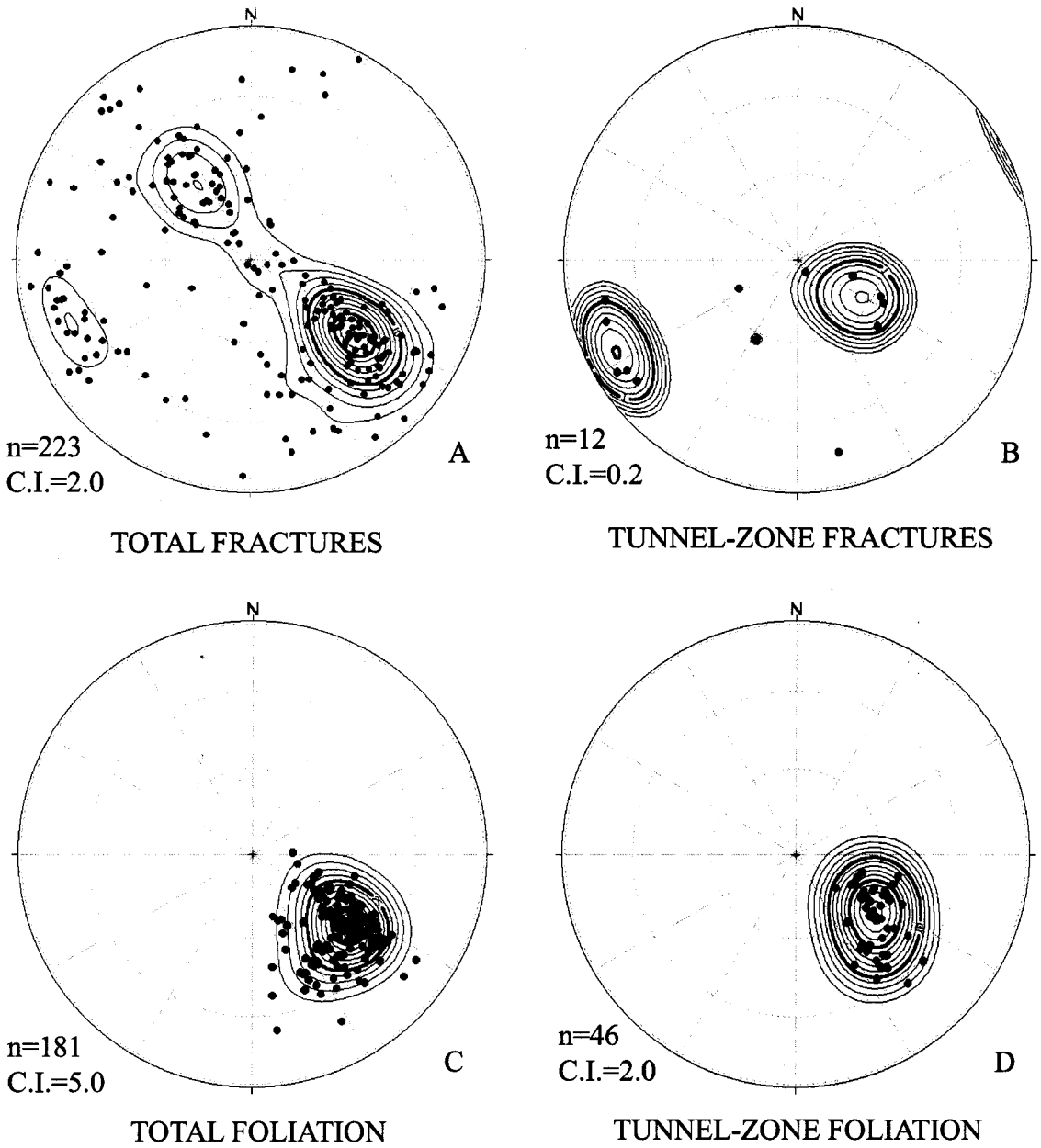

Appendix 5b. Stereonet plots of borehole E33ST-A, Manhattan Island, N.Y.,: A. Total fractures. B. Tunnel-zone fractures. C. Total foliation. D. Tunnel-zone foliation.

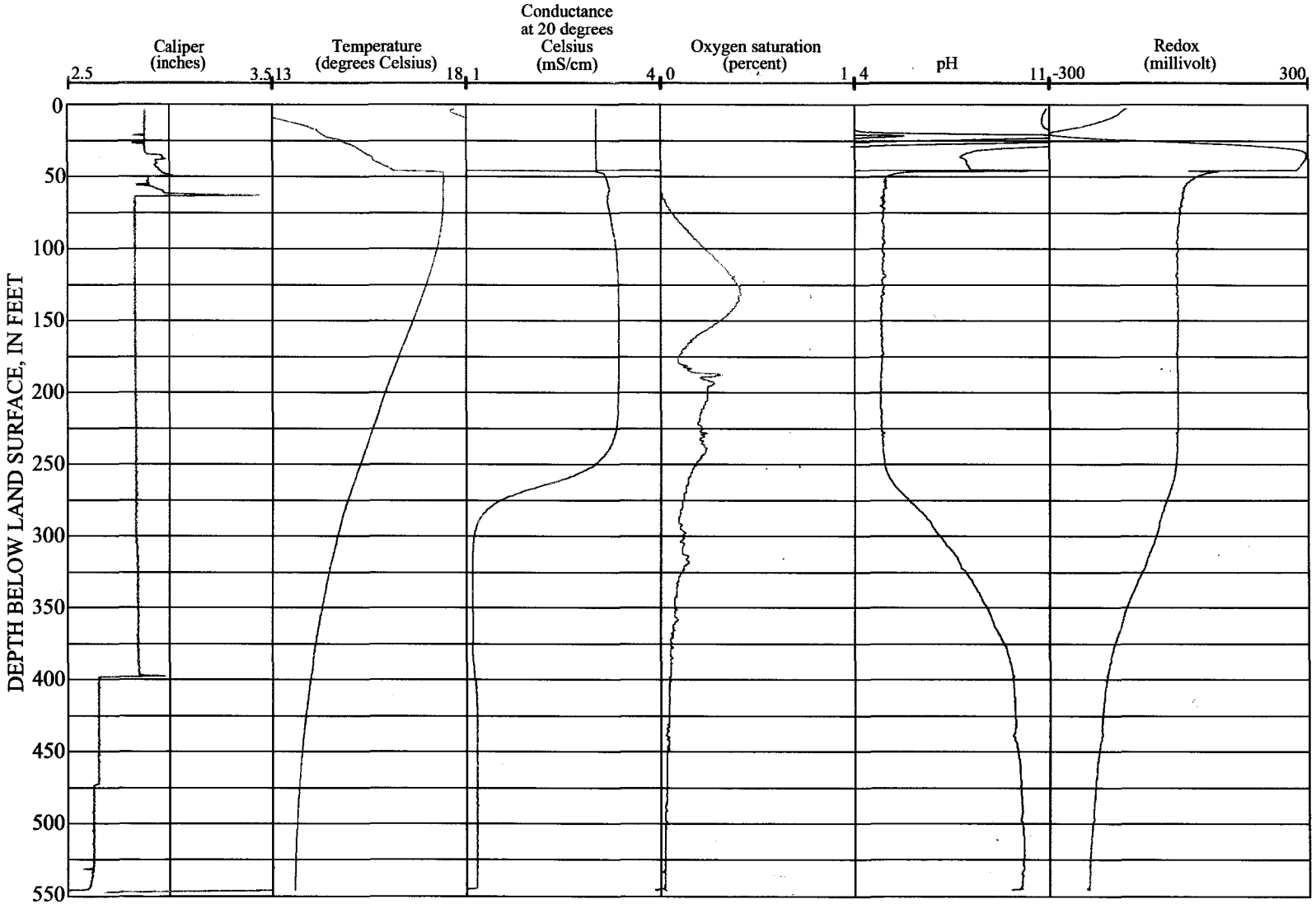

Appendix 5c. Suite of borehole-geophysical fluid logs from borehole E33ST-A, Manhattan Island, N.Y.

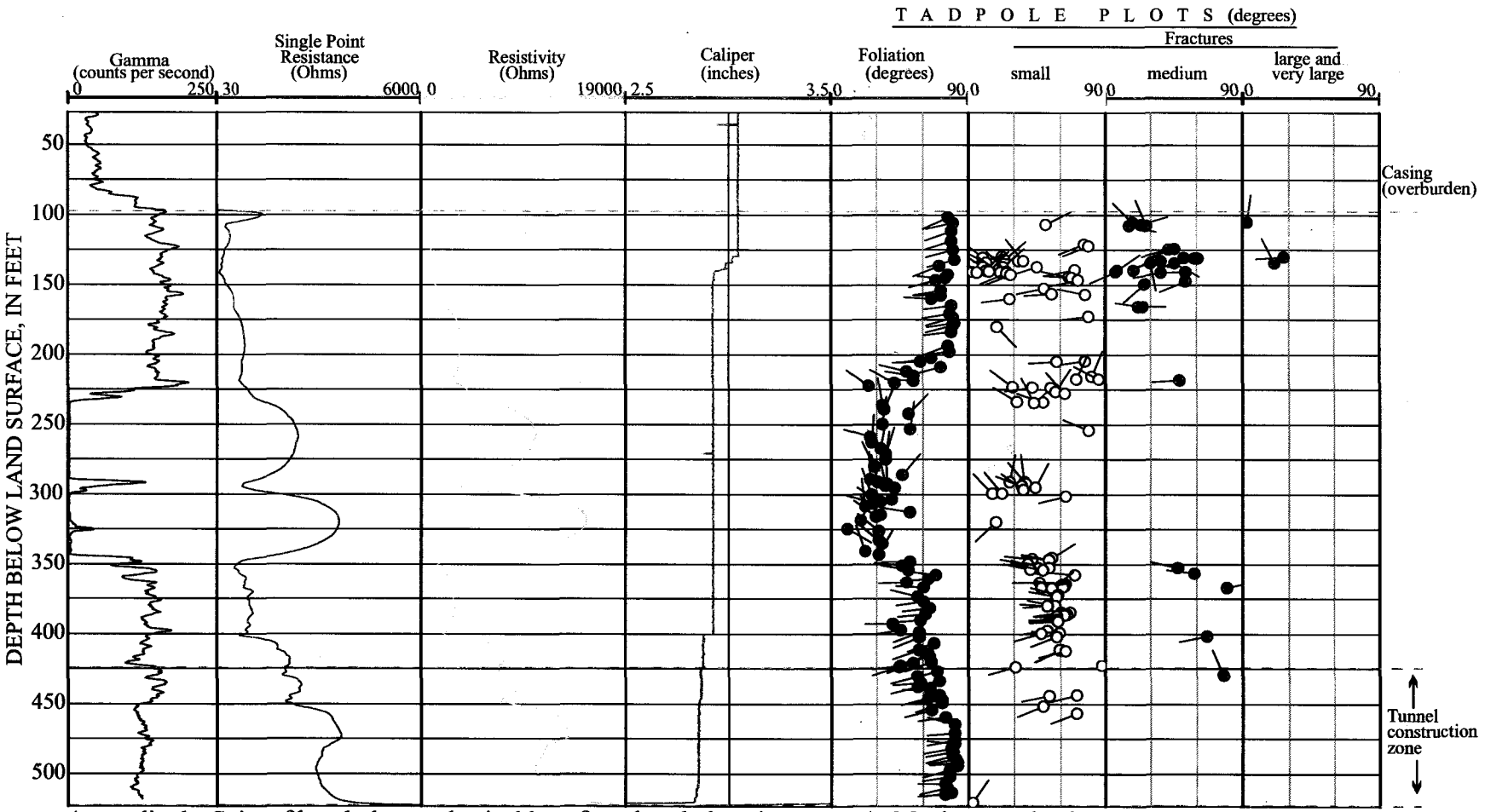

Appendix 6a. Suite of borehole-geophysical logs from borehole EricssonPL-A, Manhattan Island, N.Y.

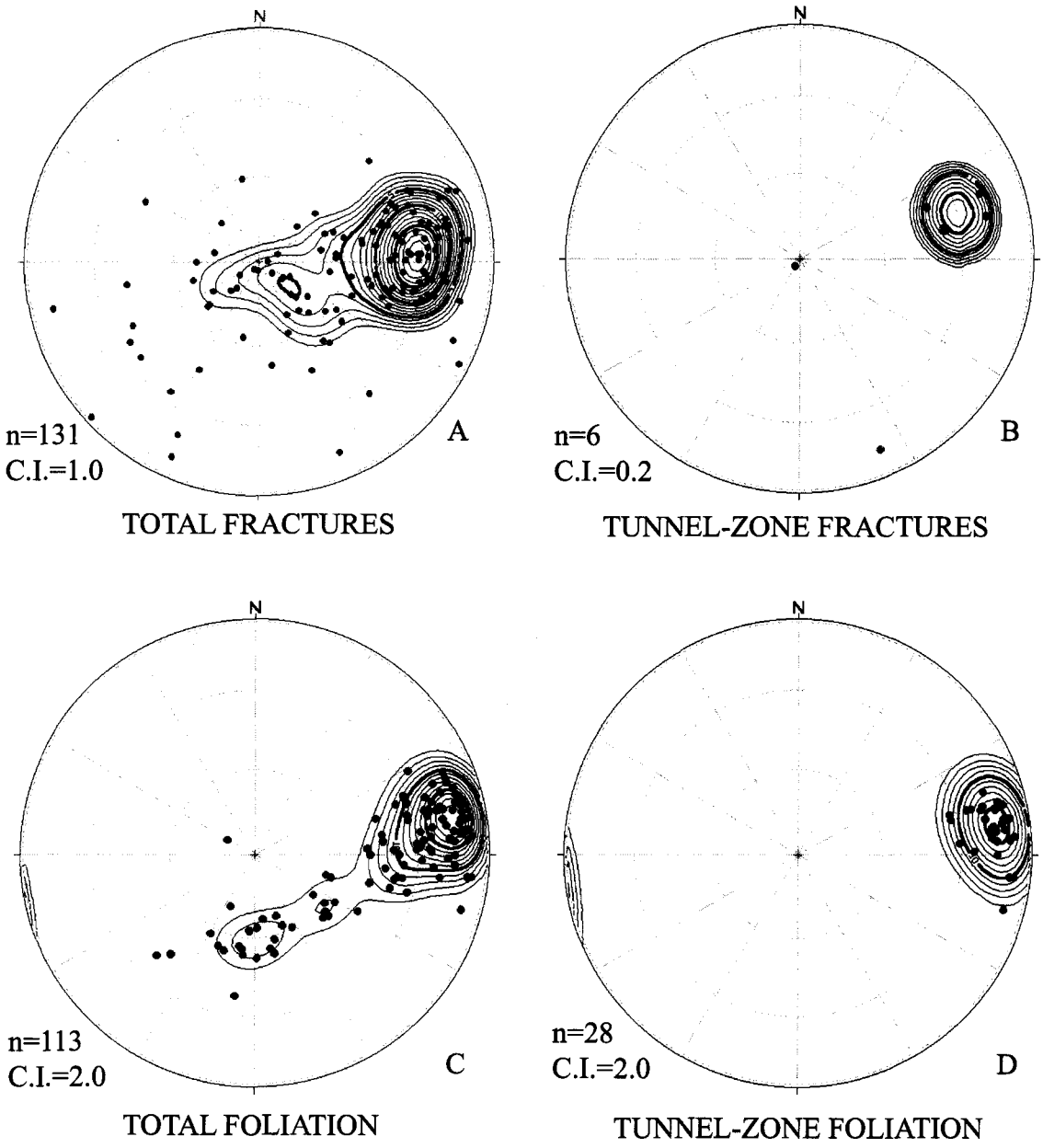

Appendix 6b. Stereonet plots of borehole EricssonPL-A, Manhattan Island, N.Y.,: A. Total fractures. B. Tunnel-zone fractures. C. Total foliation. D. Tunnel-zone foliation.

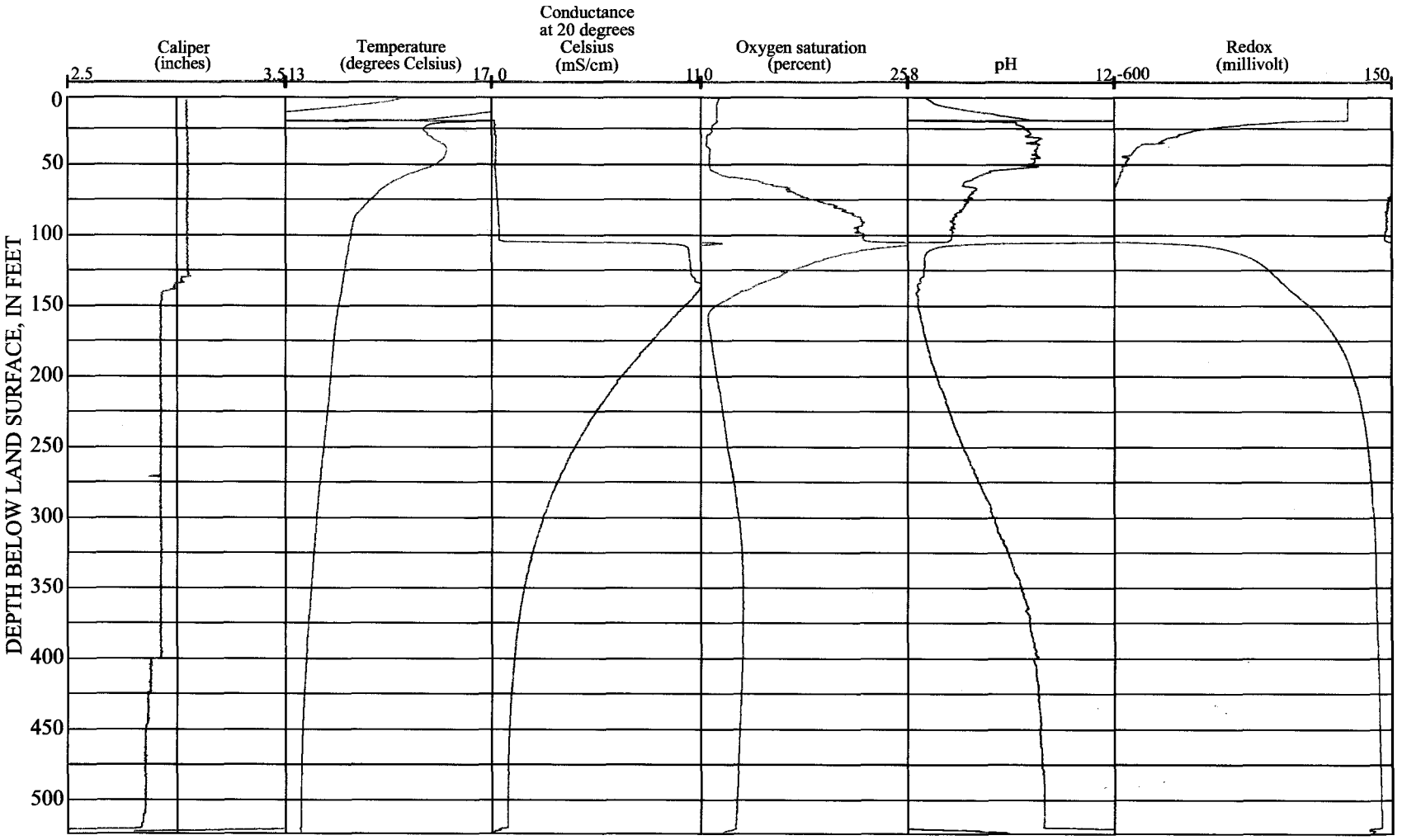

Appendix 6c. Suite of borehole-geophysical fluid logs from borehole EricssonPL-A, Manhattan Island, N.Y.

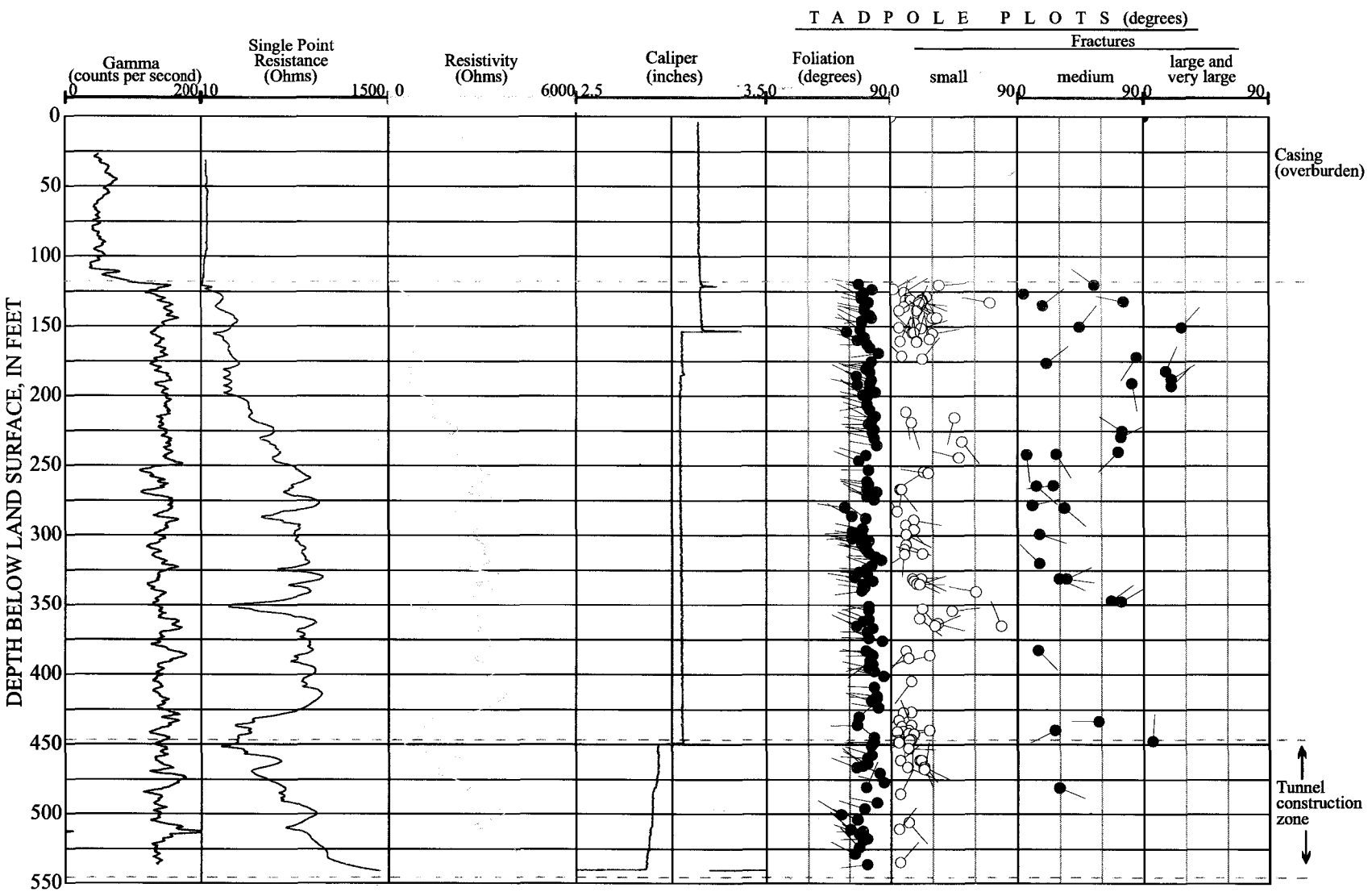

Appendix 7a. Suite of borehole-geophysical logs from borehole FranklinST-A, Manhattan Island, N.Y.

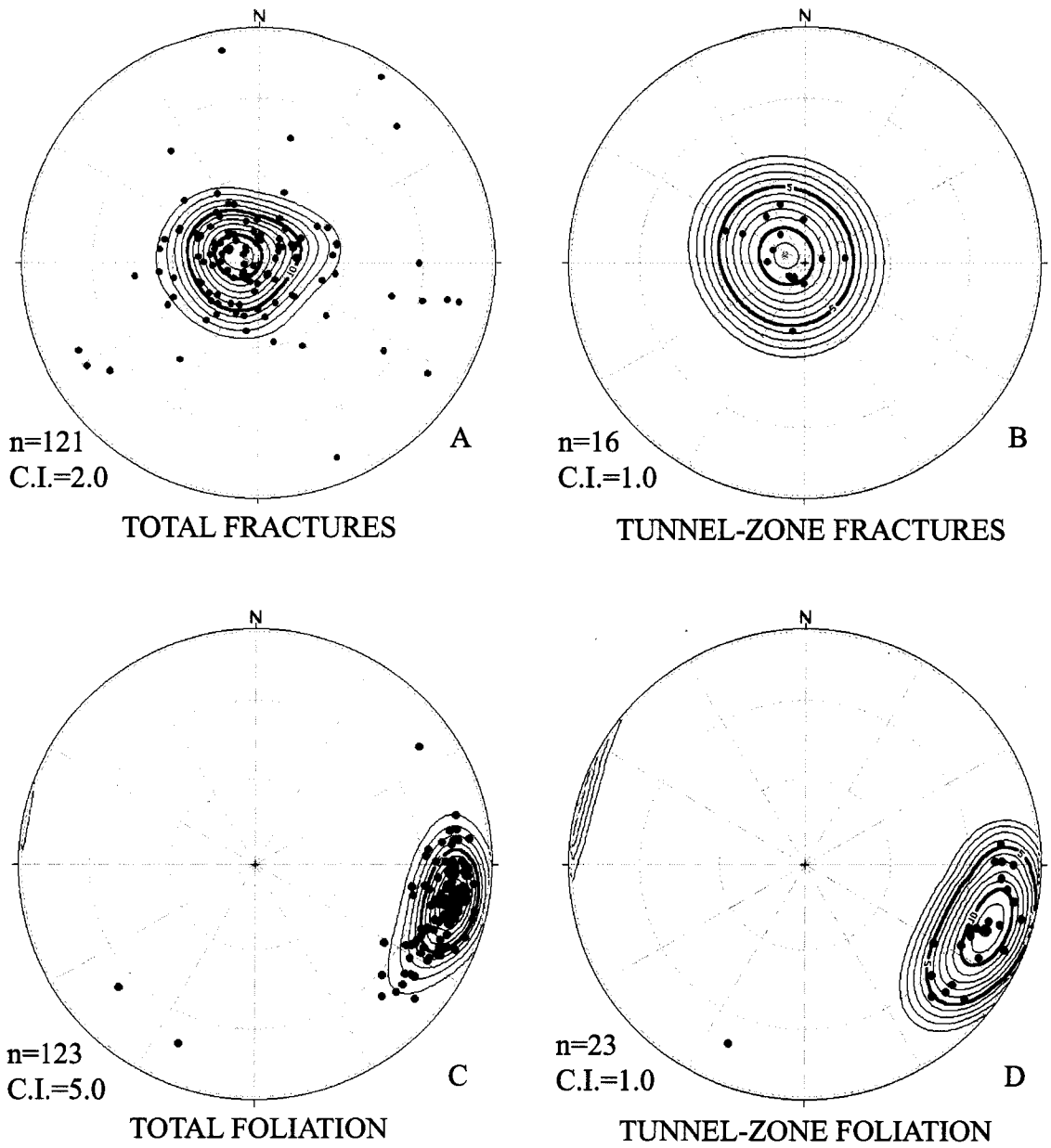

Appendix 7b. Stereonet plots of borehole FranklinST-A, Manhattan Island, N.Y.,: A. Total fractures. B. Tunnel-zone fractures. C. Total foliation. D. Tunnel-zone foliation.

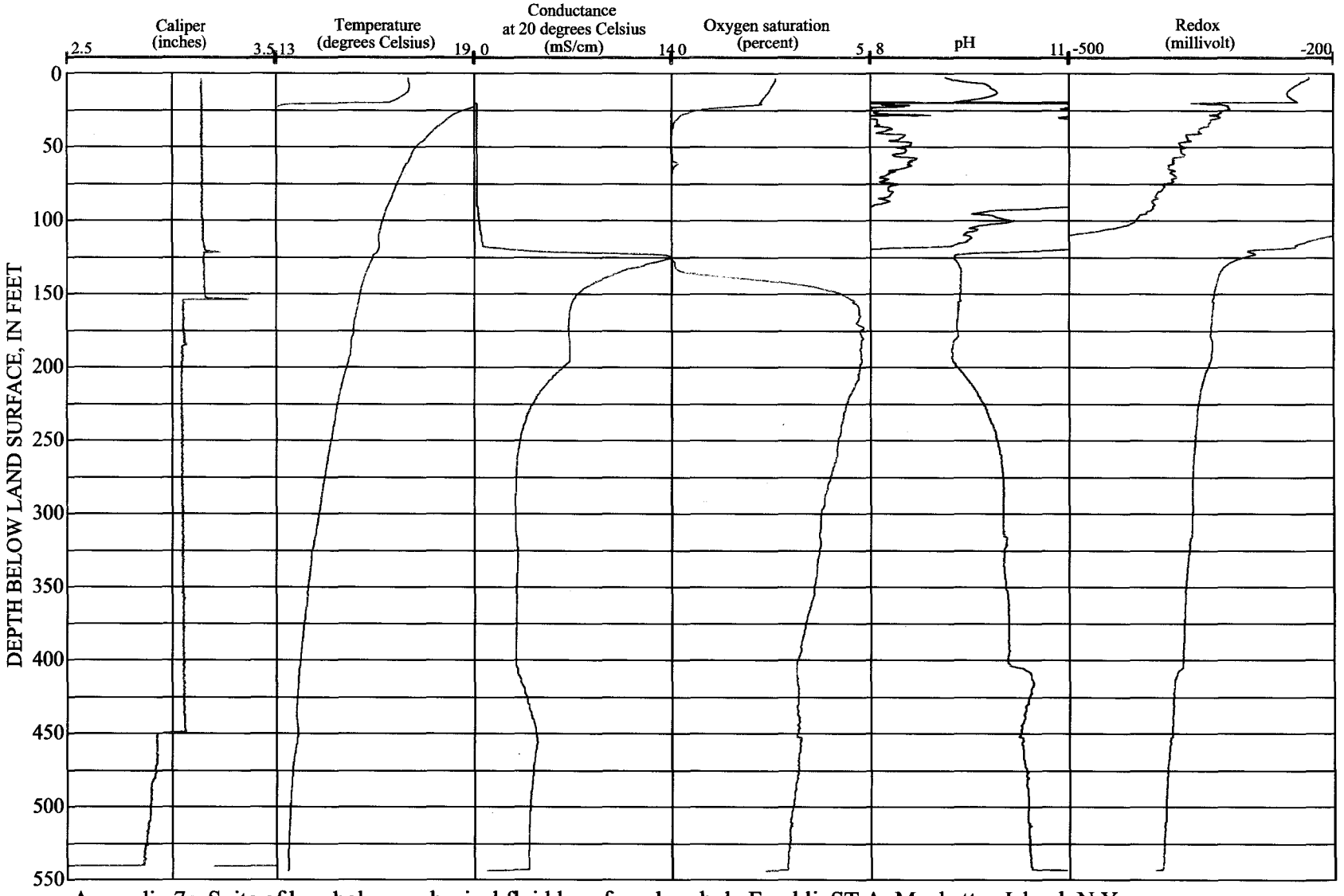

Appendix 7c. Suite of borehole-geophysical fluid logs from borehole FranklinST-A, Manhattan Island, N.Y.

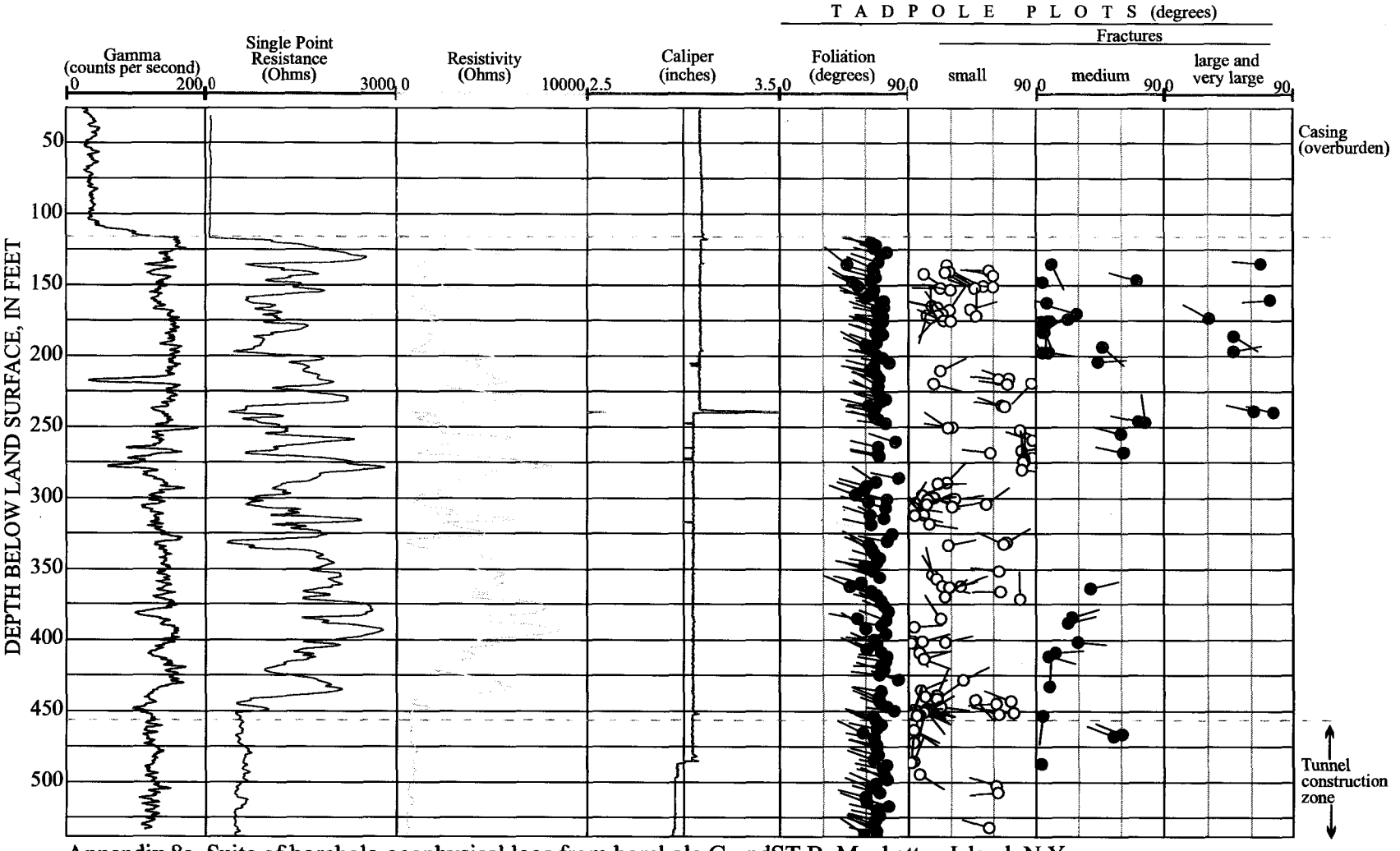

Appendix 8a. Suite of borehole-geophysical logs from borehole GrandST-B, Manhattan Island, N.Y.

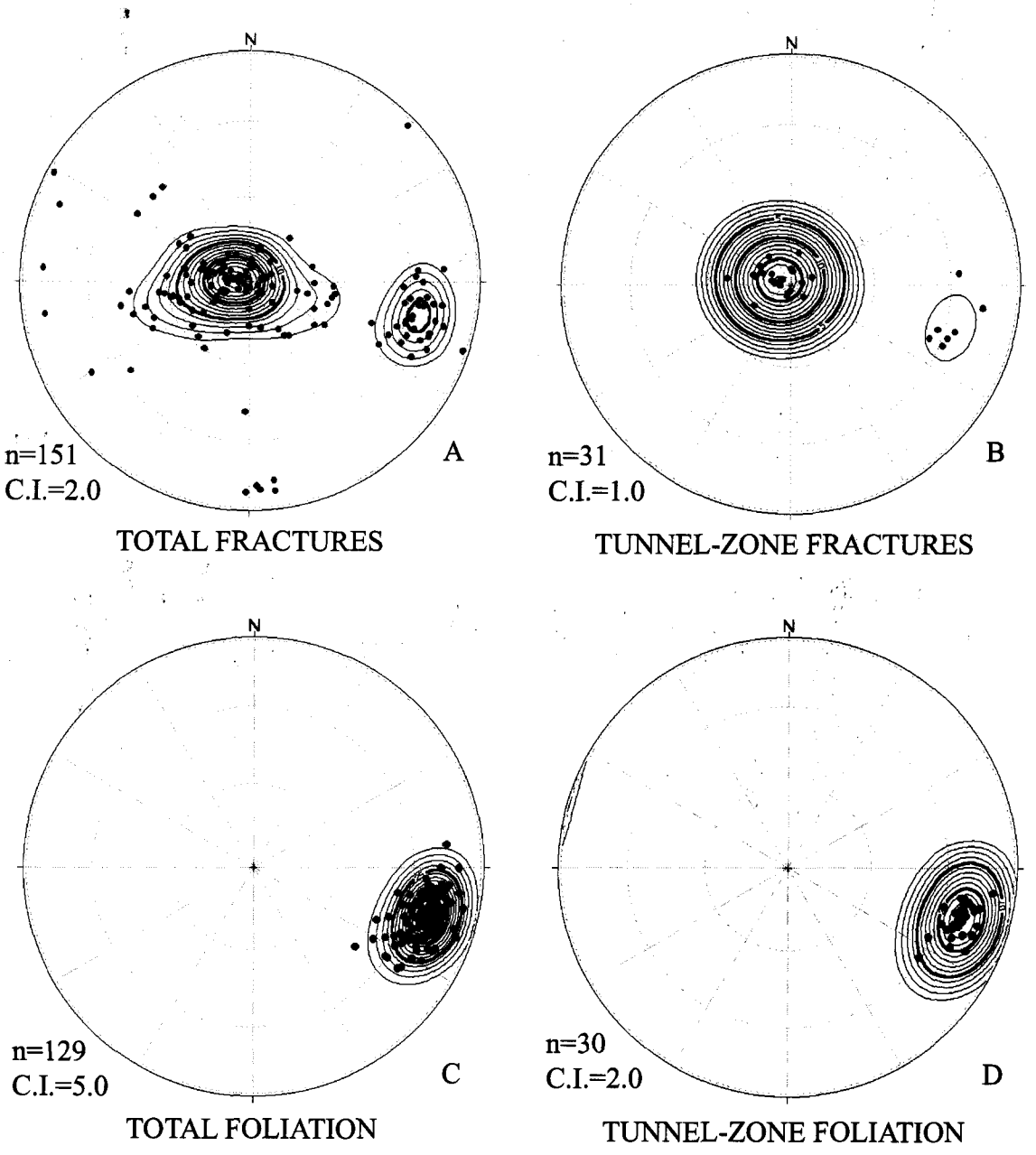

Appendix 8b. Stereonet plots of borehole GrandST-B, Manhattan Island, N.Y.,: A. Total fractures. B. Tunnel-zone fractures. C. Total foliation. D. Tunnel-zone foliation.

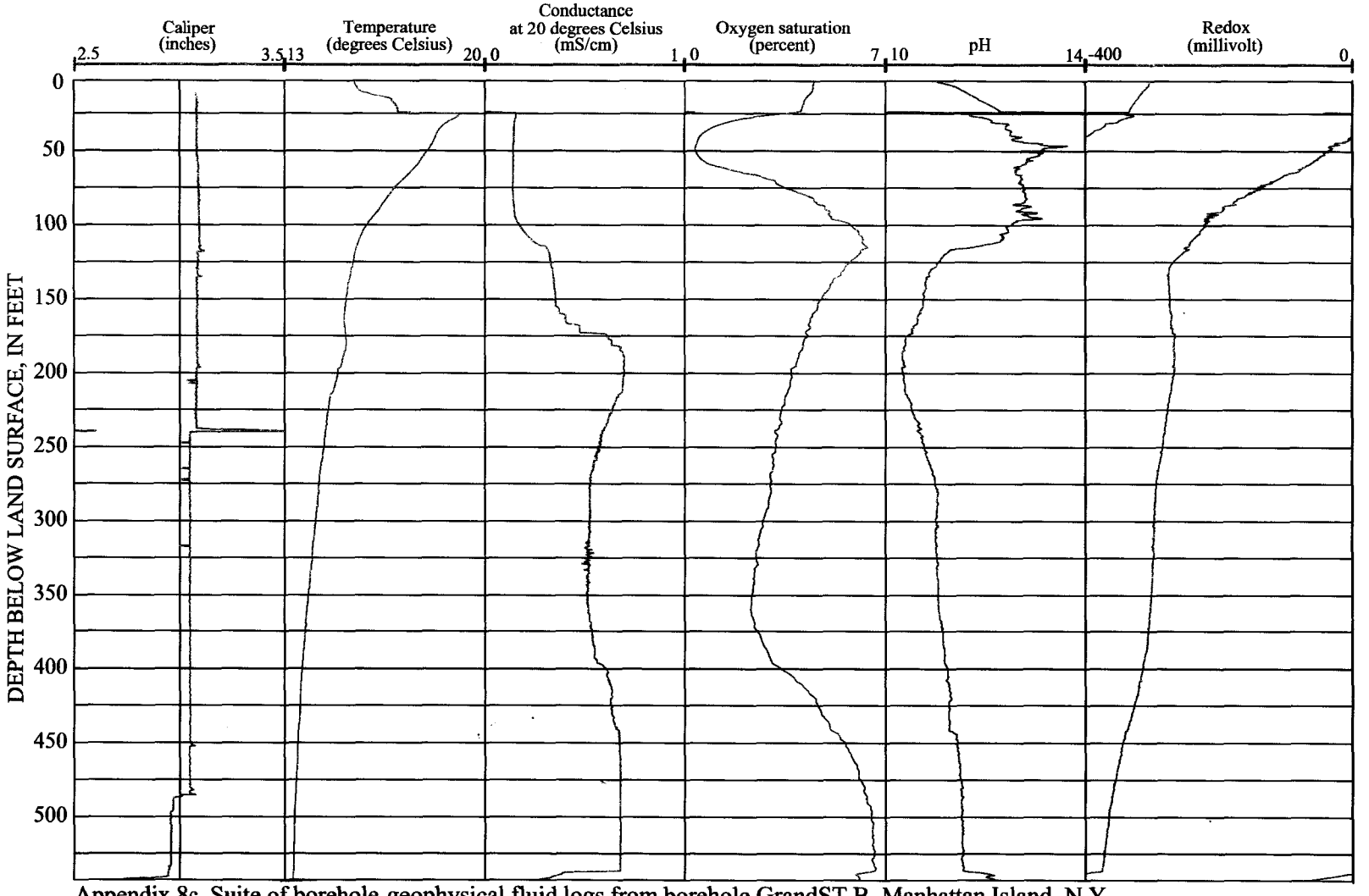

Appendix 8c. Suite of borehole-geophysical fluid logs from borehole GrandST-B, Manhattan Island, N.Y.

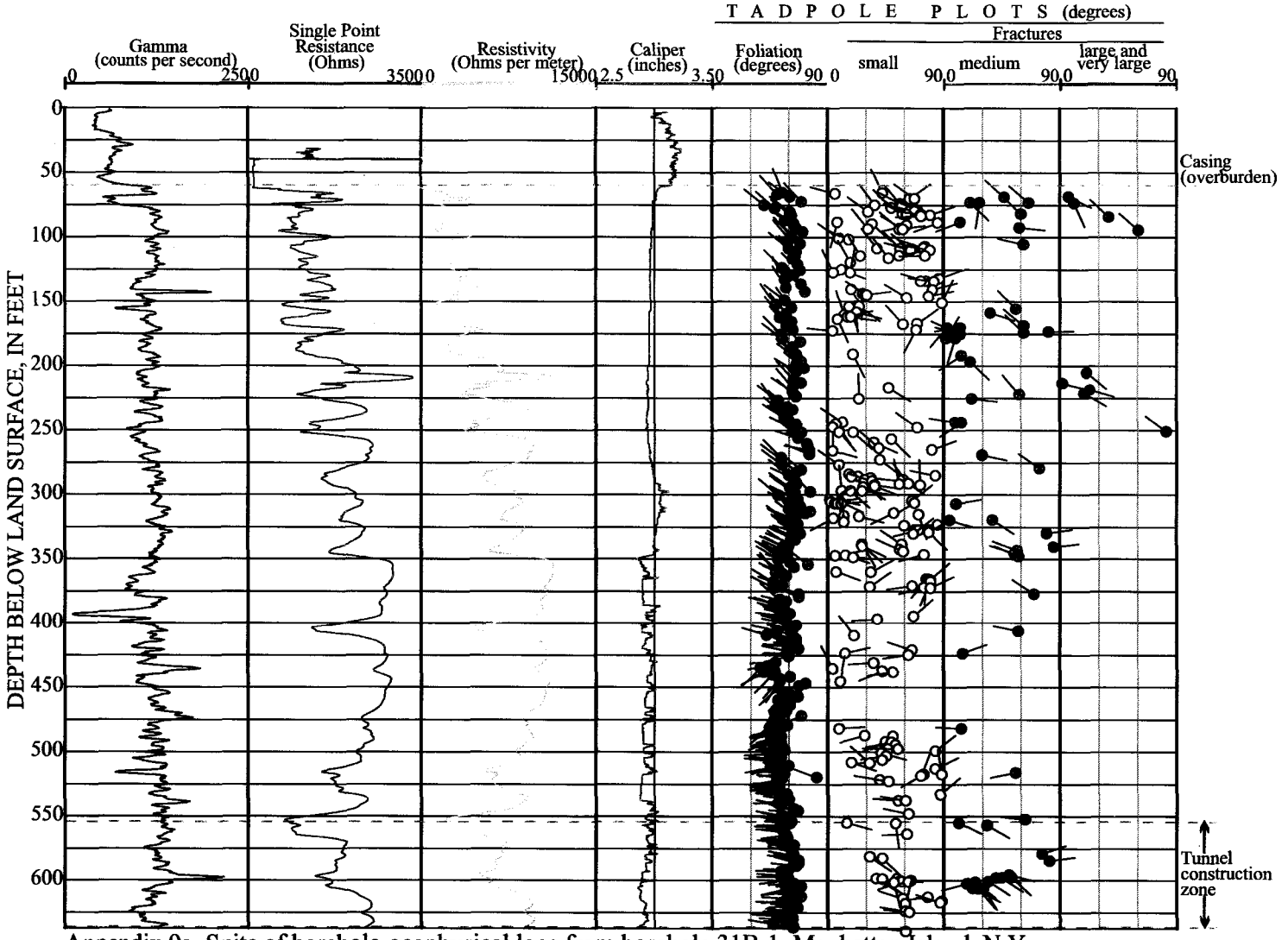

Appendix 9a. Suite of borehole-geophysical logs from borehole 31B-1, Manhattan Island, N.Y.

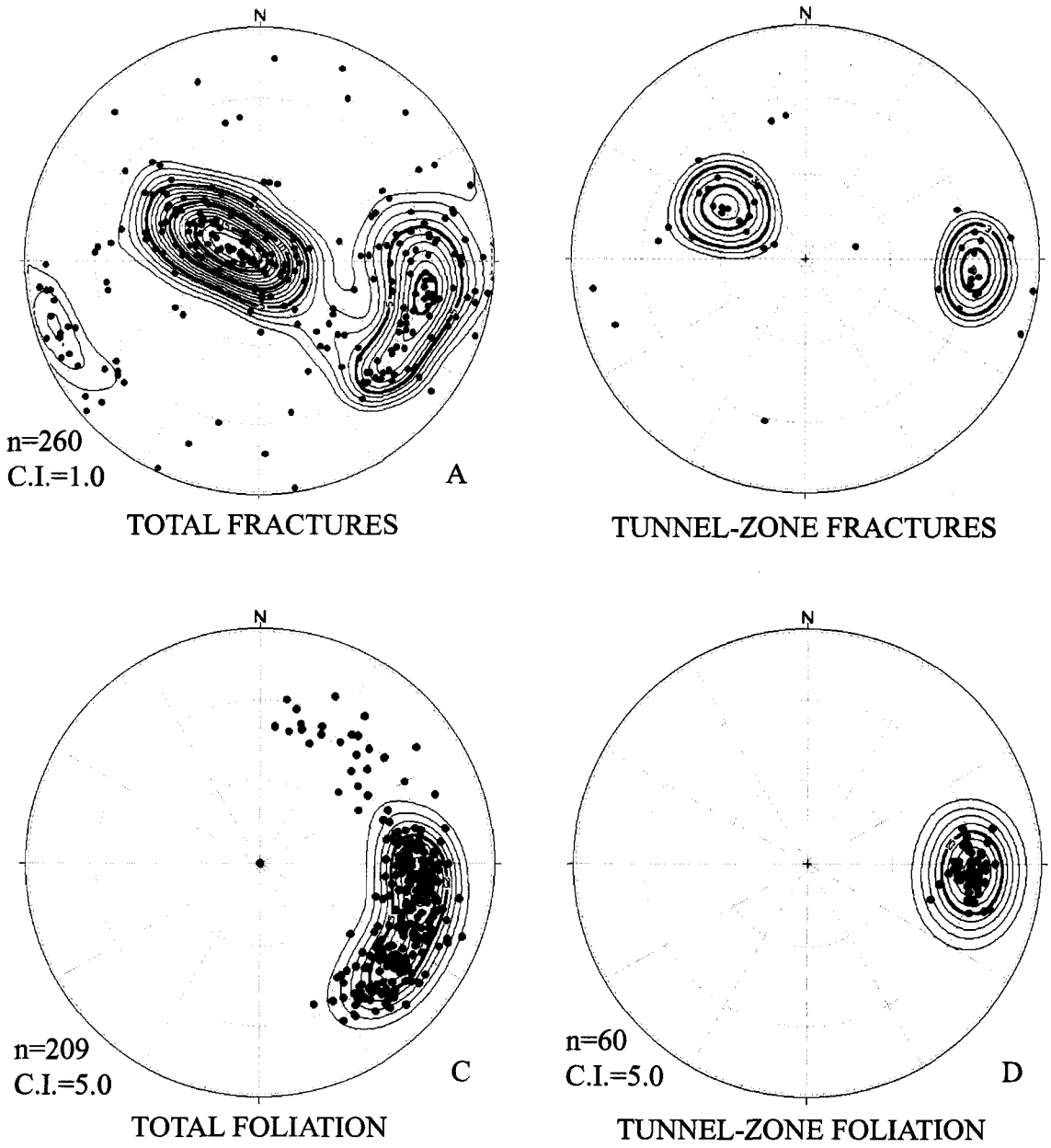

Appendix 9b. Stereonet plots of borehole 31B-1, Manhattan Island, N.Y.,: A. Total fractures. B. Tunnel-zone fractures. C. Total foliation. D. Tunnel-zone foliation.

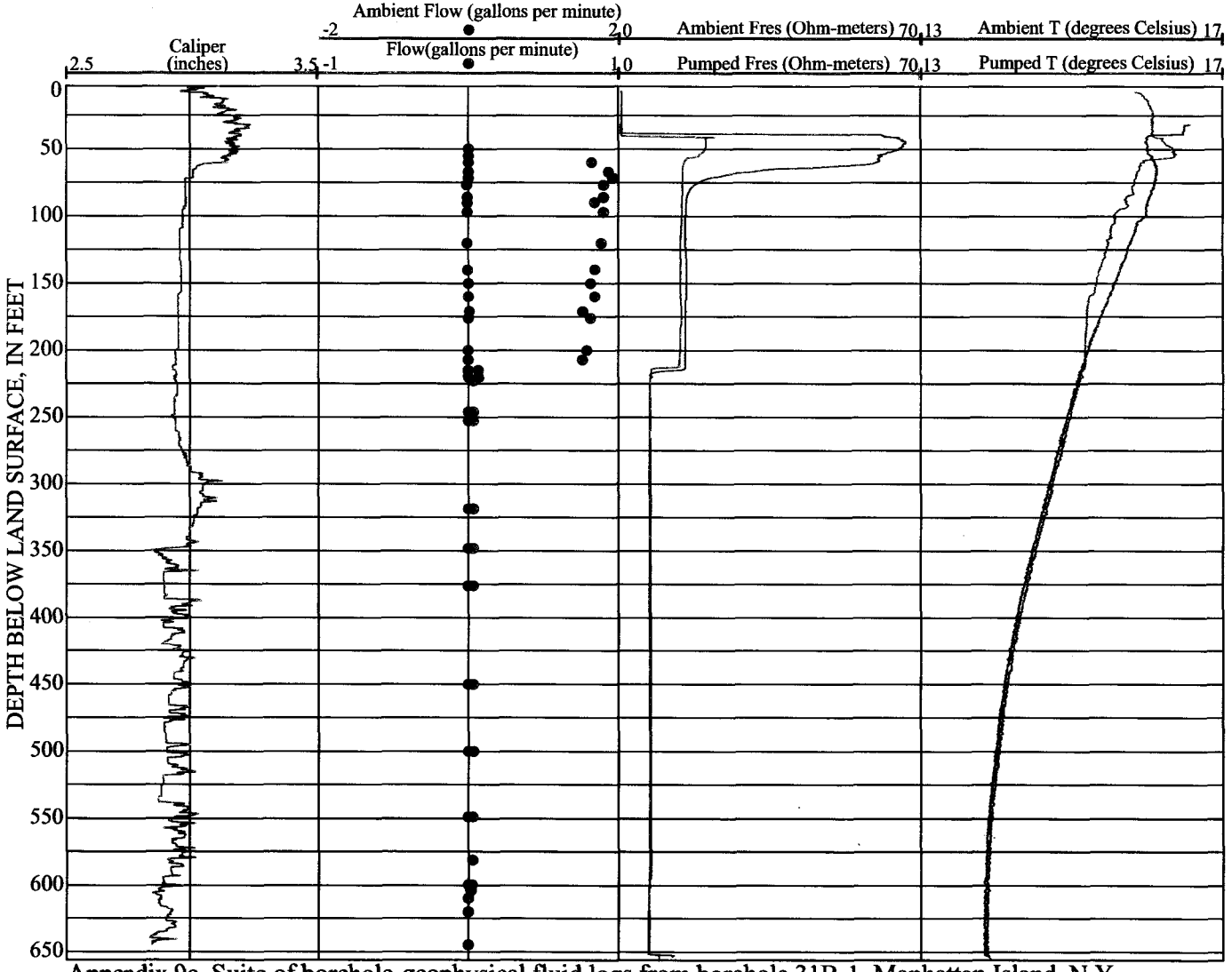

Appendix 9c. Suite of borehole-geophysical fluid logs from borehole 31B-1, Manhattan Island, N.Y.

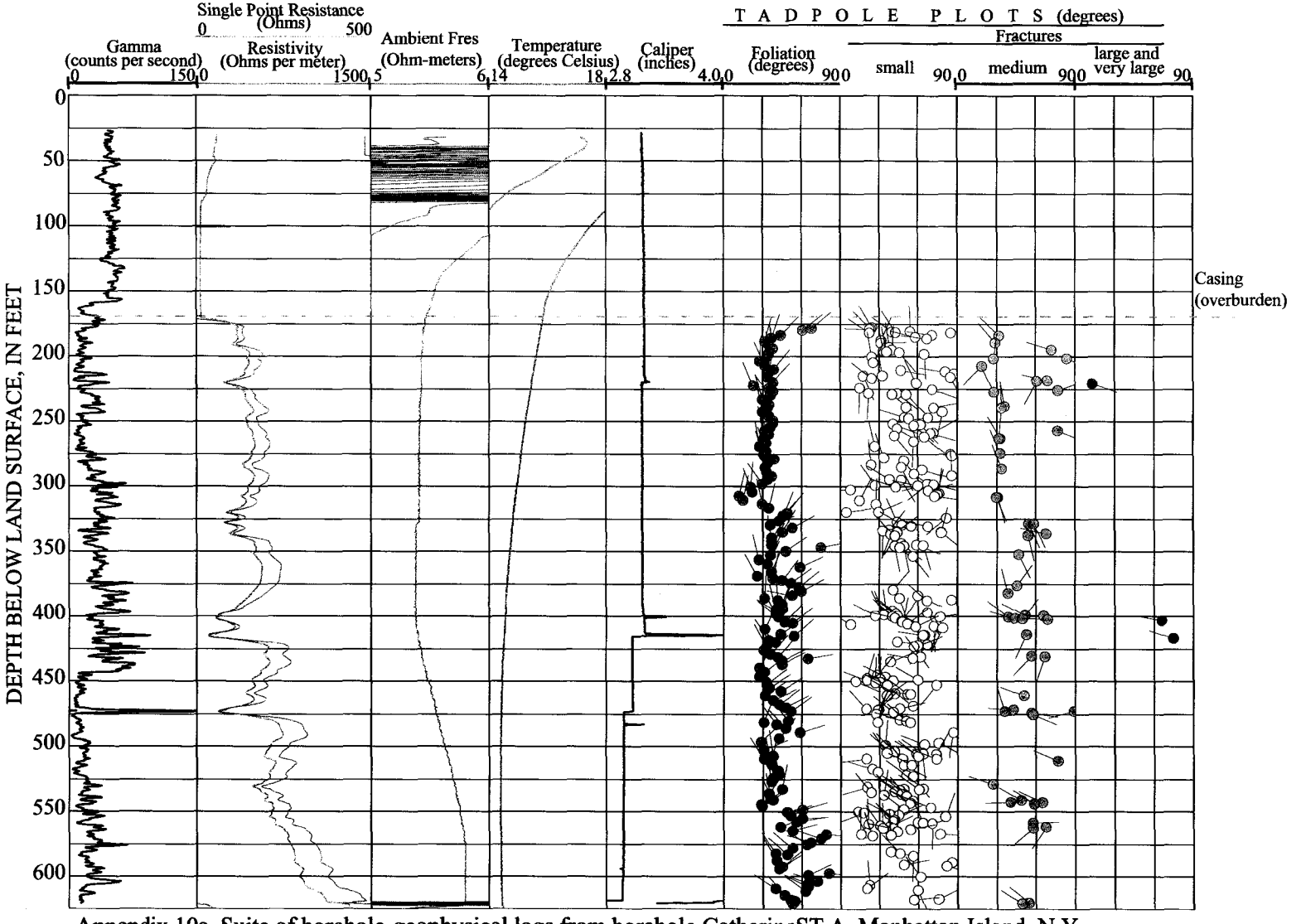

Appendix 10a. Suite of borehole-geophysical logs from borehole CatherineST-A, Manhattan Island, N.Y.

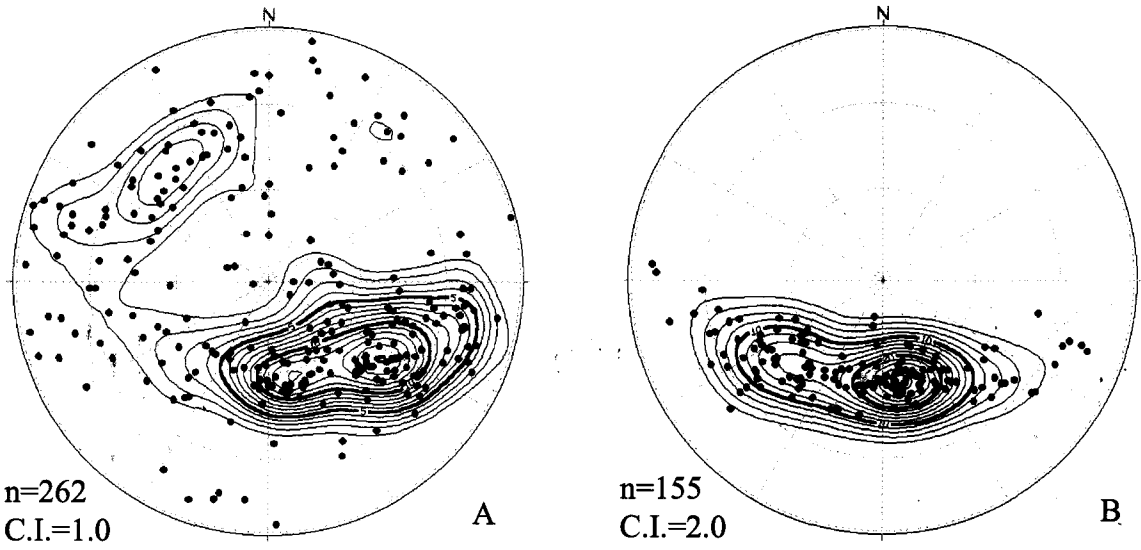

Appendix 10b. Stereonet plots of borehole CatherineST-A, Manhattan Island, N.Y.,: A. Total fractures. B. Total foliation.

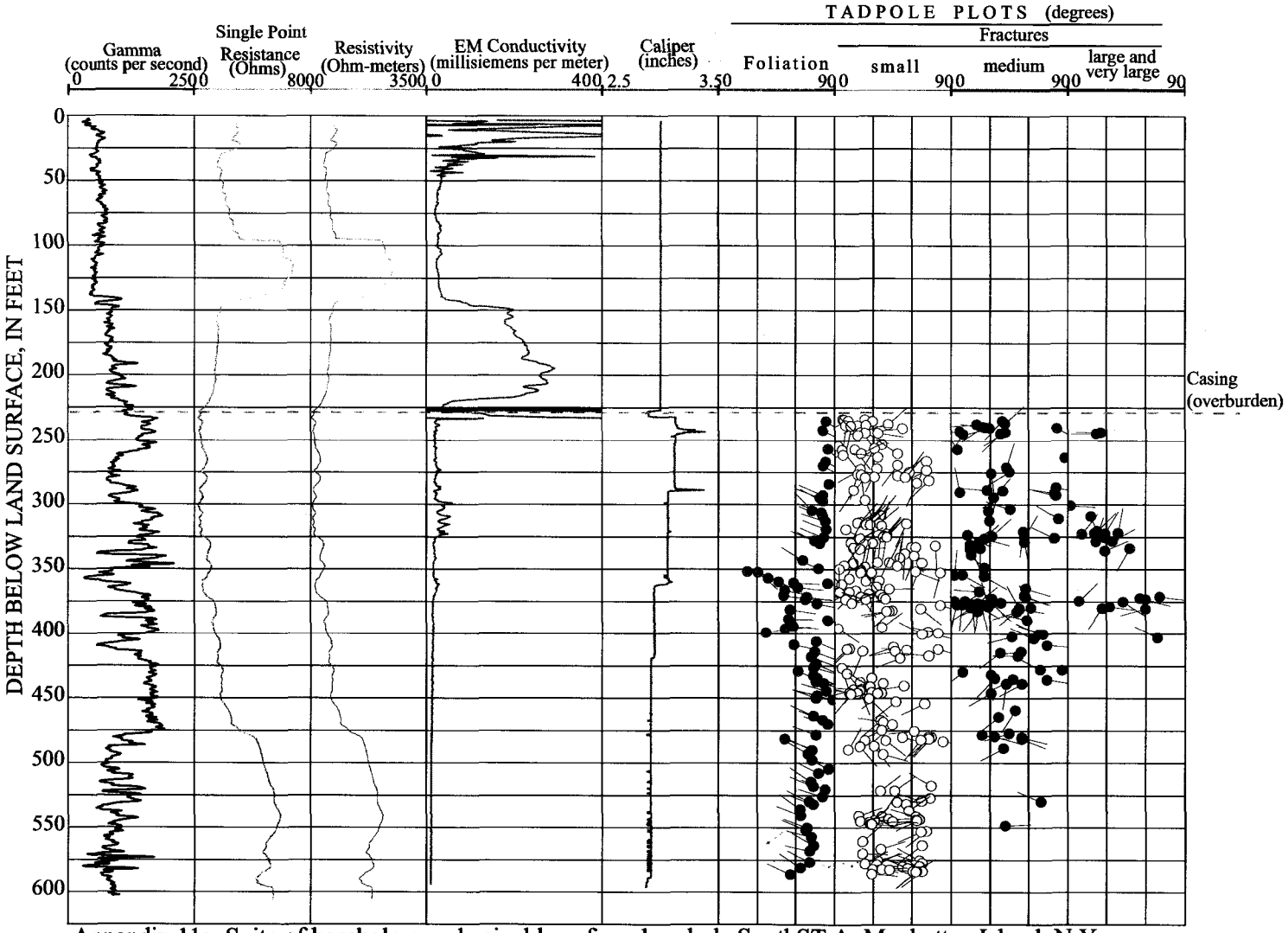

Appendix 11a. Suite of borehole-geophysical logs from borehole SouthST-A, Manhattan Island, N.Y.

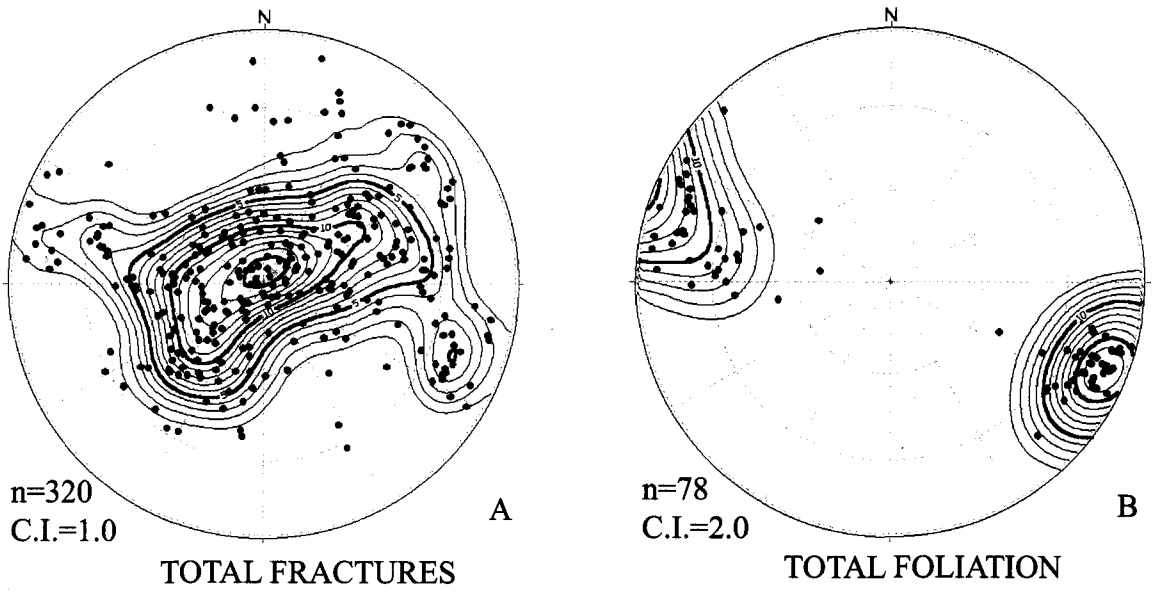

EXPLANATION

● STATISTICAL MEAN ORIENTATION

C.I. CONTOUR INTERVAL (point density contouring)

Appendix 11b. Stereonet plots of borehole SouthST-A, Manhattan Island, N.Y.,: A. Total fractures. B. Total foliation.

7. References

Baskerville, C.A, 1982, The foundation geology of New York City, *in* Legget, R.F., ed., Geology under cities: Geological Society of America Reviews in Engineering Geology, v. 5, p. 95-117.

Baskerville, C.A., 1994, Bedrock and engineering geologic maps of New York County and parts of Kings and Queens Counties, New York: U.S. Geological Survey Miscellaneous Investigations Series, map I-2306, 2 sheets, scale 1:24,000.

Berkey, C.P., 1910, Areal and structural geology of southern Manhattan Island: Annals New York Academy of Science, v. 19, no. 11, p. 247-282.

Bradbury, K.R., and Rothschild, E.R., 1985, A computerized technique for estimating the hydraulic conductivity of aquifers from specific-capacity data; Groundwater, v. 23, no. 2, p. 240-246.

Brock, P. J. C., and Brock, P.W.G., 2001, Bedrock geology of New York City: More than 600 m.y. of geologic history: http://pbisotopes.ess.sunysb.edu, 11 p.

Caine, J.S., Evans, J.P., and Forster, C.B., 2000, Characterization and modeling of fluid flow in fault and fracture zones: the reality realized: Short course manual, Geological Society of America, 153 p.

Fetter, C.W., 1999, Contaminant Hydrogeology: Prentice Hall, 503 p.

Freeze, R.A., and Cherry, J.A., 1979, Groundwater: Prentice Hall, 604 p.

Hobbs, W.H., 1905, Origin of the channels surrounding Manhattan Island, New York: Geological Society of America Bulletin, v.16, p. 151-182

Keys, W.S., and MacCary, L.M., 1971, Application of borehole geophysics to water-resources investigations: U.S. Geological Survey Techniques of Water Resources Investigations, book 2, chap. E1, 126 p.

Keys, W.S., 1990, Borehole geophysics applied to water-resources investigations: U.S. Geological Survey Techniques of Water Resources Investigations, book 2, chap. E2, 150 p.

McNeill, J.D, Hunter, J.A., and Bosner, M., 1996, Application of a borehole induction magnetic susceptibility logger to shallow lithological mapping: Journal of Environmental and Engineering Geophysics, v. 0, no. 2, p.77-90.

Merguerian, Charles, and Baskerville, C.A., 1987, The geology of Manhattan Island and the Bronx, New York City, New York, p. 137-140, *in* Roy, D.C., ed., Northeastern Section of the Geological Society of America, Centennial Fieldguide, v. 5, 481 p.

Merguerian, C., and Sanders, J.E, 1993, Geology of southern Central Park: New York Academy of Sciences, Trips on the Rocks, Trip 28, 143 p.

Merrill, F.J.H, 1890, The metamorphic strata of southeastern New York: American Journal of Science, v.39, no. 234, p 383-392.

Molz, F.J., Morin, R.H., Hess, A.E., Melville, J.G., and Guven, Oktay, 1989, The impeller meter for measuring aquifer permeability variations—evaluation and comparison with other tests: Water Resources Research, v. 25, no. 7, p. 1677-1683.

Murphy, J.J, and Fluhr, T.W, 1944, The subsoil and bedrock of the borough of Manhattan as related to foundations: Municipal Engineers Journal, Fourth Issue, Paper 212, p 119-157.

NOAA, 2005, Monthly and annual precipitation at Central Park, Manhattan, N.Y.: http://www.erh.noaa.gov/er/okx/climate/records/monthannualpcpn.htm.

Paillet, F. L., 1998, Flow modeling and permeability estimation using borehole flow logs in heterogeneous fractured formations: Water Resources Research, v. 34, no. 5, p. 997-1010.

Paillet, F. L., 2000, A field technique for estimating aquifer parameters using flow log data: Ground Water, v. 38, no. 4, p. 510-521.

Paillet, F.L., 2001, Hydraulic head applications of flow logs in the study of heterogeneous aquifers: Ground Water, v. 39, no. 5, p. 675-684

Perlmutter, N.M., and Arnow, T, 1953, Ground water in Bronx, New York, and Richmond Counties with summary data on Kings and Queens Counties, New York City, New York: U.S. geological Survey Ground Water Bulletin, GW-32, 86 p.

Schopf, J.D., 1787, Beytrage zur mineralogischen Kenntniss des Ostlichen Theils von Nord-Amerika und seiner Geburge: Munchen, Germany, 94 p.

Serra, Oberto, 1984, Fundamentals of well-log interpretation: New York, Elsevier, 423 p.

Singha, Kamini, Kimball, Kari, and Lane, J.W., Jr., 2000, Borehole-Radar Methods-Tools for characterization of fractured rock: U.S. Geological Survey Fact Sheet 054-00, 4 p.

Stumm, F., Paillet, F., Williams, J.H., and Lane, J.W., 2000, Geohydrologic assessment of crystalline bedrock for the New York City Water-Tunnel Project by use of advanced borehole-geophysical methods, in Proceedings of the Seventh International Symposium on Borehole Geophysics for Minerals, Geotechnical, and Groundwater Applications, October 24-26, 2000, Denver, Colorado, Minerals and Geotechnical Logging Society, p. 19-27.

Stumm, F., Chu, Anthony, and Lange, A.D., 2001a, Use of advanced borehole geophysical techniques to delineate fractured-rock ground-water flow, faults, foliation and fractures along the western part of Manhattan, New York: U.S. Geological Survey Open-File Report 01- 196, 46 p.

Stumm, F., and others, 2001b, Use of advanced borehole geophysical techniques to delineate fractured-rock ground-water flow and fractures along water-tunnel facilities in northern Queens County, New York: U.S. Geological Survey Water Resources Investigations Report 00-4276, 12 p.

Stumm, Frederick, 2001c, Hydrogeology and extent of saltwater intrusion of the Great Neck peninsula, Great Neck, Long Island, New York: U.S. Geological Survey Water Resources Investigations Report 99-4280, 41 p.

Stumm, F., Lange, A.D., and Candela, J.L, 2002, Hydrogeology and extent of saltwater intrusion of the Manhasset Neck peninsula, Long Island, New York: U.S. Geological Survey Water Resources Investigations Report 00-4193, 42 p

Stumm, F., and Chowdhury, S., 2003, Delineation of ground water flow in fractured rock in the southwestern part of Manhattan, New York, through use of advanced borehole geophysical methods: Groundwater Monitoring and Remediation, v. 23, no. 3, p. 42-49.

Stumm, F., Chu, Anthony, and Monti, J.Jr., 2004, Delineation of faults, fractures, foliation, and ground-water-flow zones in fractured-rock, on the southern part of Manhattan, New York, through use of advanced borehole geophysical techniques: U.S. Geological Survey Open-File Report 04-1232, 212 p.

Taterka, B.D., 1987, Bedrock geology of Central Park, New York City: Amherst, MA, University of Massachusetts Department of Geology and Geography, M.S. Thesis, contribution 61, 84 p.

Viele, E.L., 1865, Sanitary and topographical map of the City and island of New York: NYC Council of Hygiene and Public Health, 1 sheet, scale 1:10,000.

Williams, J.H., and Conger, R.W., 1990, Preliminary delineation of contaminated water-bearing fractures intersected by open-hole bedrock wells: Groundwater Monitoring and Review, v. 10, no. 4, p. 118-126.

Williams, J.H, and Lane, J.W., 1998, Advances in borehole geophysics for ground-water investigations: U.S. Geological Survey Fact Sheet 002-98, 4 p.

Williams, J.H., and Johnson, C.D., 2000, Borehole-wall imaging with acoustic and optical televiewers for fractured-bedrock aquifer investigations, in Proceedings of the Seventh International Symposium on Borehole Geophysics for Minerals, Geotechnical, and Groundwater Applications, October 24-26, 2000, Denver, Colorado, Minerals and Geotechnical Logging Society, p. 43-53.

Williams, J.H., and Johnson, C.D., 2004, Acoustic and optical borehole-wall imaging for fractured-rock aquifer studies: Journal of Applied Geophysics, no. 55, p. 151-159.